DRILLING PROCESS PARAMETER OPTIMIZATION AND MECHANICAL PROPERTY TEST ANALYSIS OF E-GLASS-SISAL FIBER REINFORCED POLYESTER COMPOSITE

Raga Sileshi Tolera

A Thesis Submitted to
The Department of Mechanical Engineering
School of Mechanical, Chemical, and Material Engineering

Presented in Partial Fulfillment of the Requirement for the Degree of Master's in Mechanical Engineering (Manufacturing Engineering)

Office of Graduate Studies
Adama Science and Technology University

September, 2022
Adama, Ethiopia

DRILLING PROCESS PARAMETER OPTIMIZATION AND MECHANICAL PROPERTY TEST ANALYSIS OF E-GLASS-SISAL FIBER REINFORCED POLYESTER COMPOSITE

Name of Candidate:

Raga Sileshi Tolera

Advisor:

Dr. Moera Gutu Jiru

A Thesis Submitted to

The Department of Mechanical Engineering

School of Mechanical, Chemical, and Material Engineering

Presented in Partial Fulfillment of the Requirement for the Degree of Master's in Mechanical Engineering (Manufacturing Engineering)

Office of Graduate Studies

Adama Science and Technology University

September, 2022

Adama, Ethiopia

Declaration

I hereby declare that this Master Thesis entitled “Drilling Process Parameter Optimization and Mechanical Property Test Analysis of E-Glass-Sisal Fiber Reinforced Polyester Composite” is my original work. That is, it has not been submitted for the award of any academic degree, diploma, or certificate in any other university. All sources of materials that are used for this thesis have been duly acknowledged through citation.

Raga Sileshi

Name of the Student	Signature	Date

Recommendation of Advisors

I/we, the advisor(s) of this thesis, hereby certify that I/we have read the revised version of the thesis entitled "Drilling Process Parameter Optimization and Mechanical Property Test Analysis of E-Glass-Sisal Fiber Reinforced Polyester Composite" prepared under my/our guidance by Raga Sileshi submitted in partial fulfillment of the requirements for the degree of Master of Science in Manufacturing Engineering.

Therefore, I/we recommend the submission of a revised version of the thesis to the department following the applicable procedures.

____________________	____________________	____________
Major Advisor	Signature	Date
____________________	____________________	____________
Co-advisor	Signature	Date

Approval Page

I/we, the advisors of the thesis entitled "Drilling Process Parameter Optimization and Mechanical Property Test Analysis of E-Glass-Sisal Fiber Reinforced Polyester Composite" and developed by Raga Sileshi, hereby certify that the recommendation and suggestions made by the board of examiners are appropriately incorporated into the final version of the thesis.

______________________	______________________	______________
Major Advisor	Signature	Date
______________________	______________________	______________
Co-advisor	Signature	Date

We, the undersigned, members of the Board of Examiners of the thesis by Raga Sileshi have read and evaluated the thesis entitled "Drilling Process Parameter Optimization and Mechanical Property Test Analysis of E-Glass-Sisal Fiber Reinforced Polyester Composite" and examined the candidate during an open defense. This is, therefore, to certify that the thesis is accepted for partial fulfillment of the requirement of the degree of Master of Science in Manufacturing Engineering.

______________________	______________________	______________
Chairperson	Signature	Date
______________________	______________________	______________
Internal Examiner	Signature	Date
______________________	______________________	______________
External Examiner	Signature	Date

Finally, approval and acceptance of the thesis is contingent upon submission of its final copy to the Office of Postgraduate Studies (OPGS) through the Department Graduate Council (DGC) and School Graduate Committee (SGC).

______________________	______________________	______________
Department Head	Signature	Date
______________________	______________________	______________
School Dean	Signature	Date
______________________	______________________	______________
Office of Postgraduate Studies, Dean	Signature	Date

Acknowledgment

First and foremost, praise and thank God, the Almighty, for His abundant blessings during my research work to complete the thesis.

I would like to express my deep and sincere gratitude to my thesis advisor, Dr. Moera Gutu, an assistant professor at Adama Science and Technology University, Adama, for allowing me to do research and providing invaluable guidance throughout this thesis work. His dynamism, vision, sincerity, and motivation have deeply inspired me. It was a great privilege and honor to work and study under his guidance. I am extremely grateful for what he has offered me. The precious advice and help he has given to me in the achievement of this research work. I would also like to thank him for his friendship, empathy, and great sense of humor. I am extending my heartfelt thanks to his family and friends for their acceptance and patience during the discussion I had with him on this thesis work.

I would like to express my sincere gratitude to Adama Science and Technology University for allowing me to fulfill my dream of attending the Technology University, the administration of the school of mechanical, material, and chemical engineering, and the school of research and graduate studies for their kind assistance in pursuing and completing my education. I would also like to thank every one of my teachers.

This thesis is wholeheartedly dedicated to my beloved parents my mother Asegedech Gebeyehu, and my father Sileshi Tolera, who has been my source of inspiration and strength when I give up, and who continually provide their moral, spiritual, emotional, and financial support. Also, I express my thanks to my sisters and brothers for their support and valuable prayers.

Friends here at Adama Science and Technology University. You all are like relatives to me. Thank you, everybody!

Table of Contents

List of Tables

List of Figures

List of Symbols and Nomenclatures

Abbreviation	Description
A:	Average cross-sectional area
ANOVA:	Analysis of variance
ASTM:	Americal standard of testing and measurement
C_i:	Circularity Error
CFRP:	Carbon fiber reinforced fiber
CNC:	Computer numerical control
d:	Drill Diameter
DF:	Delamination factor
D_{max}:	Maximum diameter
D_{min}:	Minimum diameter
E:	Poisson ratio
f:	Feed rate
F:	Ultimate tensile strength
GFRP:	Glass-fiber reinforced composite
GGGG:	Glass/glass/glass/glass
GRA :	Grey relational analaysis
GRG:	Grey relational grade
GSSG :	Glass sisal sisal glass
HCl:	Hydrochloric Acid
HSS:	High-speed steel
l:	initial length
MEKP:	Methyl ethyl ketone peroxide
NFC:	Natural fiber composite
NaOH:	Sodium Hydroxide
OA:	Orthogonal array
P:	Maximum load before failure
Ra:	Surface roughness
s:	Stacking sequence

S/N:	Signal-to-noise ratio
SEM:	Scanning electron microscope
SGGS:	Sisal glass glass sisal
SSSS:	Sisal/sisal/sisal/sisal
v:	Drilling speed
W_C:	Weight of composite
W_f:	Weight of fiber
W_F:	Fiber Weight Fraction
W_m:	Weight of matrix
W_M:	Matrix Weight Fraction
σ:	Stress
ε:	Strain
Δl:	Change in length

Abstract

When focusing on composite materials, the most important factors to consider are environmental friendliness and lightweight with high specific qualities. The growing use of composite materials in a wide range of applications raises the need for high-quality drilling of these materials. The effect of stacking sequence and drilling parameters on E-glass-sisal fiber-reinforced polyester was investigated in this paper. Hand layup was used to create hybrid fiber/polyester composites with a 40:60 ratio. A 3D optical profilometer was used to determine the surface roughness values. Delamination and circularity errors were analyzed using ImageJ software. Mechanical properties using impact, hardness, flexural, and tensile testing and drilling behavior using high-speed steel cutting tools in a CNC machine were determined. Using Taguchi L_{16} *orthogonal array and grey relational analysis methods to find optimized parameters (Speed, feed rate, stacking sequences, and drilling diameter as process control variables with multiple performance characteristics of delamination factors, circularity (roundness) error, and surface roughness are determined. Chip formation and hole morphology were also assessed. From the result, an Impact energy of 12.33J, a hardness value of 157.633HV, a flexural strength of 387.557MPa, and a tensile value of 132.7MPa were obtained. Analysis of variance has been used to find the effect percentage contribution and significance of the process parameters. Speed, feed rate, drilling diameter, and stacking sequences were found to be the significant factors affecting the entry and exit delamination factors, circularity, and surface roughness output. Lower entry and exit delamination, lower circularity error, and lower surface roughness were obtained at speed of 1500rpm, feed rate 0.02mm/rev, drill bit diameter 6mm, and sisal/glass/glass/sisal reinforced polyester composite. Conclusions contribute to the understanding combination of the Taguchi and grey relational analysis to find the optimum process parameter which minimizes the delamination factor, circularity error, and surface roughness within the range of parameters investigated.*

Keywords: Drillings, Delamination, Surface roughness, Taguchi and Grey relational analysis

CHAPTER ONE

INTRODUCTION

1.1 Background of the Study

The qualities of composite materials, which are composed of two or more different materials, cannot be attained by any one material component alone. The geometry of the reinforcing material (short fibers, long fibers, and texture), the type of reinforcement and matrix material, and the ratio of the reinforcement content and matrix materials all affect the attributes of composite materials (Caggiano, 2018). These composites exhibit good mechanical properties with increasing environmental safety (Jani et al., 2016b). During the inception stage of composite development, man-made fibers have been widely utilized as reinforcement. Later, owing to the competent characteristics of biomaterials, natural fibers extracted from plants and vegetables are used as reinforcements. The success of these bio-fiber happens mainly due to their lofty strength-to-weight ratio and the ability to degrade. Apart from these two reasons, they also provide water resistance, dimensional stability, thermal stability, and electrical resistance at a reasonable cost. These bio-reinforcements are not used in the virgin form. It needs some synthesis to remove unusable substances present in it and this is done by chemical pre-treatments (Vinayagamoorthy & Rajmohan, 2018).

Natural fibers can be used to compare to synthetic fibers such as glass in many ecological aspects, but not in mechanical strength. Significant improvements in the strength of polymer composites can be made by reinforcing natural fibers under different conditions, such as by using different chemical treatments on the fibers and hybridization with synthetic fibers. Still, the need for these treatments was identified as a lack of strength in these composites compared to other synthetic composites, whereas, the weaving of natural fibers in different orientations makes the composites stronger and comparable to those of synthetic fibers (Alavudeen et al., 2015). In addition to environmental benefits, natural fibers have a higher specific modulus than fiberglass, better damping performance than carbon fiber, and acceptable mechanical properties (Shamsuyeva et al., 2019). In some industries, it's time for natural fibers to act as a powerful alternative to synthetic fibers. In particular, natural fibers can be used as reinforcements for thermosetting resins and thermoplastic composites.

1.1.1 Hybrid Composite

Hybrid composites are materials that contain more than one reinforcement in a single matrix. Reinforcement can be two different fibers, two different filler particles, or filler particles and fibers (Vigneshwaran et al., 2019). Hybridization leads to reducing the amount of usage of synthetic fibers and improves the properties of the composites. The properties of hybrid composites are more than those of natural fiber-reinforced composites (Shireesha et al., 2019). Therefore, instead of using the individual fibers as reinforcements (synthetic or natural), combining the synthetic and bio-fibers in the same matrix through the hybridization process resulted in hybrid composites. Hybrid composites offer a good balance of mechanical performance and the cost of both fibers. The layering arrangement of fabrics will play a major role, as it affects the variety of mechanical properties such as tensile, flexural, and fatigue behavior of the laminated composites (Margabandu & Subramaniam, 2020).

Composites-based technologies have recently received increased attention. Due to their higher mechanical strength, stiffness, impact strength, damping, impact resistance, wear, thermal, chemical, and corrosion resistance, better resistance to damage, and cost-effectiveness when compared to conventional metal materials, composite technology allows for the production of exceptionally high-quality fiber-reinforced composites (John & Kumaran, 2020.; Lee et al., 2021; Singh et al., 2021). Bamboo, Sisal, Banana, Jute Flax, kenaf, and other natural fibers are inherently lightweight low-cost, environmentally friendly, and low-density (Mosisa & Batu, 2021).

Fiber-reinforced polymer composite (FRPC) is considered a substitute for metal materials in various industrial sectors such as automobiles, airplanes, wind power, railway transportation (Margabandu & Subramaniam, 2020) construction, military, and marine (Lee et al., 2021). The use of artificial synthetic fibers (carbon, glass, Kevlar) in polymer matrices is diminishing due to their non-renewability, high cost, and non-biodegradability, and can cause health and ecosystem problems. Recently, researchers have focused their interest on the development of composites reinforced with natural bio-fibers such as coir, jute, and sisal to overcome the disadvantages of synthetic fibers. Natural fibers have several advantages, such as wide availability, biodegradability, non-toxicity, low density, and low cost (Margabandu & Subramaniam, 2020). Also, some problems are there, like lower adhesion between fiber and matrix, composite degradation with an increase in temperature, and moisture absorption which limit their use in nonstructural applications (Patel et al., 2018).

1.1.2 Drilling Composite

The drilling of synthetic polymer composites was the focus of composite material machining in the 1970s. The considerable strength of composite materials comes from the fact that they can withstand a wide range of loads, depending on the type and manner of reinforcement used, as well as the matrix qualities, Fiber loss, breakage, high tool wear, delamination, fiber separation at the interface, and major environmental and health problems all result from composite machining. In FRP composite machining, the choice of reinforcing material, fiber orientation, tool type, material, and drilling parameters is crucial (Ramesh et al., 2016).

More than 40 percent of the machining process in aircraft industries contributes to drilling. Delamination around the holes becomes the major reason for their poor quality. Significant damage to the workpiece may be introduced and high wear rates of the tools are experienced. Nearly 100,000 holes have been drilled for the assembly of aircraft components. Since the holes are being drilled in finished products, poor quality may lead to the rejection of parts (Jenarthanan et al., 2017). The interaction of diverse material components during assembly in the aerospace and automotive industries may need drilling holes to permit fastening parts together. The aerospace industry in the United States uses 250 million twist drill bits per year. It is believed that 55,000 holes are bored in the Airbus A350 to simplify the assembly of one unit. Damage can occur to composite plates that have been molded or drilled with holes (Hale & Ng, 2021).

The machinability of a composite depends on the components of the composite. In particular, the properties of the reinforcement are used to determine the ease with which a composite material can be machined. Therefore, the machinability of composite materials made from man-made fibers and bio-fibers is not similar (Vinayagamoorthy & Rajmohan, 2018). The drilling operation causes serious structural damage to the laminated composites such as delamination, debonding of fiber-matrix, micro-cracks, and thermal damages, which may degrade structural integrity and also affect the mechanical performance of the composites (Rajmohan, 2019b; Vinayagamoorthy & Rajmohan, 2018) (Yallew et al., 2016). During the machining of the composites, the failure of the material starts due to the generation of the cutting force against the composite surface. The force tends to damage the material's surface. This leads to poor cutting surface, damage to fiber as well as the matrix, fiber debonding, fiber pullout, fiber layer separation (Kumar et al., 2016a; Shanmugam Vigneshwaran et al., 2021) burrs, melting of the matrix, adhesion of materials to drill, and sub-surface failures (Lee et al., 2021). Investigations have revealed that two obvious mechanisms of delamination are the peel-up and push-out of fiber (Durão et al., 2014; Kumar et al., 2016b). Among the various types of damage caused by drilling parameters, the proper choice of tool shape, and the choice of tool material is important and must be identified before machining (Rajkumar et al., 2017).

For fiber composites, fiber reinforcement orientation, fiber reinforcement, and fiber morphology are important considerations in determining processing performance. Machining is the recommended option for manufacturing composites with defined shapes and sizes to create holes and slots. However, it affects reinforcements and matrices. Machining quality can be quantified by output responses such as surface roughness, cutting force, and material removal rate. Conventional machining processes also take into account tool life and tool wear (Shanmugam Vigneshwaran et al., 2021). Delamination damage is commonly seen when drilling long fiber-reinforced composites. This defect affects the structural integrity of the laminate in terms of durability and results in poor assembly stability (Teja et al., 2020). Surface roughness and delamination are properties that can affect dimensional accuracy, machine component performance, and manufacturing costs. Reducing surface roughness and delamination factors has a significant impact on better dimensional accuracy, composite performance, and machining processes (Alagappan et al., 2020; Jenarthanan et al., 2016). To control delamination issues and achieve the quality required to machine small holes, it is necessary to understand the cutting mechanism of material removal, and the dynamics of the machining process. Precision machining is required to ensure dimensional stability and interface quality. However, the structural properties of this material make it difficult to complete the machining process. Due to the anisotropy and heterogeneity properties of composite materials, the processing of composite materials is different from that of conventional materials (Rajkumar et al., 2017; Sumesh et al., 2020; Shanmugam Vigneshwaran et al., 2021).

The effect of drilling geometry on thrust and delamination was investigated when machining carbon fiber-reinforced epoxy composites using different tool materials (Rajkumar et al., 2017). Higher thrust force, tool wear, and high feed are other main reasons for delamination. Reduction of delamination can be attained by choosing the proper machining factors, tool geometry, and material of the tool. Among the above methods, it is necessary to better understand the process of drilling CFRP under various environmental conditions, since it provides excellent machinability. In particular, temperature-assisted machining has proven to be a successful strategy when drilling composite and metallic materials (John & Ku1maran, 2021).

1.2 Problem Statement

Typically, the primary manufacturing process was used to produce products in closed or simple shapes with near-final shapes based on natural fiber composites. This primarily reduces the secondary manufacturing process's requirements (Margabandu & Subramaniam, 2020; Singh et al., 2021). Complex product assembly, on the other hand, necessitates the use of mechanical fastening or adhesive bonding. Because of its short duration, fastening is the preferred method of these two. Furthermore, the components assembled with fasteners make the parts easier to disassemble (Debnath et al., 2014; Patel et al., 2018; Singh et al., 2021). As mechanical fasteners, rivets, and bolts are used in the assembly of composite-to-composite or metal-composite aerospace system components, hole drilling is an important and unavoidable machining process. The drilled hole must be free of delamination, diameter error, burrs, and fiber pullout to avoid structural failure (John & Kumaran, 2020).

The machining process was required to assemble or join Composite materials. However, it was difficult due to the material's nonhomogeneous and anisotropic nature. The machining mechanism was quite different and more difficult than that of metals. During the process, the conventional cutting tool must alternately face the cohesive region, such as the reinforcement of hard fiber in the soft matrix. The cutting tool will fail as soon as the fiber and matrix are machined simultaneously. The poor surface finish of the composite was poor in conventional machining processes such as turning, drilling, and milling and the major failures observed were fiber pullout, delamination, subsurface damage, and bulk matrix removal (Jani et al., 2016b). While drilling natural and synthetic fiber-reinforced polymer (FRP) composite materials, it is difficult to achieve acceptable hole quality while balancing output response. The hybrid fiber-reinforced composite's heterogeneous and anisotropic properties make conventional drilling more difficult, resulting in more material failures in the matrix and reinforcement.

The stacking sequences of natural and synthetic fibers were critical in preventing tool penetration, which results in fiber pulling out, delamination, circularity error, and surface roughness. More importantly, surface fiber damage causes waviness, which was the cause of surface roughness. Delamination, circularity error, and the defects in the hole walls caused by the drilling reduce considerably the mechanical strength, fatigue resistance, and the quality of the holes in terms of dimensional and geometrical tolerances. Furthermore, chip formation and impact on hole morphology were unpredictable, making it difficult to determine the cutting mechanism. As a result, extensive research has been conducted on the machinability behavior of synthetic (glass fiber) and natural (sisal) fiber-reinforced polymer matrix composites (PMCs). The research on the machinability behavior of various stacking sequences of hybrid natural and synthetic fiber-reinforced polymer matrix composites, on the other hand, was still in its early stages. Finally, mechanical property analysis and cutting parameter optimization on drilling performance (delamination, circularity (roundness), and good surface finish) were performed on the fabricated sisal/glass fiber reinforced polyester resin composite using a CNC drill machine in dry condition.

1.3 The objective of the Study

1.3.1 General Objective of the Study

The general objective of the study was optimization of drilling process parameters and mechanical property analysis of E-glass-sisal fiber-reinforced polyester composites in dry condition.

1.3.2 Specific Objective of the Study

- To fabricate pure sisal, pure glass, and glass-sisal fiber-reinforced polyester composite materials.
- To investigate the mechanical property of the developed E-glass-sisal /polyester composite materials.
- To optimize the drilling parameters for minimum delamination, Circularity (roundness) error, and Surface finish.
- To analyze chip characteristics and their impact on the hole morphology of machined surfaces.

1.4 Significance of the Study

Now a day's manufacturing industries such as the automotive and aerospace industries are highly in need of lightweight, harder, stronger, and biodegradable components using cost-effective composite materials instead pure synthetic or natural composites. Delamination, circularity, and surface roughness is represented to be the most prevalent failure in composite structures machining where composite materials can be used such as automotive, aerospace, and any industries which are using fiber-reinforced polymer composite. The drilling process applied to FRP composites has been studied as it is one of the most widely employed machining processes of FRP materials due to the extensive utilization of mechanical joints, such as rivets, instead of welded or bonded joints. It will also be used to grasp the theoretical and practical knowledge of any reader in this research area and for students, who are studying in this research area, and for future research as literature.

1.5 Scope of the Study

This thesis was delimited to: -

- Fabrication of composite material with 0°/90° fiber orientation of sisal with acid and alkali treatment and randomly oriented synthetic glass fiber reinforced composite with uniform weight percentage ratio of natural and synthetic fiber.
- Focusing on testing of mechanical properties of sisal-glass fiber reinforced composite with polyester resin for structural application.
- Composite testing was done on the locally available testing facilities as per the standards of different ASTM.
- Experimental investigation on CNC dry drilling and the optimization of the drilling parameters was done by using Taguchi and multi-response grey relation analysis method to get better delamination, hole roundness, and surface roughness.

1.6 Limitations of the Study

For performing the research there were several constraints encountered these constraints are described as under.

- The non-availability of a sisal decortication and waving machine for fiber extraction and waving of the fiber.

- Non-availability of compression molding machine which is better than hand layup molding composite fabrication for better mechanical properties.
- The laboratories used in this work are found in different corners of the country causing time waste and the environment may affect the result.
- The malfunction of testing machines causes an unwanted reputation of the experiment in another machine and the unwillingness of different authorities for allowing machines to be used by the researcher.

1.7 Research Motivation

A lot of researchers have been researching machining single synthetic or natural composite while limited studies of research work on hybrid natural and synthetic composite drilling. Loss of properties during drilling reduces structural strength and lowers assembly tolerance which can be detrimental to the long-term performance of the composite material. By controlling machining parameters, machining can be conducted with reduced delamination, hole roundness, and surface roughness. Considering the increasing structural application of composite materials, the limitation in their machining performance should be envisaged in a detailed and systematic way for producing quality holes with reduced damage should be identified. The motivation for this work was mainly due to the above-said reasons.

1.8 Research Outline

A brief introduction to the contents of the thesis report was outlined as follows. Chapter one introduces the study, chapter two a literature review of drilling hybrid composite and related works was briefed, chapter three material, methods, and methodology implemented to achieve the objectives, chapter four comprises result and their discussions, and finally, chapter five discuss conclusions and recommendation for future work, and finally the reference and appendix.

CHAPTER TWO

LITERATURE REVIEW

2.1 Introduction

A literature review provided background material relevant to a specific area of research. It includes methodology, descriptions, and a critical evaluation of each work. The current study was primarily concerned with the machining of fiber-reinforced polymer composites to explore the machining behaviors. Based on the review, a research gap was found, and a summary review was also conducted.

2.2 Composite Materials

Composite materials are materials that are comprised of at least two different materials with one of the materials remaining in a solid state during fabrication. Glass-reinforced fiber composite materials give the engineer an alternative performance of materials for the automobile sector and building sector. Sisal fibers are a renewable resource, and the production of this fiber uses a small amount of energy. The use of sisal fibers to reinforce glass has several advantages such as reduced environmental impact from synthetic fibers and decomposability of components (Baloyi et al., 2021)

Sisal fiber: As high temperatures are encountered during the thermosets' curing step; sisal fiber's thermal resilience is essential in the production of composite materials. The walls of the sisal fiber undergo pyrolysis during high-temperature processing, resulting in the formation of charred layers. To prevent further degradation, the charred layers will form a protective layer around the lignocellulose. Thus, the thermal stability of the fiber, the bonding behavior of sisal, and the distribution of the fiber in the composites are important factors in the fabrication of sisal-reinforced composites (Baloyi et al., 2021).

E-Glass fiber: Silica is the main component of E-glass fibers (SiO_2). Other oxides, such as B_2O_2 and Al_2O_2, are added to SiO_2 to change its network structure and improve its workability (Njoku et al., 2012).

Polyester resin: A polymerizable monomer dissolved in an unsaturated (reactive) polyester solid is referred to as polyester resin. Unsaturated polyesters are long-chain, linear polymers with a high carbon double-bond concentration. They are formed as a result of the condensation reaction between glycol and an unsaturated dibasic acid (maleic or fumaric) (Njoku et al., 2012).

2.2.1 Polymer Matrix Composites

Polymer matrix composite is the most commonly used composite, because of its advantages such as high strength, low cost, and simple manufacturing principle. The requirement for polymer material in this modern dynamic world is increasing day by day because it has a wide range of advantages over traditional materials in terms of high strength-to-weight ratio, cost, high toughness, high tensile strength, and high creep resistance at increases in temperatures. Polymer matrices can be either thermoplastic or thermoset according to the effect of heat on their properties. The thermoset polymer is frequently used as the matrix material due to some advantages it has over the thermoplastic one.

Table 2.1: Qualitative comparison of thermoplastic and thermosetting resin (Nguyen et al., 2017)

Characteristic	Thermoplastics	Thermosets
Tensile properties	Excellent	Excellent
Stiffness properties	Excellent	Excellent
Compression properties	Good	Excellent
strength after impact	Good to excellent	Fair to excellent
Bolted joint properties	Fair	Good
Fatigue resistance	Good	Excellent
Damage Tolerance	Excellent	Fair to excellent
Durability	Excellent	Good to excellent
Maintainability	Fair to poor	Good
Service temperature	Good	Good
Environmental weakness	None of the hydraulic fluid	Moisture
Manufacturing scrap rates	Low	Low
Prepare shelf life and out time	Excellent	Good
Health/safety	Excellent	Excellent

The thermoset polymer matrix materials have overall, better economics and high temperature, good mechanical, wetting, and adhesion properties, and easiness for disposal. The most commonly used thermoset resin materials are epoxy, polyester, vinyl ester, and phenolic.

Table 2.2: Properties of thermoset polymers (Chaudhary and Ahmad,2020)

Name of polymers	Density (gm/cm^3)	Tensile Strength (MPa)	Compression Strength (MPa)	Young's modulus (GPa)	Elongation (%)
Epoxy resin	1.1-1.4	35-100	100-200	3-6	1-6
Polyester resin	1.2-1.5	33	90-250	1-1.3	1.5-1.8
Vinyl ester	1.2-1.4	69-83	100	3.1-3.8	4-7

2.3 Hybridization of Natural with Synthetic Fiber

Hybridization of a natural fiber composite by another natural fiber does not yield superior mechanical properties as hybridization by a synthetic fiber like glass fiber (Ramesh et al., 2013). and hence this kind of hybrid composite is suitable for low-cost applications this kind of material is very popular in the engineering market such as the automotive and aerospace industries.

2.4 Drilling of Hybrid Composites

Drilling is a complex process; it requires a systematic and quantitative study of all the major influencing parameters on machining performance to frame the rule base under a wide range of work conditions.

Several studies on the drilling behavior of composites reinforced only with synthetic or natural fibers are presented in the literature whereas few studies on the drilling behavior of composites fabricated with hybrid fibers are presented. Drilling processes were required to investigate the drilling performance of hybrid FRP composites. Some of the review works are listed down.

Margabandu & Subramaniam, (2020) experimentally investigated the thrust force, delamination, and surface roughness drilling of jute/carbon hybrid composites to study the influence of cutting parameters and it reveals that the most significant effect was the feed rate influenced the drill thrust force and the drill speed influenced both delamination factor and surface roughness of hybrid fiber-reinforced composites. From observations, the suggested combination for drilling jute/carbon hybrid composites is a carbide drill, with a spindle speed of 1,750 rpm and feed of 0.03 mm/rev.

Yallew et al., (2016) studied hole-making in woven jute fabric-reinforced polymer composites. In this experimental endeavor, drilling of woven jute fabric-reinforced polypropylene composite has been performed, and reported that the tool point angle is an important factor in deciding the delamination and hole quality in natural fiber-reinforced composites and that the drilling quality of natural fiber composites can be increased through chemical treatment of fiber and higher entry delamination than the exit delamination. This is mainly because of the increased drilling force at the exit point of the composite surface.

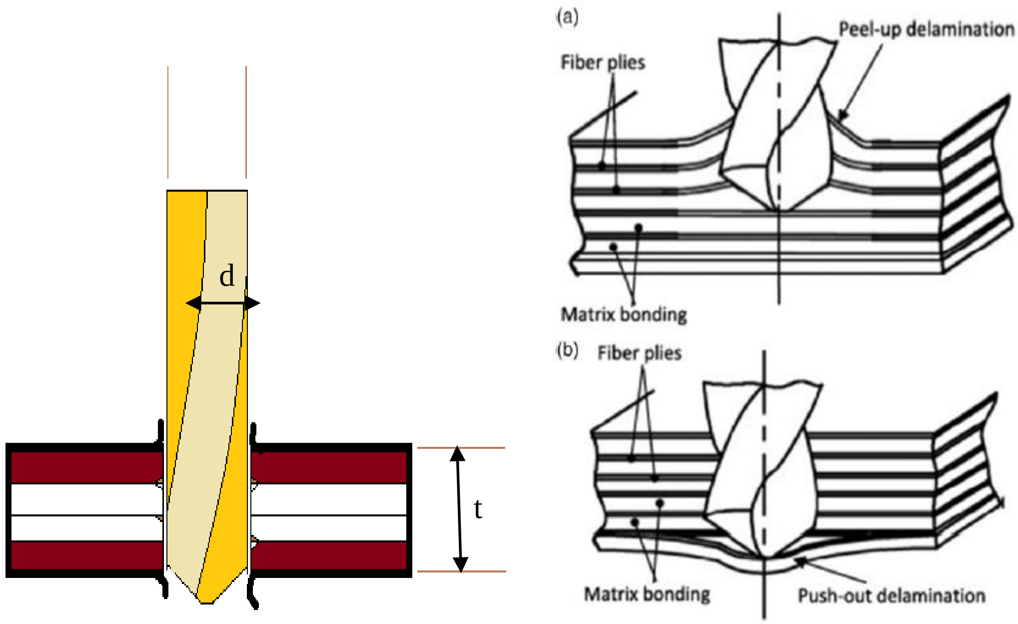

Figure 2.1: Drilling composite and its effect (Vinayagamoorthy & Rajmohan, 2018)

Debnath et al., (2014) experimentally analyzed the drilling characteristics of sisal fiber-reinforced epoxy and polypropylene composites sisal fiber-reinforced epoxy (Epoxy LY 556, and Hardener HY 951) were manufactured using the hand layup technique whereas laminates of sisal fiber-reinforced PP were manufactured using hot compression molding techniques of 4 mm film stacking method laminate was achieved. The weight percentage of natural fiber is 50-55%. This is machined using a radial drilling machine. Chip formation characteristics in the context of both thermoset and thermoplastic and Influence of drill geometry, feed, and spindle speed on drilling forces and a comparative analysis of damage characteristics of drilled holes.

Concluded that the drilling behavior of natural fiber composites depends not only on the drill geometry and cutting parameters but also on the type of polymer present in the developed composite laminates.

Shunmugesh & Kavan, (2017) on aerospace-grade T300 Bi-directional Carbon Fiber reinforced with epoxy resin composite of 8-mm thickness, holes of 6-mm diameter were drilled under the topic of investigation and optimization of machining parameters in the drilling of carbon fiber-reinforced polymer (CFRP) composites. Changing the feed rate to 0.025,0.05,0.1 mm/rev and the cutting speed to 30,40,50 m/min. In dry drill conditions, ideal drill process parameters and drill bit type effects employing HSS, Kennametal Solid Carbide (TiAlN Black Coated-KC7325 Grade), and WIDIA Solid Carbide Drill (TiN Golden Coating-WU25PD Grade) cutting tools. The multi-objective optimization of the input process parameter was carried out using the Taguchi technique in combination with the GRA. Investigated workpiece material surface roughness, hole quality, and damage due to delamination. The findings show that feed rate has a significant impact on outlet delamination damage and surface roughness, both of which are improved using TiAlN-coated carbide tools, and that cutting speed is accurate. When comparing HSS and TiN within roundness, the value of carbide TiAlN is lower when comparing case drill bit type hole quality which was the most relevant process parameter impacting roundness.

Lee et al., (2021) burr formation and tool wear in drilling CFRP and hybrid composites are being investigated. Hybrid composites of carbon fiber reinforced polymer (CFRP) and aramid fiber-reinforced polymer (AFRP) (C-AFRP) with a stacking sequence of (0°/90°) thickness 6 mm and dimensions 130 mm x 130 mm were successfully synthesized, and CNC machine maximum spindle speed and power of 10,000 rpm and 7.5kW is used for machining with a cutting tool 8 mm diameter, carbide drill with a point angle of 90°, a relief angle of 10°, a helix angle of 30°, and a total length of 63 mm. A feed rate of 200 mm/min and a spindle speed of 2000 rpm are used as process parameters, C-AFRP hybrid composite has higher tensile strength, higher tensile modulus, and smaller tensile failure elongation compared to those of CFRP and their drilling characteristics, including burr generation and tool wear, were also investigated thrust force and tool wear caused by drilling C-AFRP hybrid composites were significantly less than those by drilling CFRP. In the future, it is necessary to focus on reducing burr formation during the drilling of C-AFRP hybrid composites in the future.

Kumar et al., (2016a) investigated delamination and surface roughness in the drilling of GFRP composite material with various drills are being investigated experimentally. An asymmetric laminate of GFRP prepared by the vacuum bagging method prepared using eight layers of the plain-woven glass fiber of stacking order (0, 90/±45/±45/0, 90/±45/0, 90/0, 90/±45) with 49% of fiber volume fraction with a size of Laminates of 200 x 200 x 3.78 mm^3. Drilled using three different geometries and materials drills called a helical flute (HSS) drill, carbon tipped straight shank (K20) drill, and solid carbide eight-facet drill. Using a radial drilling machine, whose spindle power is 8 kW and has a maximum speed of 2000 rpm. Parameters used are spindle speed 250, 500, 800, 1000, 1200, and 1500 rpm and feed rate 0.02, 0.07, 0.10mm/rev. From the result, it was found that as the feed rate increases, damage around the hole increases, however, at higher spindle speed, lower delamination was measured. The surface roughness of the hole was measured at the given cutting parameters. It has been found that at higher spindle speed surface roughness was minimum. The surface quality of the hole significantly improves using a solid carbide eight-facet drill.

Jayabal & Natarajan, (2010) investigated optimizing the drilling behavior of a glass-coir-polyester hybrid composite. Feed rate played a major role in the drilling of these composites in comparison with drill bit diameter and spindle speed. The interaction between drill bit diameter and feed rate was also high in the drilling of coir-glass hybrid composites.

Jayabal et al., (2013) investigated the drilling behavior of treated and untreated woven coir fiber-reinforced polyester composite. They evaluated the influence of drill bit diameter, feed rate, and spindle speed on drilling forces and tool wear. Drill bit diameter, spindle speed, and feed rate were significant variables in their cutting forces model but drill bit diameter was the only significant variable in their tool wear model.

Singh et al., (2021) experimentally analyzed the drilling characteristics of the hybrid sisal–jute fiber epoxy matrix composites. Uses three different solid HSS drill bit geometry (Twist, Step, and Core) of 6mm nominal diameter and two process parameters (Speed and feed) with three levels with full factor analysis of L_{27} then analysis of force signals, delamination, surface roughness, and joint breaking strength was performed on the composite. Discussed that both the magnitude and mode of force signal change for the cutting lip angle because of inhomogeneity inside the fiber laminates, presence of interfaces, intermittent fracture of the composite constituents, and different thermal conductivity of fibers and matrix. Also, the oscillation of frequency is lower for the twist drill bit than for the step and core drill. This may probably be due to the line contact of the twist drill and laminates, resulting in clean and good cutting. With an increase in spindle speeds, delamination and surface roughness, both decrease. With an increase in feed, the surface roughness value increases, but delamination shows some aberrations in the results. Core drills have higher surface roughness. when we come to joint breaking strength It can be observed from the tensile test results that the hole drilled by the twist drill sample has a greater amount of tensile strength, and the core drilled sample has the lowest tensile strength.

Ramesh et al., (2014) conducted an experimental investigation in drilling hybrid glass-sisal-jute fiber-reinforced polymer composites. The outcome of their research provides evidence for the influence of the drill tool on the thrust force and delamination. The High-speed steel (HSS) tool produced high delamination and thrust force when compared to solid carbide and TiN-coated solid carbide drill tools. Cutting with the larger diameter drill tool increased the thrust force on the sisal/ glass hybrid composites because of the increased contact area and higher stress generation.

Abilash & Sivapragash, (2016) optimized the delamination failure in bamboo fiber reinforced polyester composite using critical parameters such as speed, feed, and diameter of the cutting tool, and their contribution to entry and outlet delamination were analyzed using Taguchi parameter design L_{18} orthogonal array in a single objective, the function was used, and the S/N ratio was obtained for each process parameter differently, therefore suitable multi-objective has used the function was carried out using grey analysis and reduced delamination was identified by varying the speed and feed rate on both sides. From the analysis analyzing bamboo fiber composite the push-out delamination failure effect can be minimized by controlling the feed rate at 18 mm/min with a minimum speed of 500 rpm with a 4 mm diameter drill bit. Feed rate and drill diameter are seen to make the largest contribution to the delamination effect. Generally, the use of small diameter drills and low feed favors the minimum delamination while drilling leads to better quality holes.

2.5 The Effect of Drilling Parameters

Many researchers studied the drilling mechanism and the effect of drilling parameters on fiber-reinforced polymer composites (Durão et al., 2013; Jayabal et al., 2011; Jayabal & Natarajan, 2010). An increase in speed delamination factor at entry and exit increases the reason may be the same that the dynamic rake angle increases with an increase in the spindle speed, from ANOVA analysis the drill geometry, speed, feed, and pattern have significant effects on the DF at entry. DF at entry and exit was higher for hemp polyester composites than glass polyester and hybrid composites, due to hemp fibers having more elongation before cutting than glass fibers (Patel et al., 2018). Previous studies indicated that the delamination factor increases with an increase in the feed rate. The increase in feed rate increases the chatter, and it produces incomplete machining at a faster traverse, which led to higher surface roughness, and, hence, a low limit of feed rates is advisable in machining GFRP composites (Rajkumar et al., 2017). It also has been reported that fiber-reinforced thermoplastic laminates have low damage to hole surfaces as mentioned in (Singh et al., 2021).

2.6 Mechanical Properties and Drilling Effect of Composite

When constructing a mechanically sound structure, material mechanical qualities are crucial. Tests on the samples can be used to determine this. These qualities govern how materials respond to external stresses. The Stress-Strain Curve, Stress, Strain, Elongation, Proportional Limit, Modulus of Elasticity, Yield Point, Ultimate Strength, Yield Strength, and Secant Modulus are all used to test materials for one or more of the following functions.

2.6.1 Mechanical Property of Hybrid Composite

Flynn et al., (2016) the flax/carbon hybrid composites were developed to examine the influence of hybridization on mechanical performances, and the incorporation of fibers resulted in higher mechanical strength. Rafiquzzaman et al., (2016) developed hybrid jute/glass composites to examine mechanical characteristics using experimental and numerical approaches and discovered that adding the right amount of jute with glass fiber boosted overall properties while being cost-effective. When the number of layers in a fiber-reinforced composite laminate grows, so does the load-carrying capacity of the composite from matrix to fiber, resulting in high strength and modulus of stiffness. Margabandu & Subramaniam, (2020) investigated the flexural (bending) and impact properties of hybrid jute (J) / carbon (C) composites, i.e., JCCJ and CJJC using experimental and finite element methods. The authors discovered that hybrid composites reinforced with carbon fabric on the exterior surface have high strength. The addition of natural fiber to glass fiber improves the composites' tensile, flexural, and impact strength. Manickam Ramesh et al., (2016).

(Baloyi et al., 2021) analyzed the mechanical properties of a glass/sisal/polyester composite five samples of the sisal-glass composite were prepared with varying sisal fiber content and different layering techniques. Sisal fibers were pre-treated with 20% NaOH to enhance their crosslinking with the resin and reduce chemical impurities such as lignin and waxes. Mechanical (flexural test, hardness, and tensile strength) and physical tests (density and water absorption) were conducted to analyze the properties of the composite. The composite had a tensile strength of 57.60 MPa, a flexural strength of 36 N/mm^2, moisture absorption of 10%, and a burning rate of 9.82 mm/min. These results were then compared with those of the current partition boards in the market. It was noted that the composite was suitable for use in partition boards. Again, regarding cost, these composites are cheaper to produce at a rate of \$11.33/m^2 compared to timber costing \$16/m^2.

2.6.2 Delamination of Composite

Delamination is a frequent cause of damage in the drilling of composite laminates. While drilling damage was observed both at the entry and exit of the specimen. In Jute fiber, push-out delamination was more severe than that of the peel-up reinforced composites (Yallew et al., 2016).

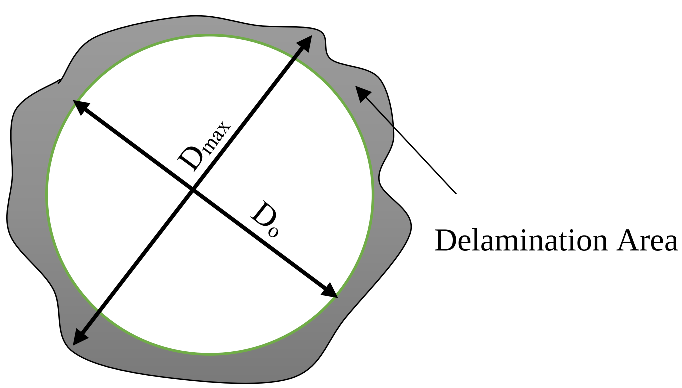

Figure 2.2: A diagram of the delamination factor measurement (Shanmugam et al., 2021)

Cracks propagated in the composite laminates due to the delamination and debonding of matrix phenomenon as the propagation of cracks is more frequent in brittle materials than ductile materials. So crack propagation is more prominent in fibers reinforced with epoxy-based polymer composites. Epoxy is a thermoset polymer matrix, and typically, thermoset polymers are comparatively brittle when compared to the thermoplastic polymer matrix, but they have properties like better chemical resistance and strong interfacial bonding, and, generally, the decomposition and glass transition temperatures of the thermosets are greater than the thermoplastic matrix (Singh et al., 2021). The delamination related to push-out is more severe than that of peel-up and is identified by the conventional drilling process using different diameters of twist drill. This happens not only because of low interlaminar shear strength between the fiber and resin interface at the exit side but also, due to the higher thrust force experienced during the machining of the specimen (Abilash & Sivapragash, 2016). The delamination at entry increases because of increased rake angle and cutting speed during drilling while the delamination at the exit of drilled samples has been influenced by the cutting tool geometry and cutting speed (Bhoopathi & Ramesh, 2020).

It is observed that hemp polyester composites exhibit more delamination factors at entry than glass polyester and hybrid composites. This was because the hemp fibers have more elongation before cutting than glass fibers. Also, hemp fibers are less brittle than glass fibers. Because of this the hybrid composite having glass at the top and bottom exhibits almost the same DF at entry as the glass polyester composite (Patel et al., 2018). The improper combination of input process parameters such as cutting speed, feed rate, depth of cut, tool geometry, and tool material affects the dimensional accuracy of a hole especially, the delamination at both the entry and exit side of the composite materials (Bhoopathi & Ramesh, 2020).

2.6.2.1 Failure criteria

Fiber buckling (compression), fiber breaking (tensile), matrix cracking, matrix crushing, delamination, or a combination of these factors can all cause failure when machining CFRP materials. Under longitudinal compression, flexural stresses in the fiber caused by buckling cause the creation of kink zones, which can result in fracture planes in carbon fibers (Figure 2.3a).

Buckling does not necessarily lead to immediate failure because the surrounding matrix supports the fibers. Under longitudinal tension, the fibers with lower ultimate strain than the matrix will fail first. When a fiber breaks in tensile stress, the matrix transmits the load across the gap created by the breakage from the broken to the adjacent fibers. The broken fibers increase gradually in density with increasing load. Stress concentrations thus created by the broken fibers produce a failure of adjacent fibers up to the point where catastrophic failure occurs in the composite (Figure 2.3b) (Seyedbehzad, 2015).

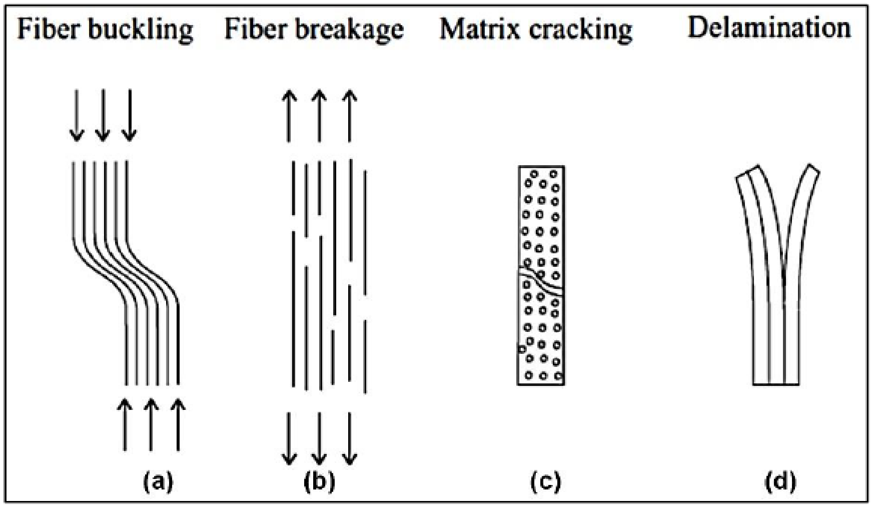

Figure 2.3: Failure modes in the machining of fiber-reinforced composite (Seyedbehzad., 2015)

Matrix cracking (Figure 2.3c) frequently occurs in composite laminates and is usually accompanied by other damages; thus, it generally does not result in the ultimate failure of a laminate. Delamination reduces the bending stiffness and strength as well as the load-carrying capability of the laminate under compression. The size of the delamination may increase to a critical point under repeated loading and cause laminate failure.

2.6.3 Surface Roughness

In tribology, rough surfaces often wear down faster than smooth surfaces and have a higher coefficient of friction. Because irregularities in the surface can produce nucleation sites for cracks or corrosion, roughness can be considered a good predictor of mechanical component performance. Roughness is an important quality parameter in drilled holes because crack propagation, wear, fatigue, creep, and corrosion mechanisms are all influenced by the level of surface roughness (Mohammed & Wolla, 2022).

Studies show that fiber orientation influenced the quality of the machined surfaces. measurement of surface roughness in FRP is less dependable than in metals, because protruding fiber tips may lead to incorrect results or at least large variations of the reading. Additional errors may result from the hooking of the fibers to the stylus. Conventional machining of fiber-reinforced composites is difficult due to diverse fiber and matrix properties, fiber orientation, inhomogeneous nature of the material, and the presence of high-volume fraction (volume of fiber over total volume) of hard abrasive fiber in the matrix. Most of the studies on FRP machining show that minimizing the surface roughness was very difficult and is to be controlled (Zitoune et al., 2012). Surface morphology and integrity depend on the machining process and workpiece characteristics such as the cutting speed, the feed rate, the fiber type, volume content, fiber orientation, and the matrix type (Seyedbehzad, 2015).

2.7 Taguchi and Grey Relational Optimization Method

2.7.1 Taguchi Method

Taguchi's experimental designs were developed to perform the machining operations on the fabricated laminates by most of the researchers by using the MINITAB software based on the cutting parameters such as tool geometry, tool materials, type of coolants, cutting speed, depth of cut, cutting feed rate, and ambient conditions (Bhoopathi & Ramesh, 2020).

2.7.2 Grey Relation Analysis

Optimization of multiple response characteristics is more complex when compared to the optimization of single performance characteristics. The Grey theory is one of the important theories and can be used for uncertainty, multi-input, and discrete data. A grey system has a level of information between black and white. The grey relational analysis is a measurement of the absolute value of the data difference between sequences and is also used to measure an approximate correlation between sequences. It is an effective means of analyzing the relationship between the sequences with fewer data and can analyze many factors. In the present investigation, the problem has three performance characteristics that need to be minimized by choosing appropriate processing conditions. The performance characteristics used are surface roughness and delamination outputs (delamination factor and delamination adjustment) (Rajmohan, 2019a).

2.8 Research Gap

During the machining process, the composite was defaced in a variety of ways. These imperfections have an impact on both the properties of the composite. A composite must be able to be machined easily and with little or no damage. Also, many researchers are only looking at either the mechanical properties or the drilling process optimization. This inspired the researcher to conduct a comprehensive survey on composite machining. There has been a lot of research done on the machining characteristics of natural or synthetic homogeneous reinforced polymer composite materials. However, little was known about the machining performance of different stacking sequences of hybrid natural and synthetic fiber-reinforced polymer composite materials, hole morphology, and chip analysis. A limited study on drilling polyester-based E-glass-sisal fiber-reinforced polyester composites with different layer arrangements has been discovered. The effects of stacking sequences on mechanical properties, as well as the effects of stacking sequences and drilling parameters on delamination, circularity error, and surface roughness of an E-glass-sisal fiber reinforced polyester composite, will be observed on the output delamination, circularity, and surface roughness. So that the mechanical properties of the prepared composite could be analyzed, a comprehensive drilling experimental test was carried out by varying the drill diameter, stacking sequences, spindle speed, and feed rate, and the significance of each parameter was analyzed on a standard CNC vertical milling machine using a hybrid Taguchi and grey relation analysis method.

CHAPTER THREE

MATERIALS AND METHOD

3.1 Introduction

In this section, the materials, method, and equipment used in the study and machines for testing different samples were presented. In addition, the methodologies used in conducting the research were also presented.

3.2 Materials and Method Used

3.2.1 Matrix material

Different methods used in the study include fiber extraction, design of experiment, fiber treatment, composite fabrication, specimen preparation, and testing methods.

Polyester resin (Grade: VBR 2303) matrix material was purchased from World Glass Fiber and Resins Private Limited, Addis Abeba, Ethiopia. The properties of the matrix material are shown in Table 3.1.

Table 3.1: Properties of the general-purpose polyester (Ramesh et al., 2019)

Property	Polyester resin
Density (kg/mm^3)	1,000-1,300
Young’s modulus (GPa)	4-6
Poisson’s ratio	0.45
Tensile strength (MPa)	15-20
Compressive strength (MPa)	80-220
Flexural strength (MPa)	25-32
Flexural modulus (GPa)	1.1-1.6

3.2.2 Fiber Material

In this experiment work natural sisal fiber (Agave sisalana) and synthetic E-glass fiber were used Sisal fibers in the form of woven mats were prepared from the local plants of sisal fiber and polyester resin as matrices were used. Woven sisal and random glass fiber laminates were made on the required dimensions (300 x 300) mm^2 which are shown in Figs 3.1. Using the hand lay-up method pure sisal polyester, pure glass polyester, and glass-sisal polyester hybrid composites with two different layering arrangements were fabricated.

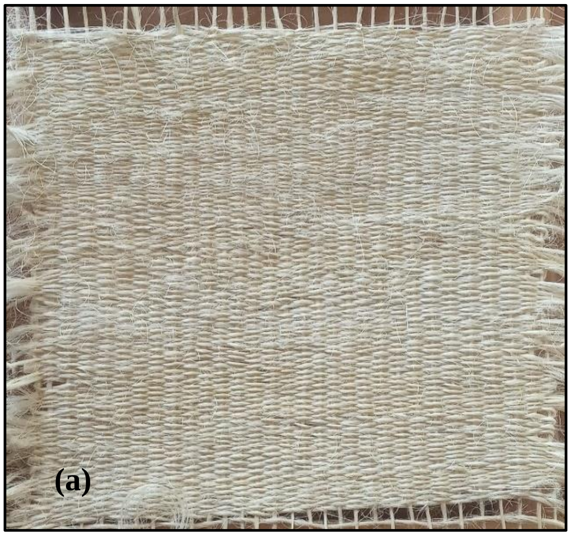

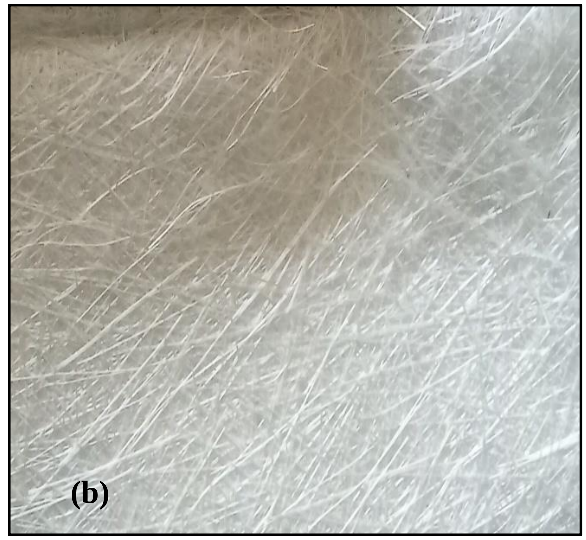

Figure 3.1: (a) Woven Sisal and (b) Random E-glass fiber

Table 3.2: Material properties of reinforcing sisal and glass fibers (Elsad et al., 2020)

Properties	Units	Sisal fiber	E-Glass fiber
Elongation	(%)	3-7	1.8-3.2
Elastic modulus	(MPa)	35	73
Moisture content	(%)	10-20	-
Density	(g/cm^3)	1.46	2.55
Tensile strength	(MPa)	700	3400
Shear Modulus	(MPa)	18.2	33
Fiber Diameter	(µm)	50-200	17
Poisson ratio	-	0.23	0.22

3.2.3 Preparation of the Fiber

General-purpose polyester was chosen as a matrix for its excellent processability, cross-linking tendency, and mechanical properties. For 100 grams of resin, 1.5 ml of Methyl Ethyl Ketone Peroxide (MEKP) and Cobalt Naphthenate were taken for room temperature curing, per the literature (Alavudeen et al., 2015). The matrix, catalyst, accelerator, and chemicals were procured from World glass fiber plc, Addis Abeba, Ethiopia. Typical properties of general-purpose polyester are listed in Table 3.1. 60:40 weight ratios of polyester and reinforcement were maintained in Table 3.3.

Most natural fibers have low processing temperatures, and cannot be processed over 150°C due to their biological nature and fiber preparation below 80°C gives better properties (Manickam Ramesh et al., 2016). Chemical surface modification was a well-known process to increase the interfacial bonding between fibers and matrix (Abilash & Sivapragash, 2016; M. Ramesh et al., 2016). So that the sisal fiber was soaked in 5% of NaOH for 3hr then washed with distilled water then again soaked in 2% of HCl acid to remove the NaOH then cleaned with distilled water too, roughened the fiber surface more and this could be expected to promote adhesion between the fibers and the matrix. The fibers were allowed to dry for 24 hrs., following which they were post-cured in an oven at 50 °C for an hour to remove their moisture (Alavudeen et al., 2015; Jani et al., 2016a).

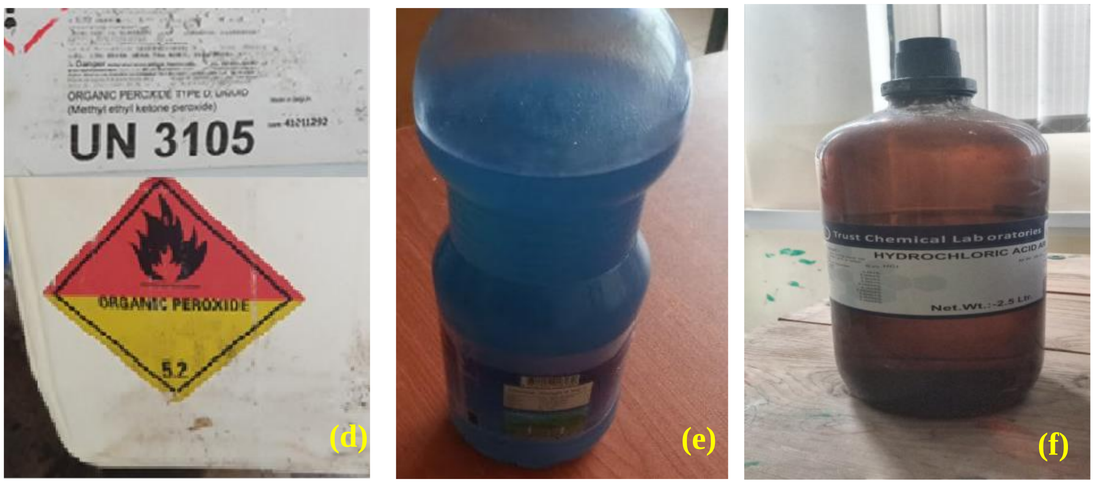

Figure 3.2: Raw material used and fiber treatment (a) NaOH, (b) Sisal fiber treated with NaOH base, (c) Sisal fiber treated in HCl acid, (d) Methyl ethyl ketone peroxide (MEKP) hardener, (e) Polyester resin, (f) HCl acid

3.2.4 Development of Composite Specimens

Manufacturing composites was another big challenge as the working conditions play a vital role in deciding the characteristics of the composite. Composites are manufactured in different ways. Amongst the different methods, hand layup and compression molding are widely used techniques for preparing the composite in the form of plates (Vinayagamoorthy & Rajmohan, 2018).

3.2.4.1 Fiber and Matrix Volume Content of the Composite

In this research, the ratio of the sisal fiber, glass fiber, and polyester resin used in sample preparation was based on mass ratio. This means the mass of both Polyester resin and fiber was measured using an electronic balance.

In the design, fabrication, and analysis of composite materials, the first and critical task was the determination of ingredient percentages such as fibers (sisal and glass) and polyester matrix fraction presence in laminate. These components are microstructural elements of the composite in which composite strength and drilling properties are determined and limited by these values.

The fiber and matrix weight fraction (WF, WM) was determined by, the compositions of the composite samples using the formulas.

Fiber and matrix weight fraction (W_F, W_M)

Weight of composite = weight of fiber + weight of the matrix

$$W_C = W_f + W_m \quad 3.1$$

$$\text{Fiber weight fraction} = \frac{weight\ of\ fiber}{weight\ of\ composite} \quad 3.2$$

$$W_F = \frac{W_f}{W_C} = \frac{W_f}{W_f + W_m} \quad 3.3$$

$$\text{Matrix weight fraction} = \frac{weight\ of\ matrix}{Weight\ of\ composite} \quad 3.4$$

$$W_M = \frac{W_m}{W_C} = \frac{W_m}{W_f + W_m} \quad 3.5$$

From these formulae, $W_F + W_M = 1$

Were, W_f: Weight of Fiber (g), W_m: Weight of Matrix (g), Wc: Weight of Composite Specimen (g), WF: Fiber Weight Fraction, WM: Matrix Weight Fraction.

Table 3.3: Details of different layering arrangements and their fiber weight fraction

Composite plate number	Layering arrangement	Weight of sisal (gm)	Weight of glass (gm)	Total weight of plate (gm)	Total fiber weight fraction (wt. %)
S1	SGGS	140	80	300	40
S2	GSSG	140	80	304	40
S3	SSSS	340	-	340	40
S4	GGGG	-	200	280	40

To fabricate hybrid composites woven sisal fibers and random glass fibers as reinforcement with different stacking sequences and polyester resin as matrices were used. Using the hand lay-up method pure sisal polyester (SSSS), pure glass polyester (GGGG), and glass-sisal polyester hybrid composites with two different layering arrangements (SGGS, GSSG) were fabricated. The accelerator was mixed with resin and air bubbles were removed by degassing. The catalyst was added to the mold, after which the mold was closed and a deadweight of 45 kg was placed over it (Alavudeen et al., 2015). In another paper, 35 kg was positioned above the entire setup and allowed to cure at room temperature for 24 hrs (Margabandu, 2020). In this research 40 dead weight was used also.

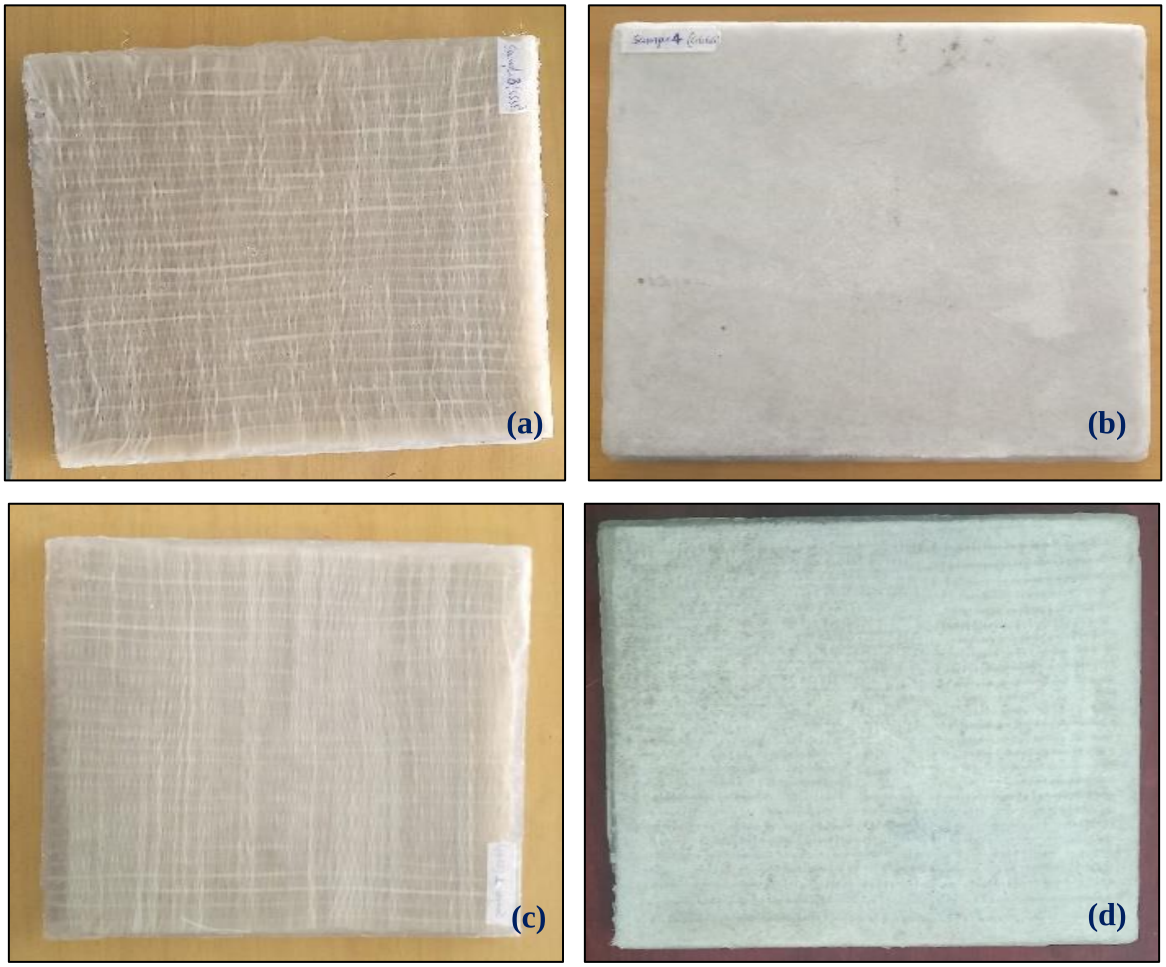

Figure 3.3: Prepared sample (a) Pure sisal (SSSS) (b) Pure glass (GGGG) (c) Sisal-glass-glass-sisal (SGGS) (d) Glass-sisal-sisal-Glass (GSSG) fiber reinforced polyester composite

The detail of different layering arrangements with fiber weight fractions were shown in Table 3.3. Figure 3.3 shows the prepared composite specimens.

The work material used consists of four plies of fiber mesh bonded together with polyester resin. The work material was fabricated by hand layup process with 40 Kg dead body mass pressing the mold. The thickness of the plate was 5 mm. The thicknesses of glass and sisal fiber are 0.2 and 0.5 mm, respectively. The plate has a dimension of 300 × 300 × 5 mm^3. Where the thickness of the composite part was built up by applying a series of reinforcing layers and liquid resin layers. A pictorial representation of raw materials and the fabricated work material was shown in Figures 3.2 and Figure 3.3.

Then it was kept in an oven at 50°C where high fiber bonding happens with the matrix thereby the delaminating tendency tends to reduce and then it was allowed for cooling at room temperature for a few hours. After that, the specimens of the required dimensions were cut using a jig saw cutter and prepared for drilling. Figure 3.3, shows the prepared composite specimens.

3.3Mechanical Testing and Characterization

Mechanical Characterization Physical and Morphological characterization of a composite material was performed according to ASTM standards and at room temperature.

3.3.1 Mechanical Testing of the composite

Representative specimens from various sections of the composite were prepared, according to ASTM D638 and ASTM D790 standards, to examine the tensile and bending (flexural) strength of the composites, respectively. The tests were done using an Instron Universal Testing Machine (UTM) (Series IX software, Ethiopian Defense College, Bishoftu, Ethiopia), which has a maximum capacity of 30 kN. All tests were performed with a crosshead speed of 1 mm/min at room temperature (25°C). Three specimens were tested for each sample and the mean values are reported.

3.3.1.1 Impact test

It is a method for determining the impact resistance of materials. An arm held at a specific height with constant potential energy was released. When the arm hits the sample, either it breaks or the weight rests it. From the energy absorbed by the sample, its impact strength was determined. The Izod impact test specimens were prepared as per the ASTM D256 standards (ASTM standard D256, 2002). The test sample was fixed in the impact test setup with the V-notched side facing the striking edge of the pendulum. The pendulum was released and allowed to strike through the sample. During the test, the maximum energy that can be stored to break the specimens was noted for the entire specimen for analysis of results. The sample dimension taken was 55 x 25 x 5mm^3.

3.3.1.2 Hardness test

Hardness is the resistance of a material to indentation load. it is determined by the depth of indentation. Vickers hardness testing relies on the use of optical measurement. Microhardness test procedure, ASTM E-384, with the dimension of the specimen $(20x20x5)mm^3$ specifies different loads using a diamond indenter to make an indentation which is then measured and converted to a hardness value. This Study used a Vickers hardness testing machine (HVS-50 Buehler, USA). The indenter was a diamond pyramid shape with a square base having an included angle of $136^0 \pm 0.5$. The indenter was forced into the sample's surface at a constant load of 10 Kgf with a dwell time of 10s. The surface-projected diagonal lengths of the resulting impression of each sample were then measured immediately after unloading using an upright optical. The flat surface was indented at three different locations and the average of the mean diagonal lengths of two indentations was calculated.

$$\mathrm{HV} = \frac{con.x\,test\ force}{surface\,area\,of\ the\ indentor} \qquad 3.6$$

$$\frac{0.102\,x\,2F(\sin\frac{136°}{2})}{d^2} \qquad 3.7$$

Where F= force, d= diagonal of indentation, and $136^{0\ is}$ the angle between the opposite surface at a vertex.

3.3.1.3 Flexural test

The flexural test determines the maximum stress induced in the outermost fiber. The three-point flexural test provides values for the modulus of elasticity in bending and the flexural stress-strain response of the material. The specimens for the flexural test are prepared according to the ASTM D790 standards (ASTM standard D790, 2002). The specimen was placed in the machine and tested by applying load with the help of the same UTM. The sample dimension was 127mm x 30mm x 5mm. The results of flexural strength and displacement of the specimen were observed for result comparison. The flexural stress was calculated by using Equation 3.16, calculation of the flexural strain was by using Equation 3.17:

$$\sigma_f = \frac{3FL}{2bd^2} \tag{3.8}$$

$$\varepsilon_f = \frac{6Dd}{L^2} \tag{3.9}$$

where σ_f = Stress in outer fibers at the midpoint (MPa), ε_f = Strain in the outer surface (mm/mm), F = load at a given point on the deflection curve (N), L = Support span (mm), b = Width of test beam (mm), d = Depth of tested beam (mm) and D= The maximum deflection of the center of the beam(mm).

3.3.1.4 Tensile testing

Factors such as the strength of the layer arrangement, fibers, matrix, the weight percentage of the fibers, and the bonding properties between the layer arrangement, matrix, and fiber determine the strength of the composites. In general, synthetic fiber reinforcement increases the tensile properties of the composites because of the enhanced stiffness and strength of the fibers. The size of the sample used for the tensile strength test was 165mm x 19mm x 5 mm.

The formulae that were used to calculate the values of tensile strength, strain, elongation, and modulus of elasticity are given below:

$$\mathrm{F} = \frac{p}{A} \tag{3.10}$$

$$\mathrm{E} = \frac{\sigma}{\varepsilon} \tag{3.11}$$

$$\varepsilon = \frac{\Delta l}{l} \tag{3.12}$$

where F = ultimate tensile strength, MPa; P = maximum load before failure, N; A = average cross-sectional area (w × h), mm^2; σ = ultimate tensile stress; E = elastic modulus; ε = strain at maximum load; Δl = change in length produced; l = initial length.

3.4 Drilling Specification and Drilling Setup

The experiment was conducted using a high-precision computer numerical control (CNC) Vertical Milling Machine (CNC) of (Model: XHS7145, No. KH1509141) at Ethio-china technical University, Addis Abeba, Ethiopia has been used to carry out drilling experiments. The experiments were conducted under dry conditions. Generally, the drilling experiments are performed using 6, 8, 10, and 12 mm diameter drill bits as recommended by (Ismail et al., 2016; Margabandu & Subramaniam, 2020).

The specifications of the CNC milling machine are given in Table 3.4. Figure 3.4 below shows the test setup for performing experiments and the fixation of the composite material by using clamps in the machining center to make sure that vibrations and unwanted displacements are eliminated. The experiments were conducted without a backing plate and coolant.

Table 3.4: Specification of the CNC milling machine

Type of machine	Unit	Specifications
Table size	Mm	1350 x 450
X, Y, and Z axis	Mm	950 x 430 x 500
Rapid traverse (X, Y, Z axis)	m/min	12 x 12 x 8
Spindle motor	kW	7.5
Max. spindle speed	Rpm	5,000
Machine weight	Kg	5300
Rated power	kW	11

Figure 3.4: Experimental setup of machining the composites (CNC vertical milling)

3.4.1 Drilling of Composite

Drilling is a process in which a rotating cutting tool was used to remove unwanted materials to produce a specific size hole. Testing the drilling ability of the composite is mandatory for assembling and joining the parts.

3.4.2 Drill Bit Material

HSS Composition:

The cutting tool used for machining was a solid High-Speed Steel (HSS) tool of 6 mm, 8 mm, 10 mm, and 12 mm diameter, Point angle of 135°, Helix angle of 33°, and Chisel edge angle of 129°.

Table 3.5: Composition of HSS tool for drilling purposes (Rathinavel et al., 2015)

Materials	Composition (%)
Carbon	1.20-1.40
Manganese	0.50
Maximum Silicon	1.00
Chromium	3.5-4.5
Vanadium	2.25-2.75
Tungsten	5.60-6.40
Molybdenum	5.60-6.40
Cobalt	5.0-7.0

Figure 3.5: Different diameters of the HSS drill bit

3.4.3 Measurement Method of Delamination

In this research, an accurate inexpensive method using a PC, cannon camera, Image j software, and image editing software, image j software was considered for measuring delamination sizes and circularity(roundness) errors. The samples with drilled holes were taken a picture directly using the cannon camera. The camera used was the ‘‘Cannon color camera’’. The image of the drilled specimen was acquired with 600 DPI resolution and saved as a JPEG image (Maleki et al., 2018). Then, the scanned images were imported into the image j and Photoshop software then each photo was magnified up to 155%. Circles were drawn on the delamination zones and to the original drill sizes. The dimensions of the delaminated zone were measured using the ruler tool of ImageJ and Photoshop software. The delamination factors and roundness(circularity) error were measured based on the pixel density of the delaminated zones.

Measurement of delamination Outputs

The widely used method of enumerating delamination depends on the delamination factor. These factors are used to determine the delamination on both sides of the workpiece. According to (Kumar D.et al 2016) delamination factor is calculated using the expression:

$$F_d = \frac{D_{max}}{D} \qquad 3.13$$

Where D_{max} = Damaged zone diameter and D = Indicates the diameter of the hole.

Some researchers have also used a ratio of the damaged area to the hole area (Patel et al., 2018) The composite material was positioned and an image was taken. That image is taken in an equal pixel which was used to measure the damage (maximum width). After the measurement of the maximum width of damage (Dmax) suffered by the material, the damage normally assigned by the delamination factor (F_d) was determined.

It was measured using open-source software image-J was used for the delamination measurement for both F_d and Circularity (roundness) error.

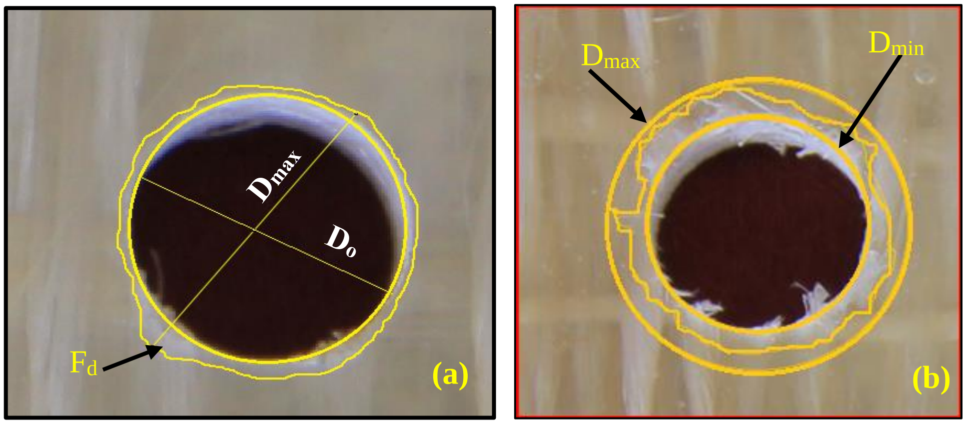

Figure 3.6: (a) Delamination and (b) Circularity(roundness) error measurement

For precise assembly of components, the hole generated should display a minimum error an error in dimension causing the failure of human life (Köklü et al., 2017).

3.4.4 Measurement Method roundness error (Circularity (C_i))

The roundness error of the drilled holes is said to be circular. The circularity is measured in terms of minimum circumscribing and maximum inscribing circle diameter (Shunmugesh & Kavan, 2017). The image of the sample taken by a camera and analyzed with ImageJ measurement is used to measure the physical characteristics of an object. The variance in diameter of all 16 individual holes of the prepared composite specimen. From each measurement, the maximum and minimum values of diameter were used to compute roundness error constantly using the equation below, and then the roundness error values were utilized in Taguchi's L_{16} OA for further analysis. where D_{max} is the maximum hole diameter and D_{min} is the minimum hole diameter. Circularity is the 2D version of cylindricity.

$$\text{Roundness}(circularity)\, error = \frac{D_{max} - D_{min}}{2} \qquad 3.14$$

3.4.5 Measurement Method of Surface Roughness

The surface roughness of drilled hole on the composite specimens was measured using a zeta 3D optical profilometer and the values are described using the arithmetic mean roughness (Ra) as it is one of the most widely used surface roughness measures. All drilled composite specimens were cut into half sections for ease of measurement and consistency, and measured surface roughness values were taken at 10×lens magnification for better precision (Mohammed & Wolla, 2022).

The setup adopted for surface roughness measurement using an optical profilometer were shown in Figure 3.8. Surface roughness in Ra means that the value generated by using Eq 3.15. was described in micrometer (μm) when only the reference length of the roughness curve was taken in the location of the mean line, the x-axis in the direction of the mean line, and the y-axis in the path of the longitudinal magnification of the sample component. Ra parameter was determined using Eq 3.15. in which y = f(x) describes the roughness curve. Where l_r represents the reference length of the roughness.

For the measurement of Ra, all the drilled composite laminates were sectioned carefully into two halves as presented in Figure 3.7(a). Sectioning was required so that it's easy to insert the sample under the lenses for the 3D optical profile measuring instrument so it would be able to measure the hole wall surface without intrepidity first scanning. The sectioning was also required for a scanning electron microscope (SEM) examination. Figure 3.7. (b) and (c) present the surface roughness measurement of the drilled hole.

$$R_a = \frac{1}{l_r}\int_0^{l_r} \{f(x)\}dx \qquad 3.15$$

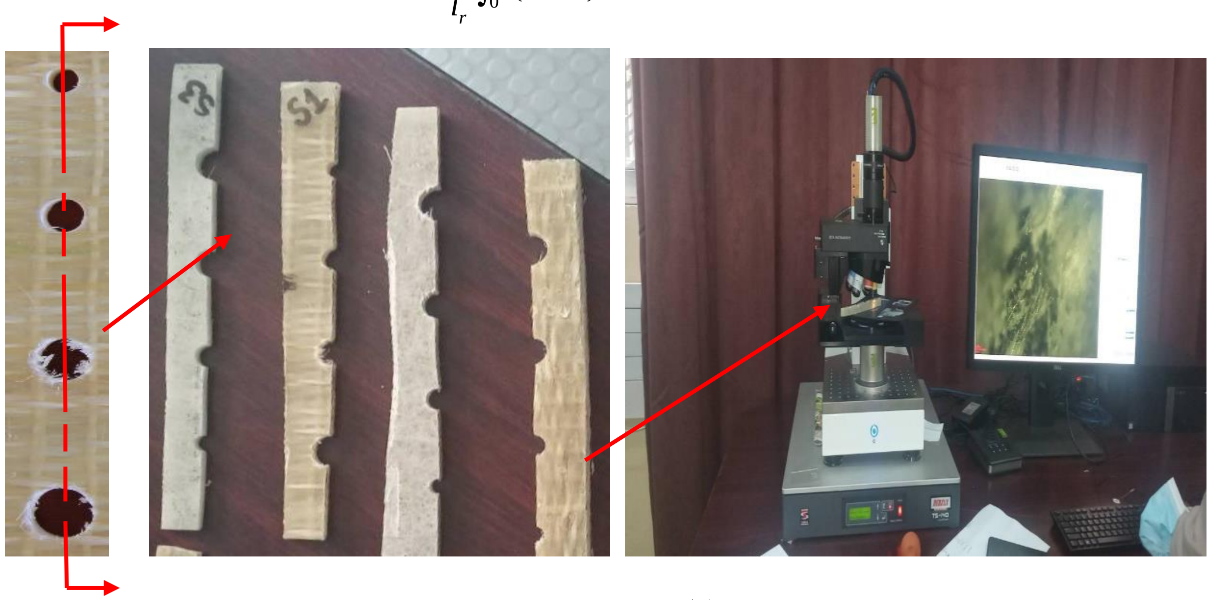

(a) (b) (c)

Figure 3.7: 3D optical profilometer surface roughness measuring instrument

The surface roughness of the composites was determined using the Zeta 20, 3D optical surface profile tester at Addis Abeba Science and Technology University, Addis Abeba, Ethiopia.

3.5 Methodology

3.5.1 Experimental Design

Delamination, circularity, and surface roughness of the workpiece are the three important factors of quality in any machining operation. During machining, many factors affect the delamination, circularity error, and surface roughness. Based on the literature (Jenarthanan A. et al 2016), the independently controllable predominant machining parameters that are having greater influences on delamination, circularity error, and surface roughness of hybrid sisal-glass fiber reinforced polymer composite workpiece have been identified, this was Stacking sequences, feed rate, cutting speed, and drill diameter for this experiment.

The drilling input parameters selected for this study were stacking sequences (layering arrangement), drill diameters, spindle speed, and feed rate.

Taguchi L_{16} orthogonal array and multi-objective grey relational analysis methodology was one of the methods that can be used to analyze the process parameters for performance characteristics, i.e., surface finish, delamination factors, circularity error, the morphology of the machined surface, and chip analysis, also be determined. Drilling parameters are chosen for achieving maximum performance characteristics for the drilling process. The desired drilling parameters are usually selected with the help of referred literature and the operator's experience.

According to the literature research, the performance of the drilling process performed with a CNC milling machine was dependent on various machining parameters. Parameters used in this drilling test have been defined to study their influence on the drilled material quality and selected from a consensus in the literature regarding the drilling process parameters and the values are selected based on the optimal drill effect on the quality of drilled holes and drilling machine set-up specifications (Yallew et al., 2016).

Table 3.6: Process control parameters and their levels

Process parameters	Units	Notation	Variable	Levels			
Feed rate	mm/rev	F	A	0.02	0.04	0.06	0.08
Spindle speed	Rpm	V	B	750	1000	1250	1500
Drill diameter	Mm	D	C	6	8	10	12
Layer arrangement	sequence	S	D	SGGS (1), GSSG (2), SSSS (3), GGGG (4).			

Taguchi method with ANOVA was used to find the influence, percentage contribution, and significance of drilling parameters on drilling-induced damages, and multi-objective grey relational analysis was used to find the overall optimum value. Scanning electron microscopy and 3D optical profilometer analysis were also conducted to understand the fracture behavior and surface morphology of the drilled holes. The different methodologies followed in performing this study were summarized. Taguchi method and grey relational analysis are applied for the optimization of process parameters to bring forth superior products with low manufacturing costs (Ghani et al., 2013).

3.5.2 Taguchi Experimental Design

The Taguchi experimental design was selected to design and analyze the significance of the control variables on output response. Based on the number of parameters/variables, a specific orthogonal array can be chosen to identify the optimal conditions leading to a desirable outcome, as well as lower the number of required experiments. The main objectives of the Taguchi method were to save time and to produce quality outputs at low costs. Both objectives can be achieved using the orthogonal array proposed by Taguchi. The total number of experiments can be reduced by using Taguchi factorial experimental design (orthogonal array) rather than full-scale factorial analysis. Additionally, variable and detailed information regarding the influence of the parameters on the experimental results can be obtained. In the present investigation, the Standard Taguchi L_{16} (4 x 4) orthogonal array was selected for experimentation. Drill bits diameter, spindle speed, stacking sequences, and feed rate were the selected control variables, and their corresponding level was shown in Table 3.5.

A unique optimal combination of input-cutting parameters was not at all possible in Taguchi's optimization approach because of the different contradictory characteristics of the output responses. The obtained results from Taguchi's optimization approach evidence that the optimization of measured responses was performed separately for each attribute such as inlet delamination, outlet delamination, circularity, and surface roughness (Bhoopathi & Ramesh, 2020).

Quality characteristics of a control variable are evaluated using a signal-to-noise (S/N) ratio, where the signal represents the "desirable" output and noise refers to the variations in the output due to "undesirable" factors. The Taguchi method uses the signal-to-noise ratio to express the scatter around a target value. In Taguchi's experimental analysis, the output response was analyzed by considering three categories: "nominal is better, larger is better, and smaller is better." In Taguchi analysis, the mean response of the experimental data was evaluated by transforming the output data into a signal-to-noise ratio (S/N). For the present experiment, the S/N ratio of the output responses was found at a "smaller is better" condition since the rate of delamination, circularity error, and Surface roughness (Ra) should be minimum. The S/N ratio condition was expressed in the logarithmic transformation of the loss function, as in Equation 3.16.

Calculate the S/N ratio for the corresponding responses using the following formula.

(a) Larger - the – better

$$\text{S/N}\, ratio(\eta) = -10\log_{10}(\frac{1}{n})\sum_{i=1}^{n}\frac{1}{Y_{ij}^{2}} \qquad 3.16$$

Where, n=number of replications, Y_{ij}^2 = Observation response value where i=1, 2… n; j=1, 2… k

This is applied to the problem where maximization of the quality characteristics of interest is sought. This is referred to as the larger-the-better type problem.

(b) Smaller- the better

$$\text{S/N}\, ratio(\eta) = -10\log_{10}(\frac{1}{n}\sum_{i=1}^{n}Y_{ij}^{2}) \qquad 3.17$$

This is termed the smaller-the-better type problem where minimization of the characteristics is intended.

(c) Nominal -the better.

$$\text{S/N } ratio\,(\eta) = 10\log_{10}(\frac{\mu^2}{\sigma^2}) \quad 3.18$$

$$\text{Where, } \mu = \frac{y_1 + y_2 + ... + y_n}{n} \text{ and } \sigma^2 = \frac{\sum (y_i - \bar{y})^2}{n-1}$$

The significance of the individual parameters was determined by the Analysis of Variance (ANOVA). The ANOVA table consists of the P-value, F-value, and percentage (%) of the contribution of each parameter. The larger the F-value of a parameter, the more notable it is. The significance of a parameter can also be understood by its probability value. If the P-value is less than 0.05 for a parameter, then it is significant in the process and the percentage of contribution of each input process parameter on the quality characteristics.

Using analysis of variance (ANOVA), the effect of input parameters was studied on the output parameters. ANOVA is a standard statistical technique that is used to analyze experimental data. The percentage contribution of each factor is found by determining the variability of the data. To evaluate the correlation between the input process parameters and the response variables. The Minitab Version 20 statistical tool was used for the statistical analysis of the experimental data. The optimum process parameters were found using Taguchi's S/N ratio graphs. The foremost objectives of this paper were to minimize the delamination factor, roundness (circularity), and surface roughness. To determine the optimal input parameters and mathematical models, it was necessary to use an optimization technique. For these purposes, it is convenient to use an experiment plan. Drilling should be optimized using the Grey relational analysis the multi-response analysis was performed (Rajkumar et al., 2017).

3.5.3 Grey relational analysis

In grey relational analysis, data preprocessing was conducted first to normalize the raw data. A linear normalization of the S/N ratio was performed in the range of (0-1), which was called grey relation generation

For the Grey Relational Analysis (GRA), the sixteen experiments become sixteen subsystems. The influence of these subsystems on the response variable was to be analyzed by using the GRA technique. The parametric conditions corresponding to the highest weighted grey relational grade give minimum values of surface roughness, roundness error, and delamination. In this manner, the multi-objective problem has been converted into single-objective optimization using the GRA technique.

In grey relational analysis, the grey relational coefficient for different process characteristics is calculated and the average of these coefficients is called grey relational grade which is used as a single response for the Taguchi L_{16} experimental plan, and the same is illustrated in the following steps.

Step 1: Transform the original response data into S/N ratio (Y_{ij}) using the appropriate formula depending on the type of quality characteristics using Eq. 3.16, Eq.3.17, and Eq.3.18.

Step 2: Selection of experimental design based on the levels of the process parameters normalize the performance characteristics. Using Y_{ij} is normalized as Z_{ij} ($0 \leq Z_{ij} \leq 1$) by the following formula to avoid the effect of adopting different units and to reduce the variability. It's necessary to normalize the original data before analyzing them with grey relation theory or any other methodologies. An appropriate value is deduced from the values in the same array to make the value of this array approximate 1. Since the process of normalization affects the rank, we also analyzed the sensitivity of the normalization process on the sequencing result. Thus, we recommend that the S/N ratio value be adopted when normalizing data in grey relation analysis.

S/N ratio with larger the better manner:

$$Z_{ij} = \frac{Y_{ij} - \min(Y_{ij}, i = 1, 2, \ldots n)}{\max(Y_{ij,}\ i = 1, 2, \ldots n) - \min(Y_{ij,} i = 1, 2, \ldots n)} \tag{3.19}$$

S/N ratio with smaller-the better manner:

$$Z_{ij} = \frac{\max(Y_{ij}, i = 1, 2, \ldots n) - Y_{ij}}{\max(Y_{ij,}\ i = 1, 2, \ldots n) - \min(Y_{ij,} i = 1, 2, \ldots n)} \tag{3.20}$$

S/N ratio with nominal the best:

$$Z_{ij} = \frac{(Y_{ij} - T\arg et) - \min(\left|y_{ij} - T\arg et\right|, i = 1,2,...,n)}{\max(\left|Y_{ij} - T\arg et\right|, i = 1,2,...,n) - \min(\left|y_{ij} - T\arg et\right|, i = 1,2,...,n)} \quad 3.21$$

Step 3: Calculation of the grey relational coefficient and the grey relational grade.

$$\gamma(Y_o(k), Y_i(k)) = \frac{\Delta \min + \xi \Delta \max}{\Delta_{oj}(k) + \xi \Delta \max} \quad 3.22$$

Where, a. j=1, 2…n; k=1, 2…m, n is the number of experimental data items and m is the number of responses.

b. $Y_o(k)$ is the reference sequence ($Y_o(k)$=1, k=1, 2…., m; $Y_j(k)$ is the specific comparison sequence.

c. $\Delta_{oj} = \left\|Y_o(k) - Y_i(k)\right\|$ The absolute value of the difference between $Y_o(k)$and $Y_j(k)$.

d. $\Delta \min = \min\limits_{\forall j \in i} \min\limits_{\forall k} \left\|Y_o(k) - Y_j(k)\right\|$ is the smallest value of $Y_j(k)$.

e. $\Delta \min = \max\limits_{\forall j \in i} \max\limits_{\forall k} \left\|Y_o(k) - Y_j(k)\right\|$ is the largest value of $Y_j(k)$.

f. ζ is the distinguishing coefficient which is defined in the range $0 \le \zeta \le 1$ (the value may adjust based on the practical needs of the system).

Step 4: ANOVA for grey relational grade to analyze the experimental results.

$$\bar{\gamma} = \frac{1}{k} \sum_{i=1}^{m} \gamma_{ij} \quad 3.23$$

Where, $\bar{\gamma}$ is the grey relational grade for the j^{th} experiment and k is the number of performance characteristics.

The grade is considered for optimizing the multi-response parameter design problem.

Step 5: Selection of optimal parameters using the graph method or ANOVA response table for the grey relational grade.

The highest grey relational grade implies better product quality; therefore, based on the grey relational grade, the factor effect can be estimated and the optimal level for each controllable factor can also be determined (Abilash & Sivapragash, 2016).

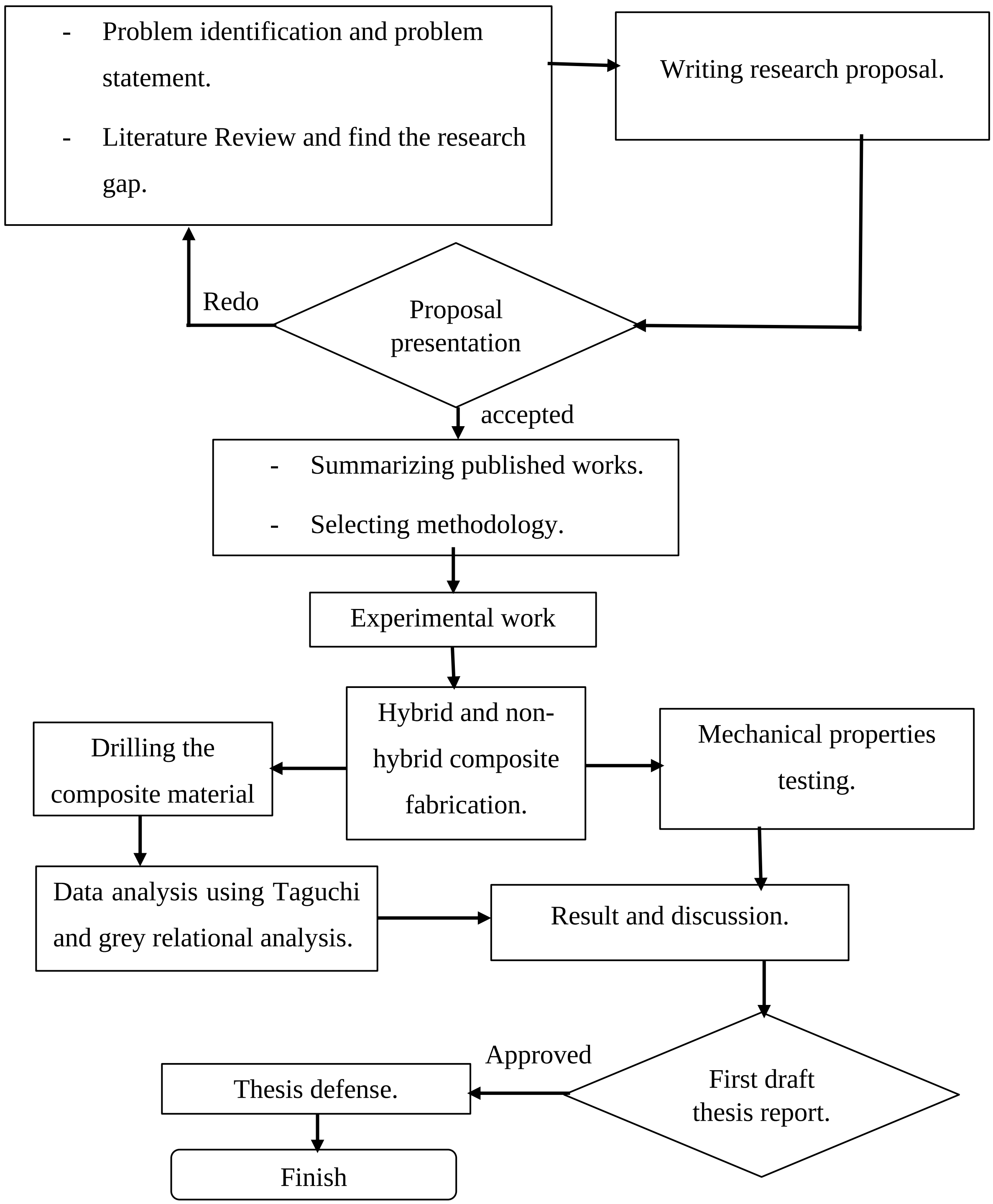

Figure 3.8: Flow chart for the methodological approach and progressive steps

CHAPTER FOUR

RESULTS AND DISCUSSIONS

4.1 Introduction

In this analysis part, the result of the experimental work of the study has been discussed in detail in different sections and sub-sections. To obtain the properties of the fabricated composite, four different layer samples of fiber and matrix were prepared. From each of the samples, three test specimens were obtained and subjected to impact, hardness, flexural, and tensile tests to analyze the mechanical property of the composite. The drilling response of the composite such as delamination, circularity error, and surface roughness evaluation was very important for many fundamental problems such as friction, contact deformation, heat and electric current conduction, tightness of contact joints, and positional accuracy. The result was analyzed as a single response characteristic for (delamination, roundness (circularity) error, and surface roughness) using Taguchi's S/N ratio and as multi-response characteristics using Grey relational analysis. The study also contains chip analysis and hole morphology, of the prepared FRP composites depending on many factors (speed, drill diameter, feed rate, and stacking sequences) for a given workpiece set-up.

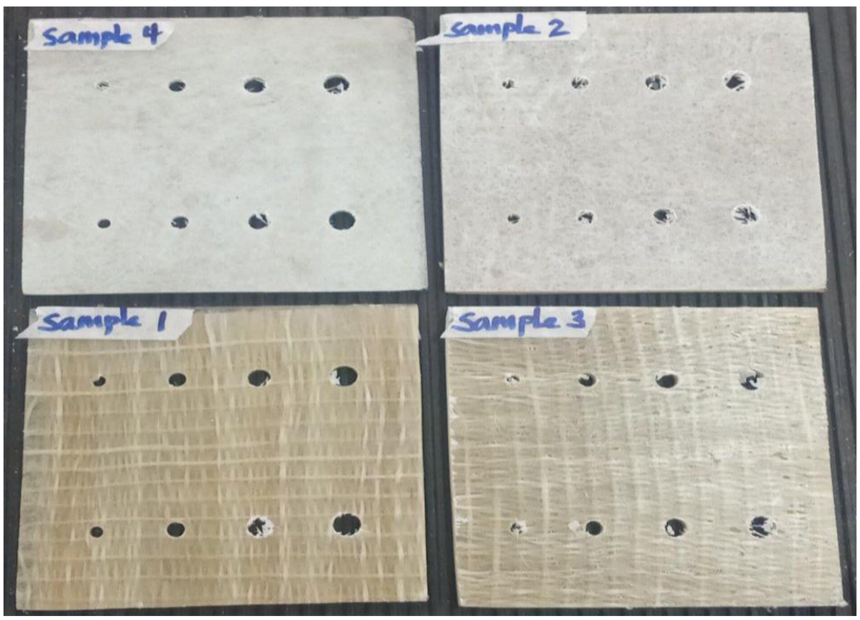

Figure 4.1: Machined composite specimens

4.2 Analysis of Mechanical Properties

In general, the properties of composites were determined by various parameters such as properties of fiber and resin, fiber content, length, the orientation of fiber, layer arrangement, and interfacial adhesion between the matrix and fiber. Therefore, fiber arrangement has more influence on mechanical properties and was taken as the major factor in this investigation. (Manickam Ramesh et al., 2016). Mechanical properties of the developed fiber composite were necessary to elaborate on the interfacial bonding strength, layer arrangement between fibers, and the matrix of composite samples.

4.2.1 Impact Test

Impact properties provide information about the energy absorbed by a material during fracture. The Charpy impact test was used to determine the impact strength of the fabricated composites. V-notched specimens with 1.25 mm depth were tested, and the results are presented in Figure 4.2.

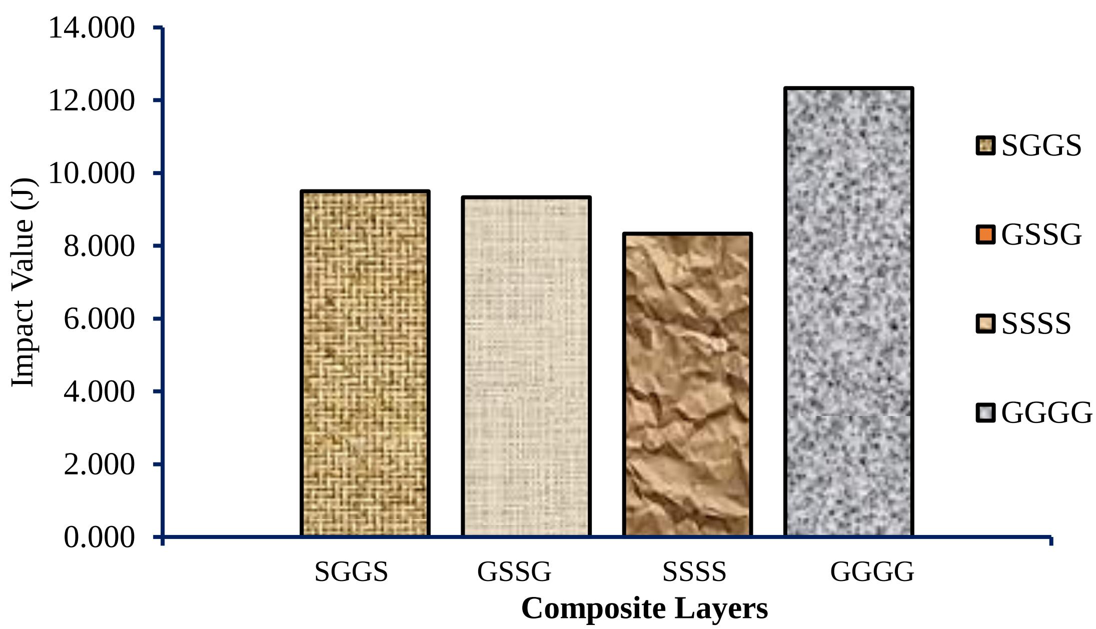

Figure 4.2: Impact value of sisal/glass FRP composites

Figure 4.2. Showed the graph of the impact strength defined by the Charpy impact test in this experiment showed that the sisal composite has an impact strength of 8.333J, whereas the impact strength of glass was 12.333J which was very high. The comparison of two glass/sisal composites showed that the hybrid composites with outer layers made of sisal 9.50J have better mechanical and impact absorption than those with outer glass layers having an impact value of 9.333J that was due to the interlaminar effect of glass to sisal. These results are induced by the mechanical properties of fibers and the fiber-matrix adhesion in a composite. Regarding the impact properties of hybrid glass/sisal composites, the stacking sequence significantly affects the results. Particularly, sisal composites show a dual-natured failure mode, consisting of fiber breakage accompanied by a fiber pullout from the matrix and a local fiber debonding from the matrix. Both of these failure modes promote the dissipation of energy during impact testing. However, due to the low fiber-matrix adhesion and low mechanical properties of natural fibers, the overall energy absorption was low. On the other hand, glass composites possess several failure modes, whereas two primary failure modes are fiber debonding and fiber breakage. Since the fiber-matrix adhesion in glass composites was better than in sisal fiber composites, a greater energy dissipation takes place during the fiber-debonding event. Similarly, due to the higher mechanical properties and directions of glass fibers which are random, more energy was required to break a glass fiber than a sisal fiber of 0°/90° fiber orientation. The results follow a similar pattern to the results published by other researchers (Margabandu & Subramaniam, 2020).

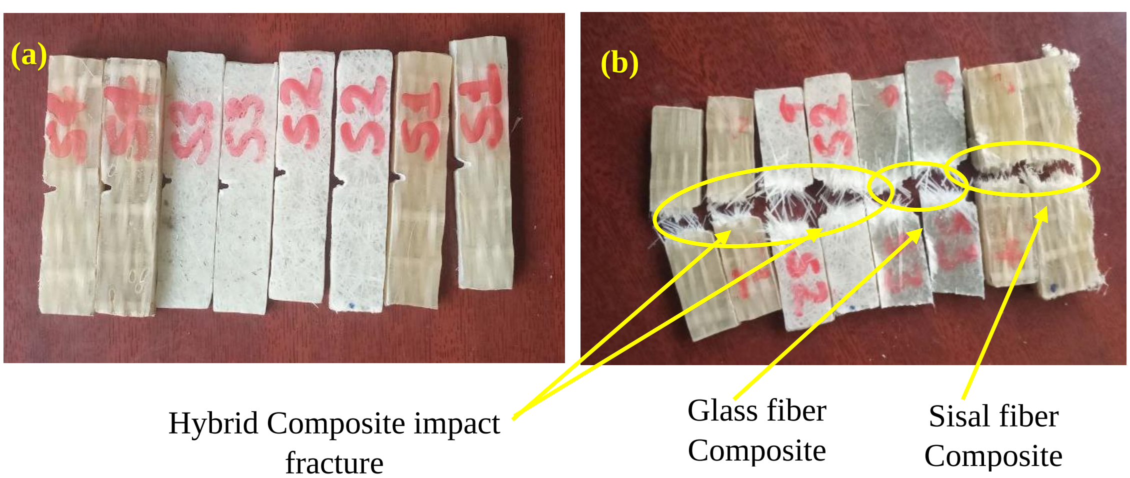

Figure 4.3: Impact (a) Prepared sample with v notches (b) Fracture of composites

The fractured zone of selected impact specimens of the non-hybrid and hybrid sisal-glass reinforced polyester composites was depicted in the fracture analysis of the impact specimens in Figure 4.3 (b). The fracture was quite localized for all composites; hence the specimen showed no signs of damage in the regions outside of the crack. The glass fiber composite displayed a complete fracture and full specimen separation.

4.2.2 Hardness Test

Hardness tests determined the resistance of the composite to deformation caused by low-impact forces such as indentations.

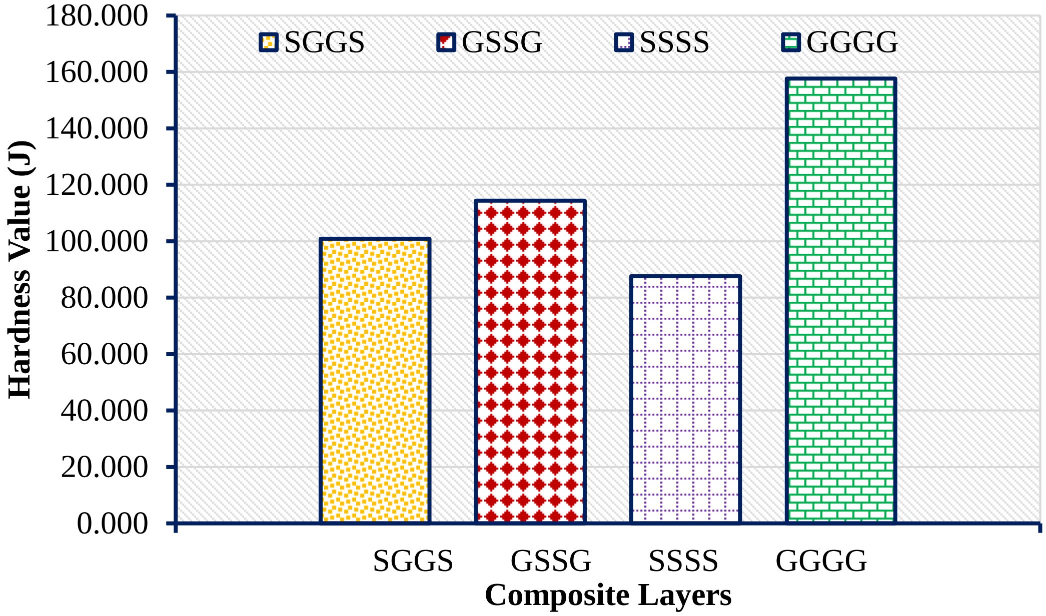

Figure 4.4: Hardness value sisal/glass FRP composites

Figure 4.4. Show the graph of the impact resistance and impact strength of glass/sisal fiber-reinforced hybrid composites. From the result, the pure sisal (SSSS) has a low hardness number (87.567HV). The hardness number increased due to the introduction of synthetic glass fiber within the composite. The sisal-glass-glass-sisal (SGGS) and glass-sisal-sisal-glass (GSSG) hybrids are fabricated from the stacking sequences of fiber but the hardness number of GSSG (114.367HV) was lower than SGGS (100.867HV). The GGGG has a higher hardness number (157.633HV). From these values, we observe that the inter bonding of sisal fibers reinforced polyester composite was low due to this composite's higher brittleness nature than the natural

fiber. The inter bonding of glass fibers reinforced with polyester composite was higher due to the synthetic glass fiber having a good surface property which increases inter bonding of the fiber with the polyester material. From this, we conclude that the hardness number of hybrid composite increases or decreases by layer arrangement difference between natural and synthetic fibers.

4.2.3 Flexural Strength Test

A flexural test was conducted to determine the material's ability to withstand bending forces by measuring the flexural strength and flexural modulus of the specimen for the applied load. In the three-point bending test, the maximum load was applied in the middle of a freely supported beam specimen and the average values of the flexural test results of three samples were tabulated. These results are shown in Figure 4.5.

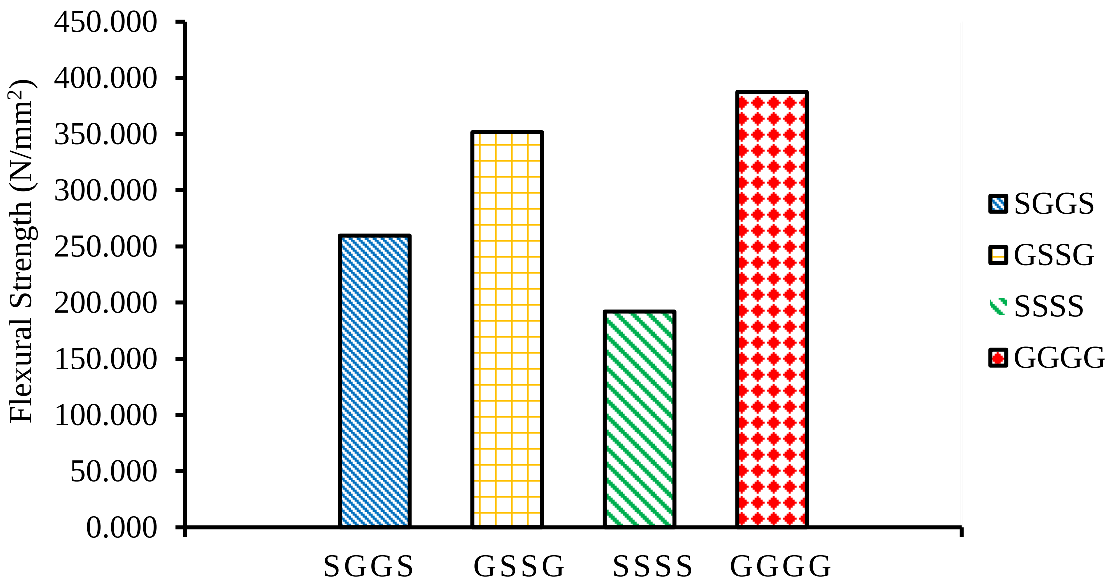

Figure 4.5: Flexural strength test of sisal/glass fiber reinforced polyester composites

The bending properties of glass-sisal/polyester composites show dependency on the weaving art and stacking sequences. The result obtained was that the use of glass layers at outer layers results in flexural strength and maximum testing force of 351.76MPa and 1023.33N, respectively, whereas the use of the same glass layer at inner layers results in 259.683MPa and 1023.333N, respectively. The hybrid composites result in a closer bending modulus in comparison with non-hybrid glass composites which were 387.557MPa and 1536N are significantly higher than the bending modulus of non-hybrid sisal composites with a flexural strength of 192.040MPa and 756N. Pure glass has the highest flexural strength than pure sisal FRP composites. By using the glass fiber as the outer layer and arrangement stacking sequence, the bending strength of the hybrids would give the best performance. Bending properties are significantly influenced by the stacking sequence of the hybrid composites. The reason for this was that during the bending, the testing specimen were subjected to different loads at the top and bottom and in the middle, namely, compression, tension, and shear loading. Refaai et al., (2022) also mentioned that the outer layer of the hybrid composite laminates played an important role as the main load-carrying member. It controlled the bending strength and stiffness of the composites.

Figure 4.6: (a) Prepared samples for flexural strength test (b) Fractured flexural samples

Using Figure 4.6 (b). None of the specimens exhibited a fully ruptured state. Additionally, it was discovered that the fracture was quite localized, meaning that no damage was found in areas far from the fracture. Since the glass fiber reinforced composite displayed similar behavior, this shows that the composites performed well under flexural loading and that the hybridization procedure has no impact on the material's fracture behavior.

4.2.4 Tensile Test

Composite specimens were tested for tensile characteristics using tensile strength. Different layering sequences of sisal-glass hybrid and non-hybrid composite materials have been put to the test till the samples fail. To illustrate the load–extension relationship for various stacking schemes, the hybrid composites in Figure 4.7. are shown. They were utilized to determine the composite's ultimate tensile strength and modulus. The point of eccentricity from the span reveals the failure start in glass layers, and all curves exhibit nonlinear behavior. Sample GGGG (Glass/glass/glass/glass) has a somewhat higher tensile strength than the other sample composites. GGGG–polyester of (Glass/glass/glass/glass) composites has a higher tensile strength of (132.7MPa), and the tensile strength of the SSSS (Sisal/sisal/sisal/sisal)–polyester composite has a lower (112 MPa) than that of SGGS (Sisal/glass/glass/sisal)-polyester hybrid composites with the tensile strength of (105.1MPa), and GSSG (Glass/sisal/sisal/glass)-polyester hybrid composites having a tensile strength of (99.6MPa) which shows better tensile strength than natural sisal fiber reinforced composite. As can be seen from the data, hybridizing sisal fiber with glass fiber improved the tensile strength of the sisal fiber composites, resulting in higher tensile strength. The mechanical properties became higher when the high-strength material was used in the outer plie’s specimen due to the better load transfer from the weak sisal fabric and consequently, the crack arrest was improved. In comparison to the sisal fiber reinforced composite, the tensile strength of glass and sisal-glass hybrid composites with two different stacking sequences improved the properties. Higher lignin content weakens the interfacial bond between the fiber and the polymer components, resulting in a weak composite. As a result, most researchers employed fiber treatment to lower lignin concentration to strengthen the inter-facial connection and increase the composite’s mechanical properties (Bekele et al., 2022). Alkaline treatment increases fiber surface adhesion properties by eliminating both natural and manufactured contaminants from the fibers, resulting in better fiber matrix interaction and better fiber integration(Refaai et al., 2022).

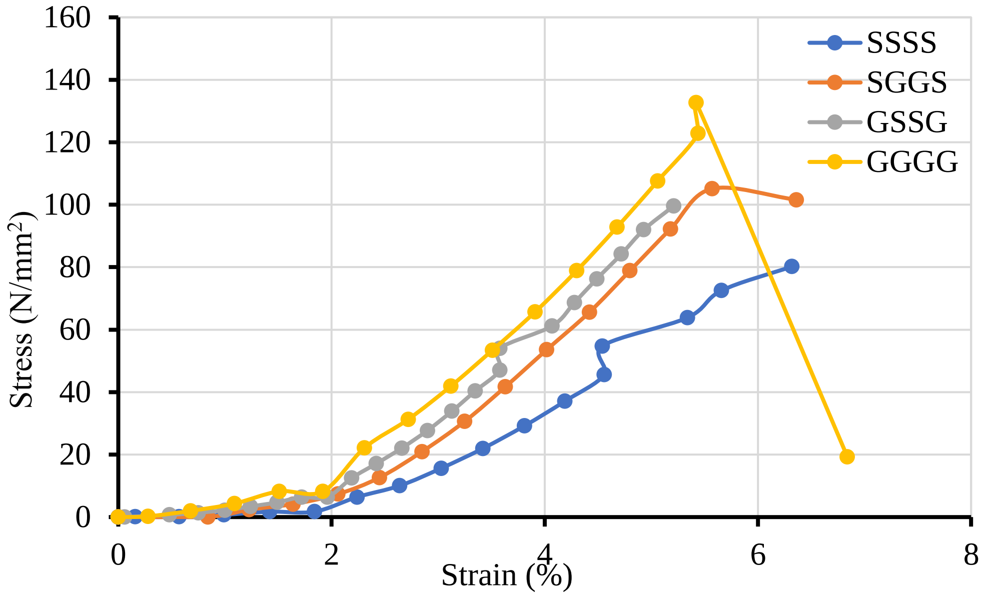

Figure 4.7: Stress vs strain curve for sisal/glass composites

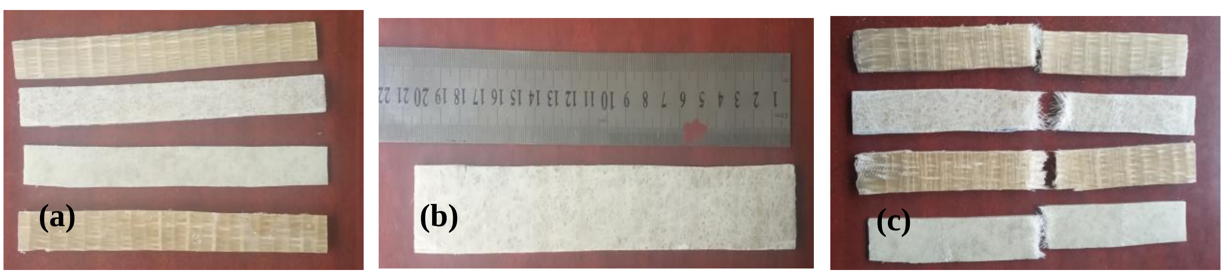

Figure 4.8: (a) Prepared samples (b) Sample dimension (c) Fractured samples of tensile test

Fracture analysis of the tensile specimens. Figure 4.8 (c). showed the fracture region of tensile specimens of the hybrid composites. The fracture was quite localized for all composites (hybrid and non-hybrid), which means the specimen did not present evidence of damage in the areas distant from the fracture. The pure glass and sisal fiber composite presented a complete fracture with a total separation of the specimen. On the other hand, the specimens of the hybrid composites maintain partial ligament after the fracture.

That the synthetic layers located at the outer surfaces of the laminate improved the mechanical properties of the composite. This showed that the hybridization of the laminate composite produced a novel material with intermediate tensile properties between the glass and sisal woven fibers used alone. Moreover, the mechanical behavior of the natural fiber-reinforced composites was lower due to the different nature of the hydrophobic matrix and the hydrophilic fibers, resulting in the reduction of adhesion and compatibility of the matrix-fiber interaction. To improve the tensile properties of natural fiber composites, hybridization with the glass fiber technique should be used.

Generally, when we consider the mechanical properties of hybrid and non-hybrid composites, the properties of woven sisal fiber and the hybrid sisal/glass fiber composite properties are closer to that of other non-hybrid glass fiber reinforced composites.

4.3 Investigation of Drilling Characteristics

4.3.1 Analysis of Entry and Exit Delamination

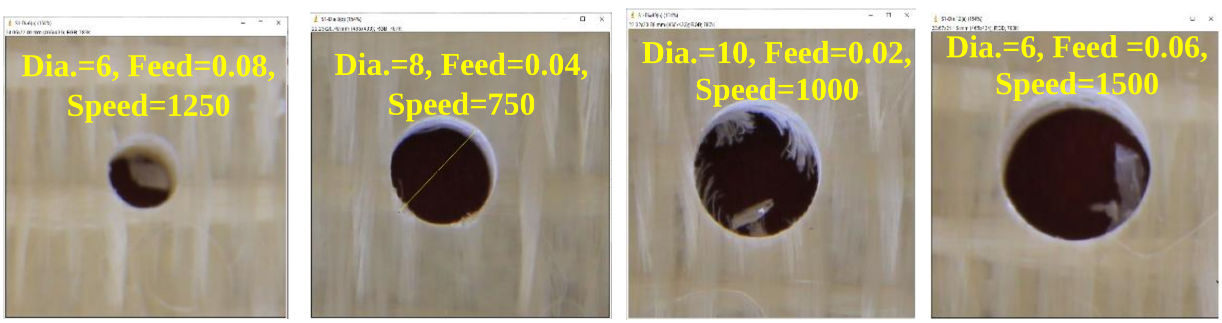

(a) Entry Delamination

(b) Exit Delamination

Figure 4.9: Entry and exit delamination of sisal-glass-glass sisal (SGGS) FRPC layer.

(a) Entry Delamination

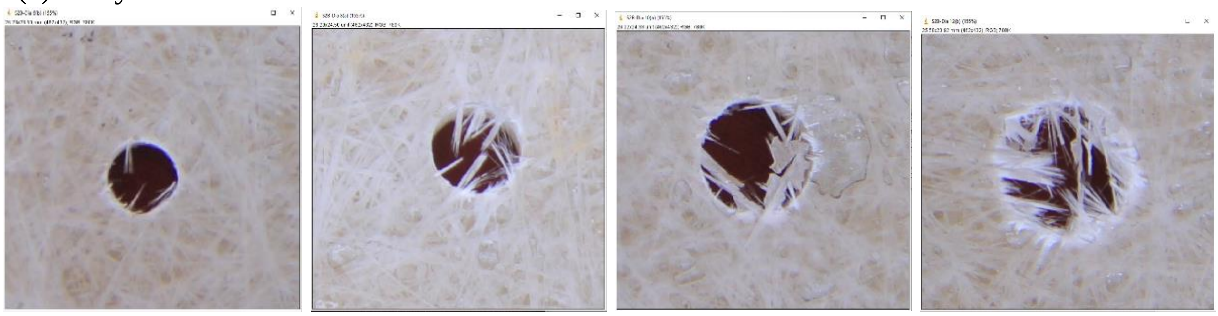

(b) Exit Delamination

Figure 4.10: Entry and exit delamination of glass-sisal-sisal glass (GSSG) FRPC layer

(a) Entry Delamination

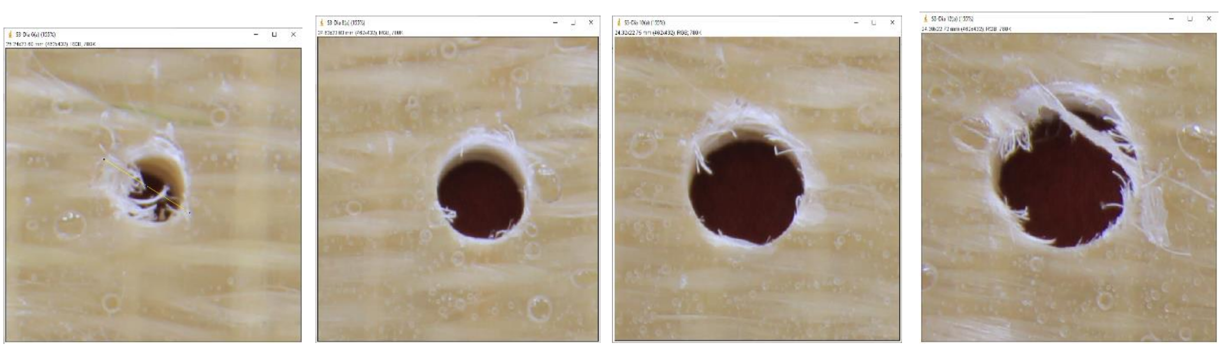

(b) Exit Delamination

Figure 4.11: Entry and exit delamination of sisal-sisal-sisal-sisal (SSSS) FRPC layer

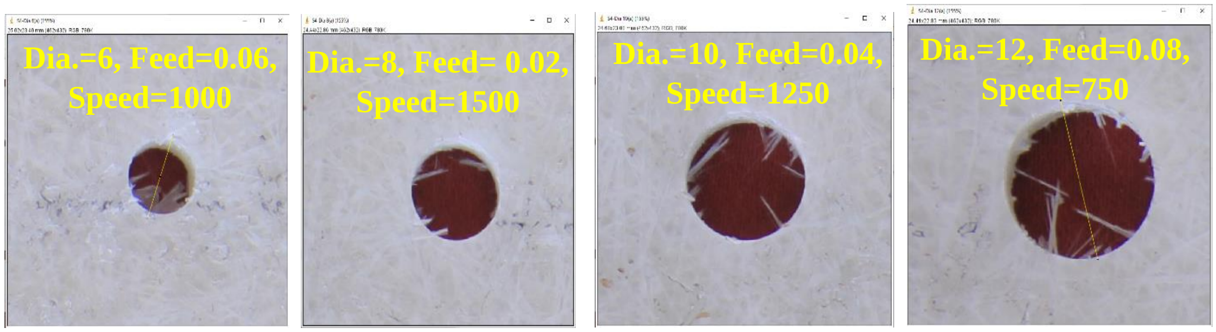

(a) Entry Delamination

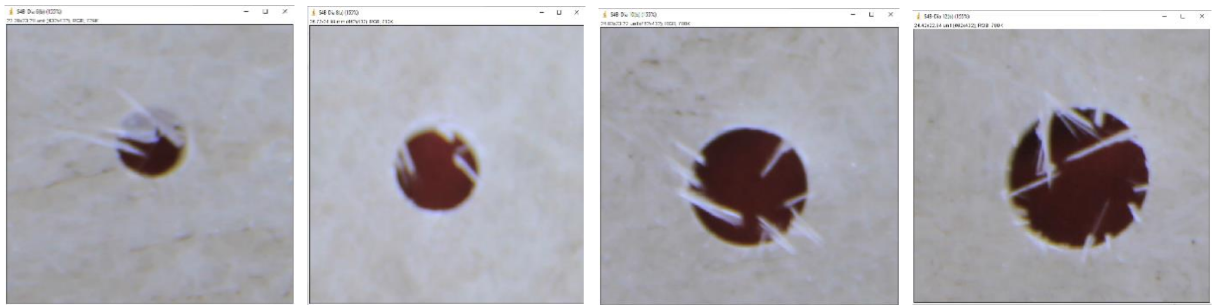
(b) Exit Delamination

Figure 4.12: Entry and exit delamination of glass-glass-glass-glass (GGGG) FRPC layer

During the drilling of the fiber-reinforced composites, delamination was observed both at the entry and exit sides of the specimens (sample) drilled. From the experimental result delamination at the exit side of the hole was more severe than that of entry side delamination, which was evident in Figures 4.9, 4.10, 4.11, and 4.12. It was observed that the SGGS composite offers a better performance regarding entry and exit delamination.

4.3.1.1 Effect of Cutting Parameters Entry Delamination Factor at Entry Side

A. Effect of Speed on entry delamination

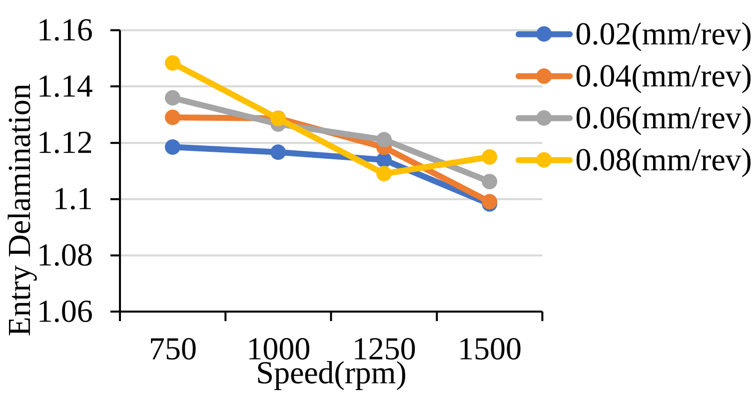

Figure 4.13: Effect of speed on entry delamination at a constant feed rate

Figure 4.13. Showed the variation of entry delamination against the different cutting speeds for constant feed rates. Generally, the entry delamination of the hybrid and no-hybrid sisal/glass FRP decrease as the speed increases. In this experiment, the entry delamination gradually reduces when the spindle speed was 1500rpm. Then, the entry delamination value gradually reduces when the drilling speed decreases to 1250rpm and 1000rpm. Then finally it attains a minimum as the speed decreases to its minimum i.e., 750rpm.

It observed that the entry delamination can be reduced to a larger extent by machining the composite sample at a feed rate of 0.02mm/rev and cutting speed of 1500rpm. The entry delamination was reduced with an increase in drilling speed.

4.3.1.2 Effect of Feed Rate on Entry Delamination

Figure 4.14 shows the relationship between average entry delamination and feed rate. As the feed rate increase, the entry delamination increases for constant drilling speeds. shows the variation of entry delamination and feeds for a drilling speed of 750rpm, 1000rpm, 1250rpm, and 1500rpm which reveals that as the feed rate increases, there was almost a large increase in entry delamination for all samples prepared.

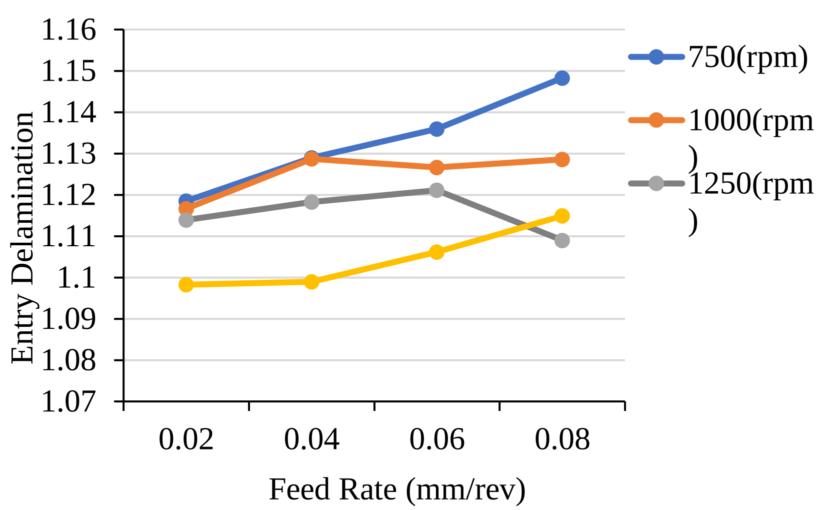

Figure 4.14: Effect of feed rate on entry delamination at a constant speed

Moreover, entry delamination was high for the 750rpm drilling speed, 0.08mm/rev feed rate, and low for 1500rpm speed, 0.02mm/rev feed rate which reveals the fact that the entry delamination increased along with an increase in feed rate and vice versa.

4.3.1.3 Effect of Drill diameter on Entry Delamination

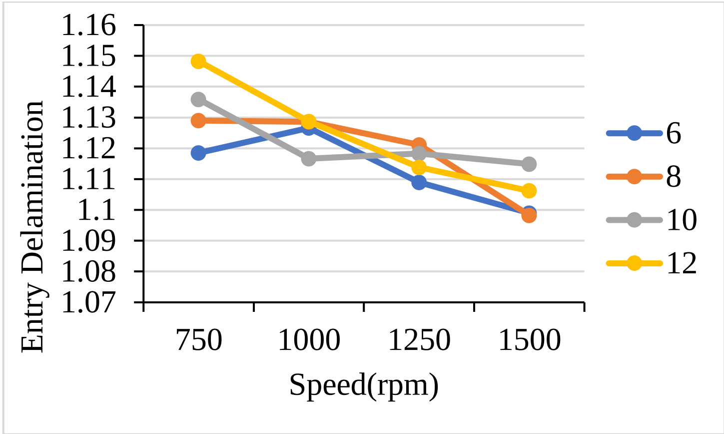

Figure 4.15: Effect of speed on entry delamination at constant diameter

Figure 4.15. shows the variation of entry delamination against the different drill diameters for different speeds. Generally, the entry delamination of the hybrid and no-hybrid sisal/glass FRP decreases as the drilling diameter decreases. In this experiment, the entry delamination gradually reduces when the drill diameter was 6mm. Then, the entry delamination value gradually increases when the drill bit diameter increases to 8mm, 10mm. Then finally it attains maximum as the drilling diameter increase to its maximum i.e., 12mm.

It observed that the entry delamination can be reduced to a larger extent by machining the composite sample at a drill diameter of 6mm and cutting speed of 1500rpm. The entry delamination was reduced with a decrease in drill diameter.

4.3.1.4 Effect of material layer arrangement on Entry Delamination

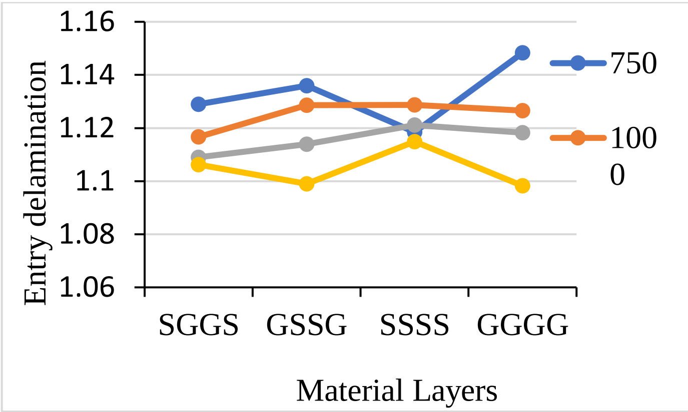

Figure 4.16: Effect of materials layer on entry delamination at a constant speed

Figure 4.16. shows the relationship between average entry delamination and composite material layers. The entry delamination increases with a decrease in drilling speed. Figure 4.16. shows the variation of entry delamination and different materials layer arrangements for constant drilling speeds of 750rpm, 1000rpm, 1250rpm, and 1500rpm which reveals that as the material layer varies, there was almost a large increase in entry delamination for all samples prepared. Moreover, entry delamination was high for the 750rpm, 1000, 1250, and 1500 drilling speeds respectively. Stacking sequences reveals the fact that the entry delamination shows different along with speed.

Interaction effect of the process parameter on the entry side of the composite

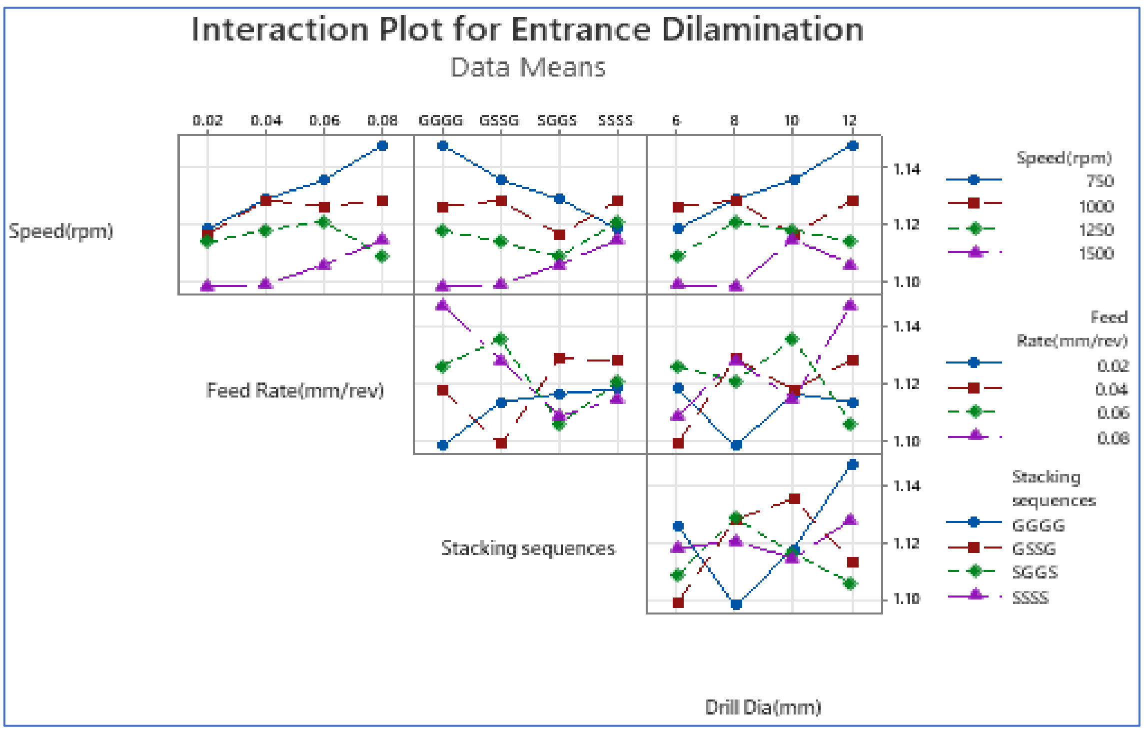

Figure 4.17: Interaction plot for entry-side delamination

Figure 4.17. The interaction plot shows the variation of entry delamination factor values with the operating parameters (cutting speed, feed rate, layering arrangement, and drill diameter) with each other. The entry delamination factor increases with an increased feed rate. The drilling process for sisal/glass/glass/sisal (SGGS)-polyester composite results in a considerably smaller delamination factor compared with the drilling process of other composites at a constant feed rate. This phenomenon should be related to the fracture response of sisal and glass fibers. This

result showed that in addition to the role of selected cutting parameters, stacking sequences (layer arrangement) of materials themselves determine the entry delamination factor. The peel-up action on the layer of materials from laminates as chips has been performed with the corresponding rake angle of the drill. The delamination at entry increases because of increased feed rate, drill diameter during drilling, and decrease in cutting speed. A similar result was shown by (Ramesh et al., 2014)

It's observed that glass/glass/glass/glass (GGGG) (4)-polyester composite exhibited more entry delamination factors than sisal polyester and both hybrid composites. Because sisal fiber has more elongation before cutting than glass fibers as mentioned in Table 3.2. Which results in the resistivity of the natural fiber.

Figure 4.17. It's seen that increase in feed rate and decreasing speed increased the entry delamination. While decreasing the feed rate and increasing the speed reduced the entry delamination in all composite types. The stacking sequences of GGGG fiber reinforced composite show the highest entry delamination when the cutting speed was low which that 750rpm and the least entry delamination was shown when the speed was 1500rpm, also seen that the entry delamination was low on natural fiber composite with the stacking sequences of SSSS this was due to the lower hardness, elongation, and brittleness nature of the natural fiber than the glass fiber.

This characteristic was due to the variation in the cutting temperature. In other words, the cutting temperature produced at lower spindle speed was minimum, and the delamination due to this condition formed because of the shearing stress induced while drilling. At a high feed rate, the composite surface exhibited high stress due to interference from the tool. Therefore, when the tool started penetrating the composite surface, the material surface near the tool edge developed higher stress against penetration. This created high delamination at the entry side of the tool. At a high feed rate, the tool was also worn due to the formation of buildup edges (Jayabal & Natarajan, 2010). That matched the rise in the entry delamination factor exactly. Fast temperatures generated at high speeds, however, caused the formed accumulation edges to disappear. Additionally, the matrix softened at high speeds as a result of the elevated temperature, which aided in quick surface cutting and chip removal without any delamination. It was acceptable to argue that the greater spindle speed and lower feed rate were suited for generating holes with a lower entry delamination factor. The study concluded that the matrix and fiber characteristics affected quality. Therefore, by regulating the fiber and matrix arrangement and enhancing interfacial bonding, delamination can be decreased in fiber composites. This displays the same outcome as (Shanmugam et al., 2021).

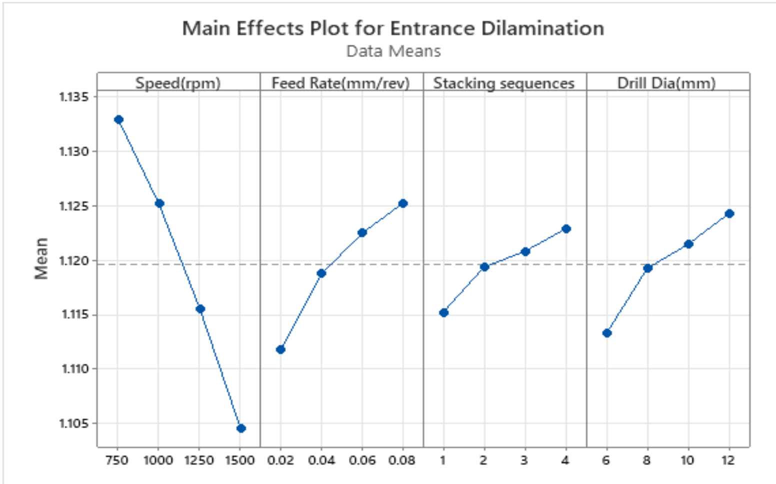

Figure 4.18: Main effect plot for entry delamination

4.3.1.2 Optimization of process parameters for entry delamination

Signal-to-noise ratios(S/N) for entry delamination

Taguchi signal-to-noise ratios(S/N) are served as the objective functions for the optimization of data analysis and prediction of optimum results. In the Taguchi method, entry delamination was studied with the help of the signal-to-noise(S/N) ratio. To measure and characterize the entry/inlet/ delamination, the statical formula for the smaller-the-better has been used. The ratio of signal-noise ratio can be given by Equation 3.16.

Table 4.1: Response table for signal-to-noise ratios for entry delamination

Level	Speed(rpm)	Feed Rate(mm/rev)	Stacking sequences	Drill Dia. (mm)
1	-1.0836	-0.9205	-0.9469	-0.9317
2	-1.0241	-0.9741	-0.9787	-0.9779
3	-0.9499	-1.0030	-0.9905	-0.9953
4	-0.8638	-1.0238	-1.0054	-1.0165
Delta	0.2198	0.1033	0.0585	0.0849
Rank	**1**	**2**	**4**	**3**

Table 4.1. shows the influence of spindle speed, feed rate, stacking sequences, and drill diameter on the entry delamination factor of glass-sisal with different fiber-reinforced composites drilled with different diameter HSS drill bits. It was found that the cutting speed and feed rate made the largest contribution to the entry delamination factor (F_d) assigned as the rank of first and second with a delta value which represents the predominant factor affecting entry delamination with the value of 0.2198 and 0.1033 while drill diameter and stacking sequences affect in third and fourth order with the delta value of 0.0849 and 0.0585. It was observed that there was a decrease in values of the entry delamination factor with an increase in cutting speed. The entry delamination was found to increase with the feed rate increase. Further, it was noticed that the entry delamination damage of the drilled hole obtained with the increased diameter HSS drill was higher than the smaller drill for all the process parameters in the considered composite.

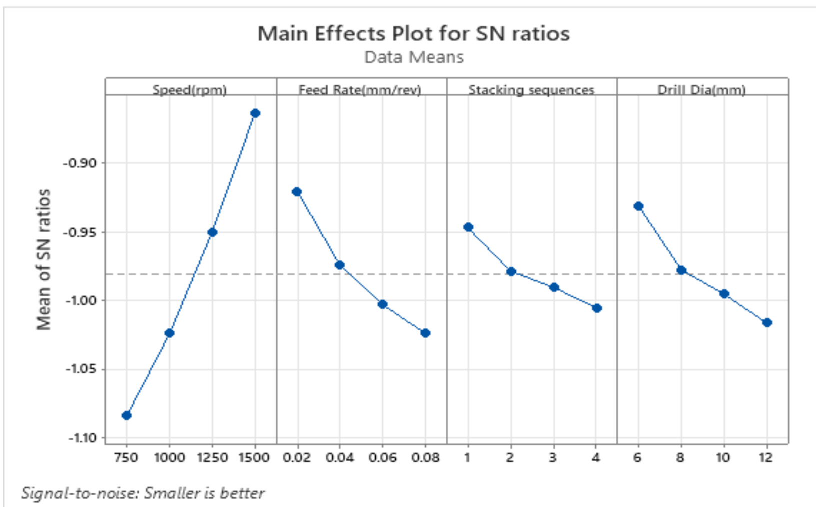

Where stacking sequences of SGGS=1, GSSG=2, SSSS=3, GGGG=4

Figure 4.19: Signal-to-noise ratio of entry delamination

Figure 4.19. Shows the optimal parameter combination of process parameters for entry delamination (the smaller the better for entry delamination). Since the S/N ratio used for this study was lower the better and lowest S/N ratio was selected. In the S/N ratio, the numerical value of the maximum point in each graph shows the best optimum combination of the factors and the above figure shows the maximum value for speed at level 4, feed rate at level 1, stacking sequences of level 1, and drill diameter of level 1 are 1500rpm, 0.02mm/rev, SGGS, and 6mm respectively (i.e.: **A4B1C1D1**) was selected.

Analysis of variance of entry delamination factor

Analysis of variance (ANOVA) was used to identify the most significant factors which affect the entry delamination and the percentage contribution of each factor. Where DF = degree of freedom, Adj SS = sum of squares, Adj MS = Mean Sum of squares, and F = fisher ratio generated by Minitab 20 software.

Table 4.2. shows the calculated ANOVA results of the entry delamination factor. The results show that the entry delamination was mostly affected by the cutting speed. The analysis shows the significance of all parameters in affecting entry delamination. F-values of spindle speed, feed rate, drill diameter, and stacking sequences were 215.68, 46.33, 29.87, and 14.33, respectively, and their corresponding P-values were 0.000, 0.000, 0.000, and 0.003. F-value and P-value show that the cutting speed contributed more to affecting the entry delamination factor. Thus, the 67.99% contribution of the cutting speed was the primary factor in deciding the inlet/entry/ delamination factor, followed by the feed rate of 14.60%, drill diameter of 9.43%, and stacking sequences of 4.52%, i.e., at a level of confidence of 95%.

Table 4.2: Analysis of variance results of entry delamination

Source	**DF**	**Adj SS**	**Adj MS**	**F-Value**	**P-Value**	**% Contribution**
Regression	4	0.002540	0.000635	76.55	0.000	
Speed(rpm)	1	0.001789	0.001789	215.68	0.000	67.99
Feed Rate(mm/rev)	1	0.000384	0.000384	46.33	0.000	14.60
Stacking sequences	1	0.000119	0.000119	14.33	0.003	4.52
Drill Dia. (mm)	1	0.000248	0.000248	29.87	0.000	9.43
Error	11	0.000091	0.000008			3.46
Total	15	0.002631				100
S=0.0028802 R-sq=96.53% R-sq(adj)= 95.27% R-sq(pred)= 91.86%						

DF-degrees of freedom; SS-sum of squares; MS-mean squares; F - and P-values.

By comparing the F-values with the tabulated ones (critical F-values), the significance of the factors can be understood. If the obtained F value of the parameter was greater than the tabulated one, then the particular parameter has a significant influence over the response variables. From Table 4.2, the F-value of Speed (215.68) > F0.05,1,15 = 4.54, feed rate (46.33) > 4.54

($F_{0.05,1,15}$), stacking sequence (14.33) > 4.54, and Drill diameter (29.87) > 4.54 Therefore, speed, feed rate, stacking sequence, and drill diameter have a significant influence over entry delamination factor.

The analysis of variance with P values also shows that the P-value of spindle speed, feed rate, stacking sequence, and drill diameter are (P = 0.000 < 0.05), (P = 0.000 < 0.05), (P = 0.003 < 0.05), and (P = 0.000 < 0.05) respectively which show they are significant on affecting entry delamination factor.

Regression Analysis: Entry Delamination versus Speed(rpm), Feed Rate(mm/rev), Stacking sequences, and Drill Dia. (mm).

$$\text{Entrance Delamination} = 1.12923 - 0.000038\, v(rpm) + 0.2192\, f(mm/rev) + 0.002438\, s + 0.001760\, d(mm) \quad (4.1)$$

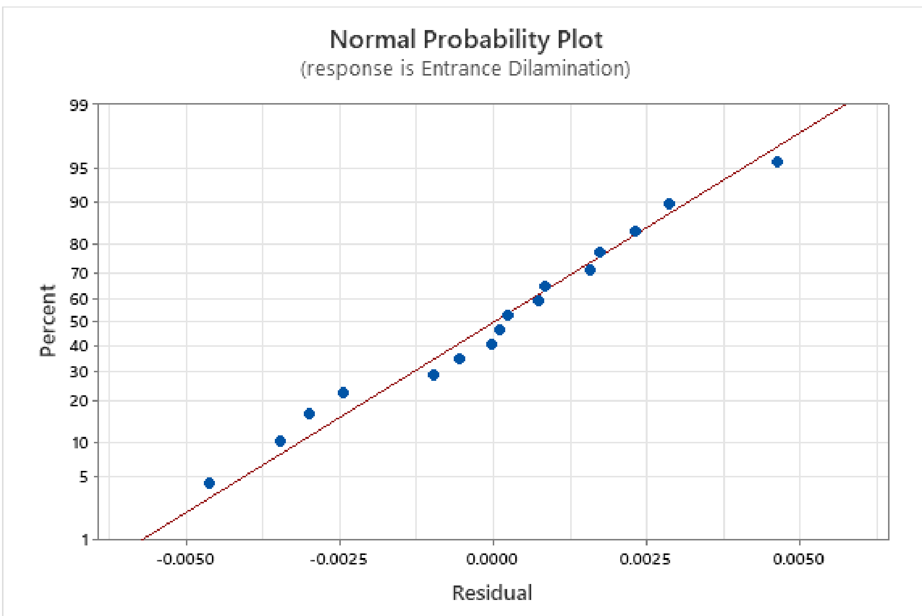

Figure 4.20: The normal probability plot for entry delamination

One of the assumptions in all the statistical models used in the design of experiments was that the experiment error (residuals) was normally distributed and a normal probability plot of effects was used to judge the significance of effects. If all the residuals fall along a straight line drawn, it is inferred that the residuals/errors follow a normal distribution. Figure 4.20. shows the data points are relatively close to the fitted normal distribution line. The results are scattered around the line which shows the minimum error value to be obtained from the experiment.

Determining optimum conditions for entry delamination factor

The optimum prediction condition for the S/N ratio in which, the lower entry delamination results are obtained with the terms set in Table 4.3. As shown in Table 4.1, The selected optimum parameters in this study were a lower feed rate, the highest spindle speed, on sample two which was GSSG layer arrangement, and a smaller drill diameter which was (**A4B1C1D1).**

Table 4.3: The optimum condition for entry delamination result prediction setting

Factors	Levels	Value of level	Rank of affecting	Prediction S/N Ratio	Values Mean
Spindle speed(v)	4	1500rpm	1	-0.753576	1.09037
Feed rate(f)	1	0.02mm/rev	2		
Stacking sequences (s)	1	GSSG	4		
Drill diameter(d)	1	6mm	3		

4.3.2 Delamination factor at Exit Side

4.3.2.1 Effect of process parameters on exit delamination factor

Effect of feed rate on exit delamination

Figure 4.21. shows the relationship between average exit delamination and feed rates. As the feed rate increase, the exit delamination increases for constant drilling speeds. Figure 4.21. shows the variation of exit delamination and feeds for a drilling speed of 750rpm, 1000rpm, 1250rpm, and 1500rpm which reveals that as the feed rate increases, there was almost a large increase in entry delamination for all samples prepared. Moreover, exit delamination was high for the 750rpm drilling speed, 0.08mm/rev feed rate, and low for 1500rpm speed, 0.02mm/rev feed rate which reveals the fact that the exit delamination increased along with an increase in feed rate and vice versa.

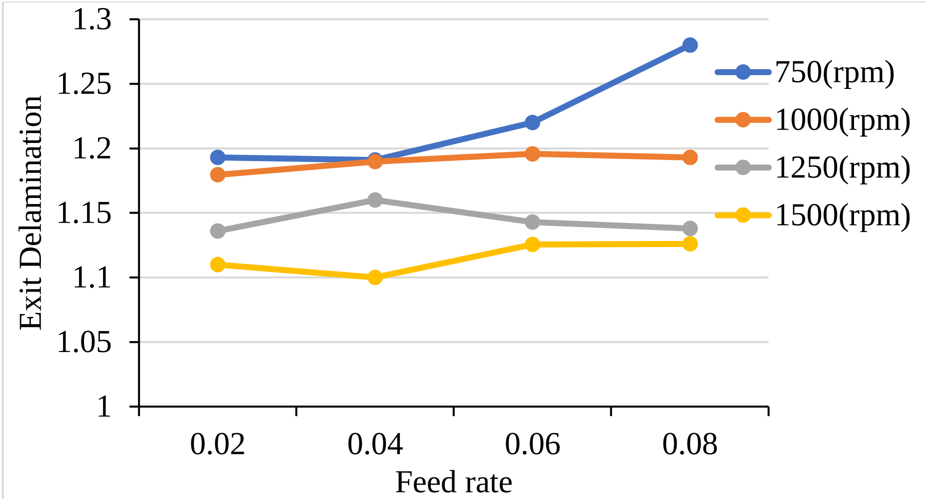

Figure 4.21: Effect of feed rate on exit delamination at a constant speed

Effect of drill diameter on exit delamination

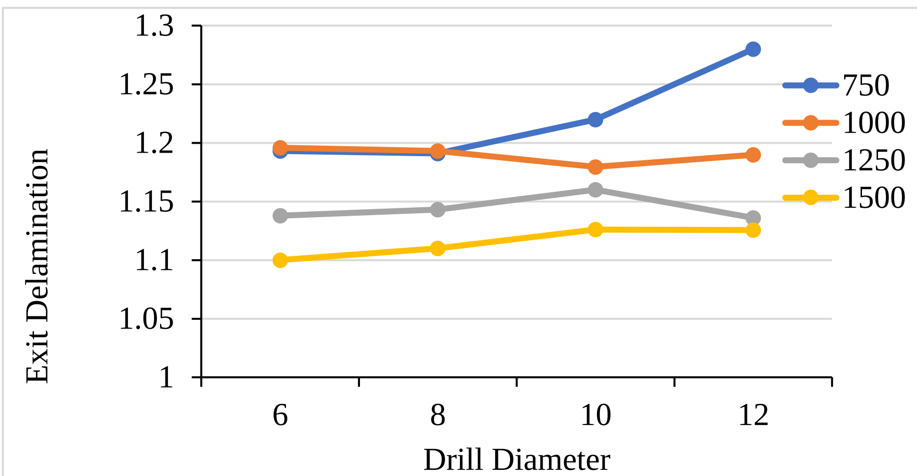

Figure 4.22: Effect of diameter on exit delamination at a constant speed

Figure 4.22 shows the variation of exit delamination against the different drill diameters for constant speeds. Generally, the exit delamination of the hybrid and no-hybrid sisal/glass FRP decreases as the drilling diameter decreases. In this experiment, the exit delamination gradually reduces when the drill diameter was 6mm. Then, the exit delamination value gradually increases when the drill bit diameter increases to 8mm, 10mm. Then finally it attains maximum as the drilling diameter increase to its maximum i.e., 12mm. Also, from Figure 4.22 the influence of speed was that when the speed increased from 750rpm to 1500rpm the exit delamination decreases.

It observed that the exit delamination can be reduced to a larger extent by machining the composite sample at a drill diameter of 6mm and cutting speed of 1500rpm. The exit delamination was reduced with a decrease in drill diameter.

Effect of materials layer arrangement on exit delamination

Figure 4.23 shows the relationship between average exit delamination and composite material layers. The exit delamination increases with a decrease in drilling speed. Figure 4.23 shows the variation of exit delamination and different materials layer arrangements for constant drilling speeds of 750rpm, 1000rpm, 1250rpm, and 1500rpm which reveals that as the material layer varies, there was almost a large increase in entry delamination for all samples prepared. Moreover, exit delamination was high for the 750rpm, 1000, 1250, and 1500 drilling speeds respectively. Stacking sequences reveals the fact that the exit delamination shows different along with speed. Poor exit delamination is seen at a point of 750rpm with glass FRP composite and good quality at 1500rpm with GSSG FRP composite.

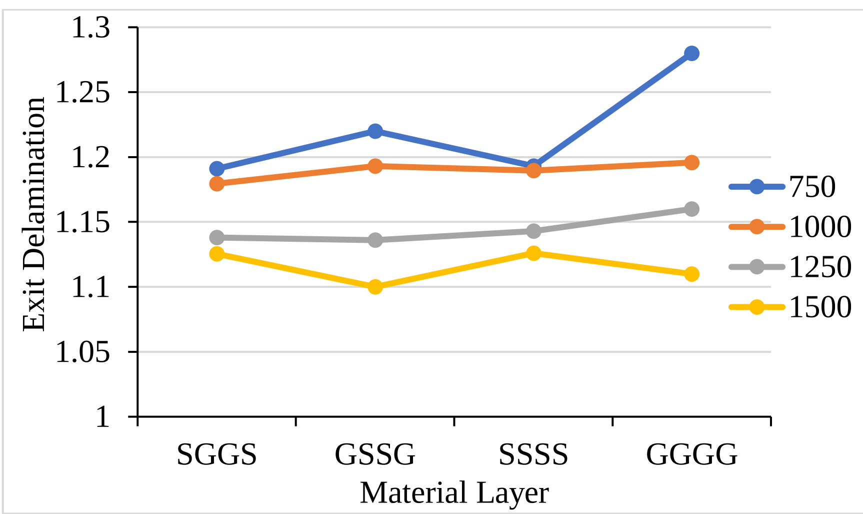

Figure 4.23: Effect of the material layer on exit delamination at a constant speed

While drilling composite laminates, as the drill approaches the exit of the specimen, the number of uncut plies supporting it reduces, and the resistance to bending decreases. At a critical thickness, the bending stress becomes greater than the interlaminar strength between the plies and the laminate at the bottom may get disconnected from its interlaminar bond around the hole. In some areas around the hole, the loading exceeds the interlaminar bond strength and delamination occurs. Delamination occurs before the laminate was fully penetrated by the drill bit (Maleki et al., 2018). This phenomenon was also seen in sisal glass hybrid fiber-reinforced composite the bondage between different fibers has influenced the result.

At the exit, the uncut plies bend elastically due to the compressive force exerted by drills. When the drill approaches the exit, resistance to the bending decreases due to the reduction of pressure on the uncut plies. Next, as bending stress increased, then the inter-laminar strength of plies was weaker, due to this reason, cracks developed around the hole. When the drill point pushes down further, it causes the crack to propagate and the flexural rigidity of plies becomes weaker. As a result, the inter-lamina bonding failure produces pushout delamination.

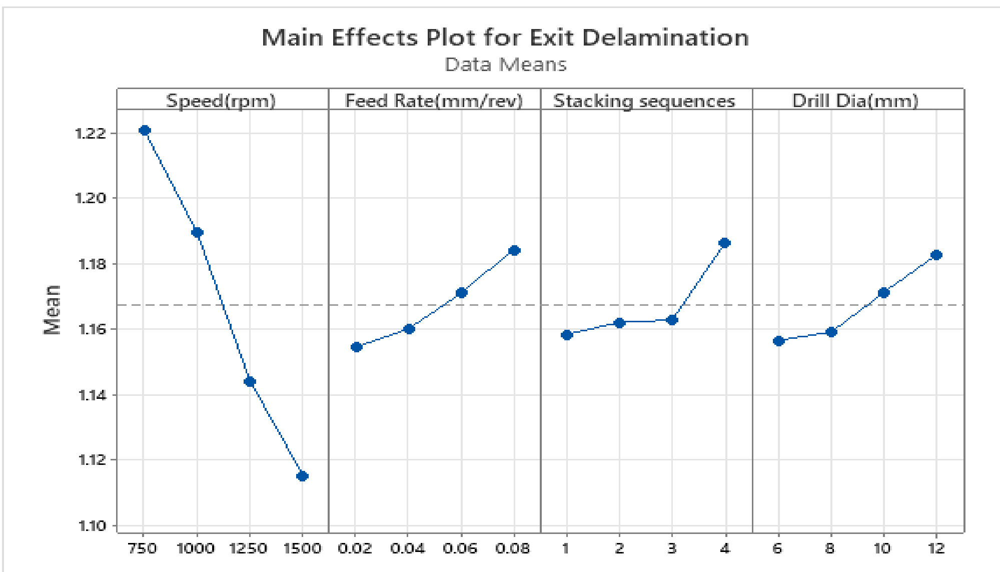

Figure 4.24: Main effect plot for exit delamination factor

Interaction effect of the process parameter on the exit side of the composite

The main effect plot for the delamination factor at the exit was shown in Fig. 4.24 and the interaction plot is in Figure 4.25. It shows that increasing the speed and decreasing the feed rate resulted in a decrease in the delamination factor at the exit side. It also shows that the delamination factor at the exit side was higher for glass polyester composites than sisal polyester and hybrid composites.

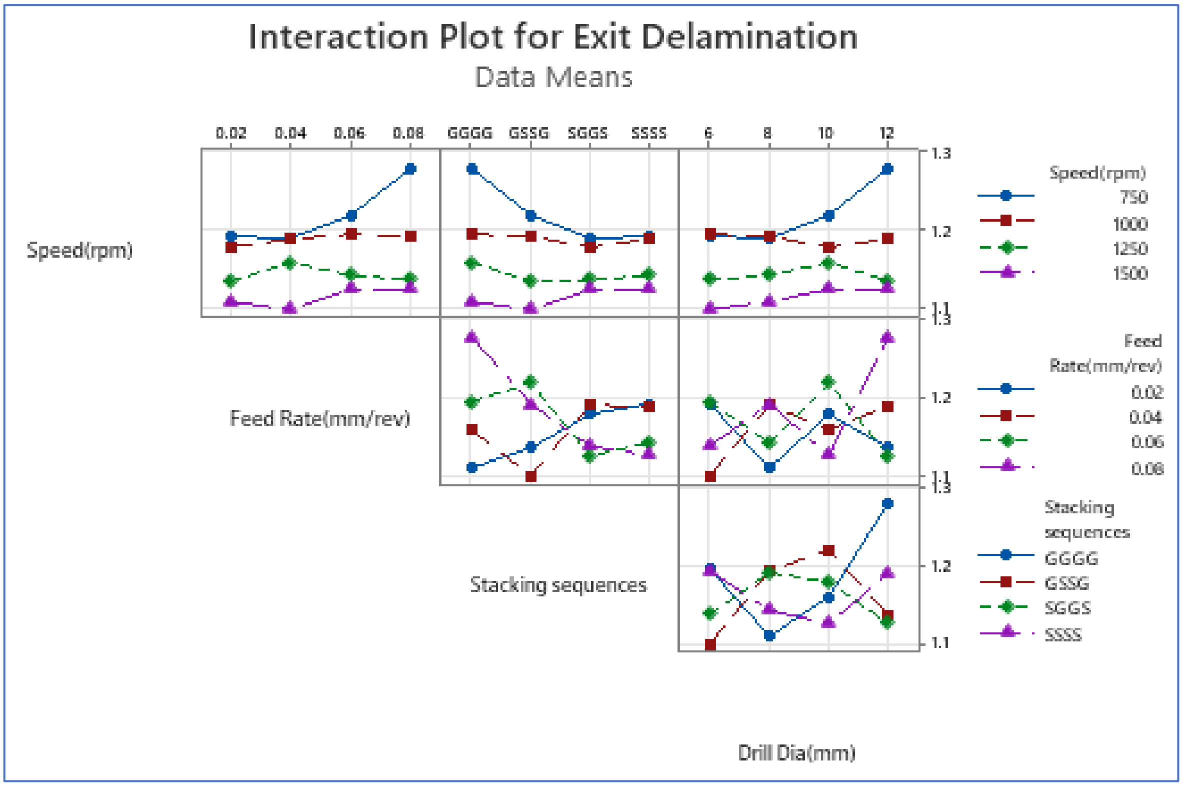

Figure 4.25: Interaction plot for exit delamination

The reason may be the same the sisal fibers have more elongation before cutting than glass fibers. So, it increases the surface roughness and delaminates the layer. Due to this GSSG (2), the composite delamination factor at the exit side was higher than SGGS (1) and sisal polyester composite. Also, the larger drill diameter bit generated a higher delamination factor at the exit compared to the smaller drill bit.

4.3.2.2 Optimization of process parameters for exit delamination

To measure and characterize the exit delamination, the statical formula for the smaller the better has been used. In the case of smaller is the better, the ratio of signal noise ratio can be given by Equation 3.16.

Analysis of the S/N ratio for exit delamination

Moreover, in drilling glass-sisal/polyester composite, the material on the exit side determines the delamination factor. Experimental data support this argument from Figures 4.9, 4.10, 4.11, and 4.12 and (Appendix). When the exit side of GSSG consists of glass/polyester, the delamination factor was extremely larger than that of the exit side consisting of sisal/polyester. All SGGS/polyester, GSSG/polyester, Glass/polyester, and Sisal /polyester composites consist of 4 layers. Given this arrangement, SGGS/polyester composite has a more compact structure and was more rigid than others. Given that SGGS/polyester composite was more resistant due to its being compact and rigid against bending stress during drilling compared with GSSG/polyester, less delamination damage occurs in an exit. The non-woven glass fiber was more exposed to exit delamination.

Table 4.4: Response table for the signal-to-noise ratios for exit delamination

Level	**Speed(rpm)**	**Feed Rate(mm/rev)**	**Stacking sequences**	**Drill Dia. (mm)**
1	-1.7304	-1.2450	-1.2755	-1.2592
2	-1.5072	-1.2860	-1.2987	-1.2794
3	-1.1701	-1.3669	-1.3083	-1.3701
4	-0.9478	-1.4577	-1.4731	-1.4469
Delta	0.7826	0.2127	0.1976	0.1877
Rank	**1**	**2**	**3**	**4**

The delta statistics of the S/N ratio for exit delamination depicted in Table 4.4 shows the ranks of factors affecting responses based on the S/N ratios obtained via the Taguchi orthogonal array. The delta statistics were computed based on the difference between the highest and lowest average value of each factor. The value of delta was assigned the first rank and represents the predominant factor affecting the exit delamination factor. The analysis showed that the cutting speed was assigned as rank 1 with a delta value of 0.7826 signifying that it was the predominant factor that affects the exit delamination factor of glass-sisal composite. The feed rate, stacking sequences, and drill diameter were assigned second (0.2127), third (0.1976), and fourth (0.1877) ranks respectively.

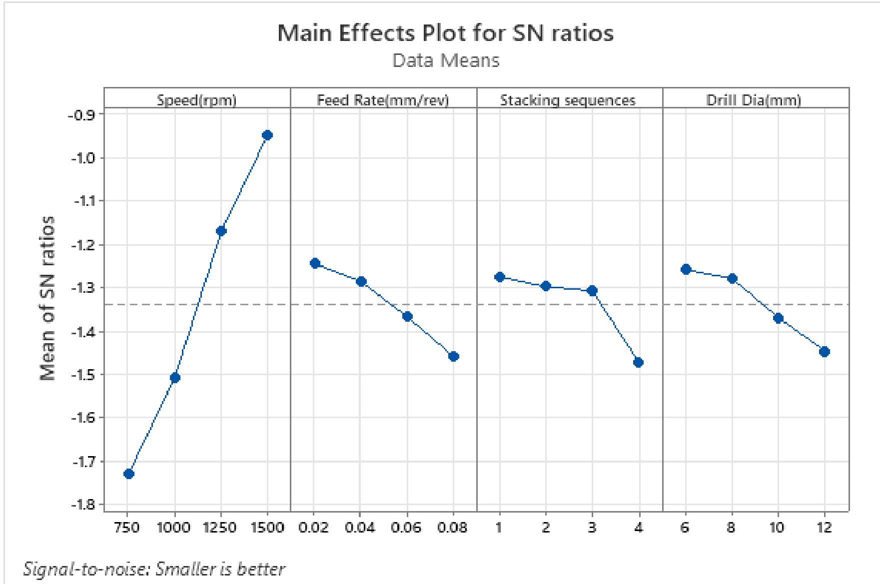

Figure 4.26: Main effect plots for S/N value of exit delamination factors

Fig 4.26 Illustrates the main effect plots for S/N ratios of delamination at exit during the drilling on pure sisal, pure glass, and the hybrid sisal glass fiber composites based on different combinations of input cutting parameters. The main effect plots of the S/N ratio for delamination at the exit pure sisal, pure glass, and the hybrid sisal glass fiber composites show the reduced exit delamination effect while performing the drilling operation with a 6mm diameter drill bit, a cutting speed of 1500 rpm, and feed rate of 0.02 mm/rev than other combination of process parameters (i.e.; **A4B1C1D1**). This was due to the quick penetration of the drill on the material which was not having a high contact time with the composite material and drill diameter.

Analysis of variance for exit delamination factor

Table 4.5 showed the calculated ANOVA results of the exit side delamination factor. The results show that the delamination was mostly affected by speed. The analysis shows the significance of the four parameters in affecting exit delamination. F-values of spindle speed, feed rate, stacking sequences, and drill diameter were 223.76, 17.00, 12.18, and 13.95, respectively, and their corresponding P-values were 0.000, 0.002, 0.005, and 0.003. The F-value and P-value show that the speed contributed more to affecting the exit delamination factor. Thus, the 80.52% contribution of the speed was the primary factor in deciding the exit delamination factor, followed by the feed rate of 6.12%, drill diameter of 5.02%, and stacking sequences of 4.38%, i.e., for a level of confidence of 95%.

Table 4.5: Analysis of variance response of exit delamination of sisal-glass composite

Source	DF	Adj SS	Adj MS	F-Value	P-Value	% Contribution
Regression	4	0.031282	0.007821	66.72	0.000	
Speed(rpm)	1	0.026227	0.026227	223.76	0.000	80.52
Feed Rate(mm/rev)	1	0.001993	0.001993	17.00	0.002	6.12
Stacking sequences	1	0.001427	0.001427	12.18	0.005	4.38
Drill Dia. (mm)	1	0.001635	0.001635	13.95	0.003	5.02
Error	11	0.001289	0.000117			3.95
Total	15	0.032572				100
S=0.0108263 R-sq=96.04% R-sq(adj)= 94.60% R-sq(pred)= 90.13%						

DF-degrees of freedom; SS-sum of squares; MS-mean squares; F - and P-values.

Table 4.5 ANOVA table also consists of the F-values and P-values. By comparing the F-values with the tabulated ones (critical F-values), the significance of the factors can be understood. If the obtained F value of the parameter was greater than the tabulated one, then the particular parameter has a significant influence over the response variable. From Table 4.5 the F-value of Speed (223.76) > F0.05,1,15 = 4.54, Feed rate (2.19) < 4.54 (F0.05,1,15), Stacking sequence (12.18) > 4.54, Drill diameter (13.95) > 4.54. Therefore, speed, feed rate, stacking sequences, and drill diameter has a significant influence on exit delamination.

The analysis of variance with P values also shows that P values of spindle speed, feed rate, stacking sequence, and drill diameter are (P = 0.000 < 0.05), (P = 0.002 < 0.05), and (P= 0.003 < 0.05) respectively which show they are a significant factor affecting the entry delamination. The P-value from the ANOVA table denotes that all parameters have significant effects on the delamination factor at the exit.

Regression analysis of exit delamination factor

The regression analysis helps to approximate the value of one variable from the given value of another. Regression modeling was done to propose empirical models for the surface roughness, and delamination factor at entry and exit. The empirical models were developed by applying regression analysis to predict delamination factors at the exit.

Regression Analysis: Entrance Delamination versus Speed(rpm), Feed Rate(mm/rev), Stacking sequences, Drill Dia. (mm)

Exit Delamination = 1.2437 - 0.000145 v(rpm) + 0.499 f(mm/rev) + 0.00845s + 0.00452d (mm)… (4.2)

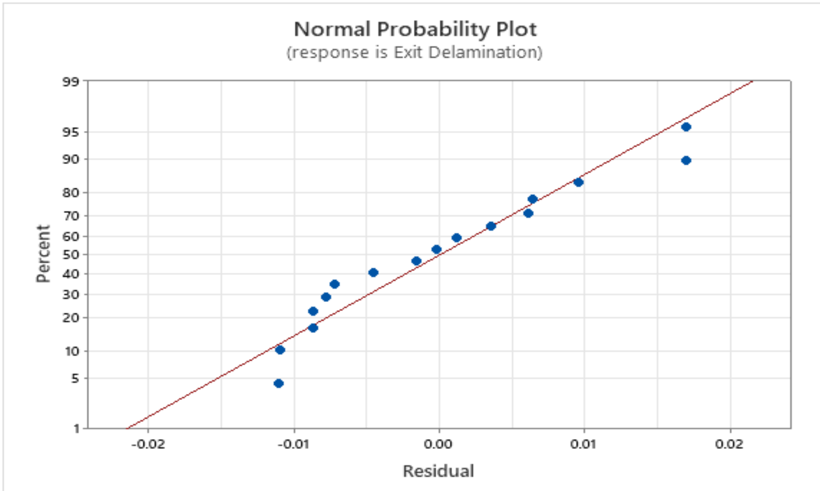

Figure 4.27: The normal probability plot for exit delamination

Determining Optimum Conditions for Exit Delamination Factor

The optimum prediction condition for the S/N ratio in which, the lower exit delamination results are obtained with the terms set in Table 4.6 The selected optimum parameters in this study were a lower feed rate, highest spindle speed, on sample two which was the SGGS layer arrangement, and smaller drill diameter which was (**A4B1C1D1).**

Table 4.6: The optimum condition for exit delamination result prediction setting

Factors	Levels	Value of level	Rank of affecting	Prediction S/N Ratio	Values Mean
Spindle speed(v)	4	1500rpm	1	-0.710814	1.08259
Feed rate(f)	1	0.02mm/rev	2		
Stacking sequences (s)	1	SGGS	3		
Drill diameter(d)	1	6mm	4		

4.3.2 Determination of Roundness (Circularity (Ci)) Error

4.3.2.1 The effect of drilling parameters

Effect of Drill diameter on Roundness (Circularity (Ci)) Error

Figure 4.28 shows the variation of roundness (circularity) against the different drill diameters for constant speeds. Generally, the roundness (circularity) of the hybrid and no-hybrid sisal/glass FRP decreases as the drilling diameter decreases. In this experiment, the roundness (circularity) gradually reduces when the drill diameter was 6mm. Then, the roundness (circularity) value gradually increases when the drill bit diameter increases to 8mm, 10mm. Then finally it attains maximum as the drilling diameter increase to its maximum i.e., 12mm. Also, from Figure 4.28 the influence of speed was that when the speed moves from 1500rpm to 1500rpm the roundness (circularity) decreases.

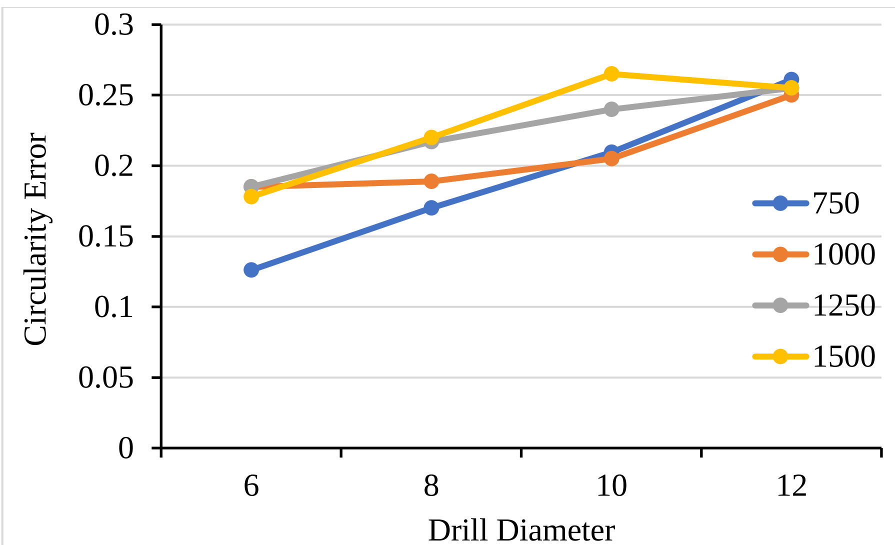

Figure 4.28: Effect of drill diameter on roundness error at a constant speed

It observed that the roundness (circularity) can be reduced to a larger extent by machining the composite sample at a drill diameter of 6mm and cutting speed of 750 rpm. The roundness (circularity) was reduced with a decrease in drill diameter.

Effect of Feed Rate on Roundness (Circularity (Ci)) Error

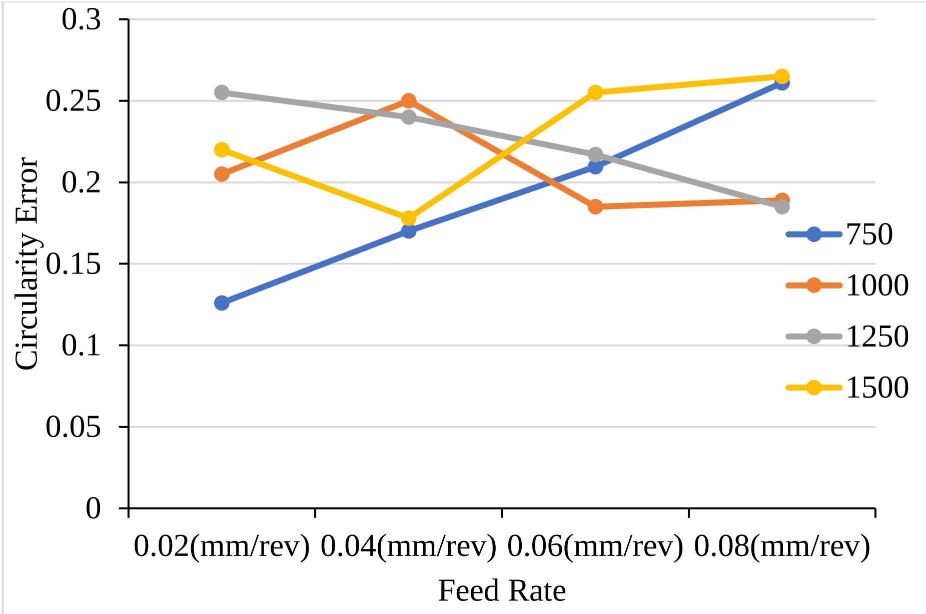

Figure 4.29: Effect of feed rate on roundness error at a constant speed

Figure 4.29 shows the relationship between average roundness error and feed rate. As the feed rate increase, the roundness error increases for lower drilling speeds in this case 750rpm. Figure 4.29 shows the variation of roundness error and feeds for a drilling speed of 750rpm, 1000rpm, 1250rpm, and 1500rpm which reveals that as the feed rate increases, there was almost a large increase in roundness error except for the speed of 1250rpm which shows the decrease in roundness error. Moreover, roundness error was high for the 1500rpm drilling speed, 0.08mm/rev feed rate, and low for 750rpm speed, 0.02mm/rev feed rate which reveals the fact that the roundness error decreased along with the decrease in feed rate and vice versa.

Effect of Speed on Roundness (Circularity (Ci)) Error

Figure 4.30 shows roundness error for natural fiber and synthetic fiber was showing opposite that in pure sisal FRP composite and the hybrid composite containing sisal fiber at the outer layer showed a decrease in roundness error at a lower speed of 750rpm while the synthetic fiber of glass and hybrid composite containing glass fiber at outer layer shows a decrease in roundness error at the higher speed of 1500rpm. This was due to the nature of the fibers in the composite, that sisal fiber has high elongation than glass fiber which decreases the tendency to be removed and promotes slide.

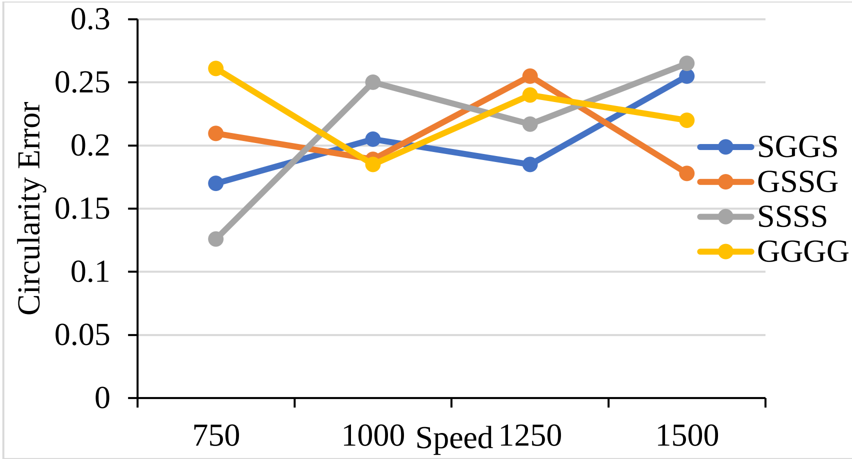

Figure 4.30: Effect of drill speed on roundness error at constant material layers

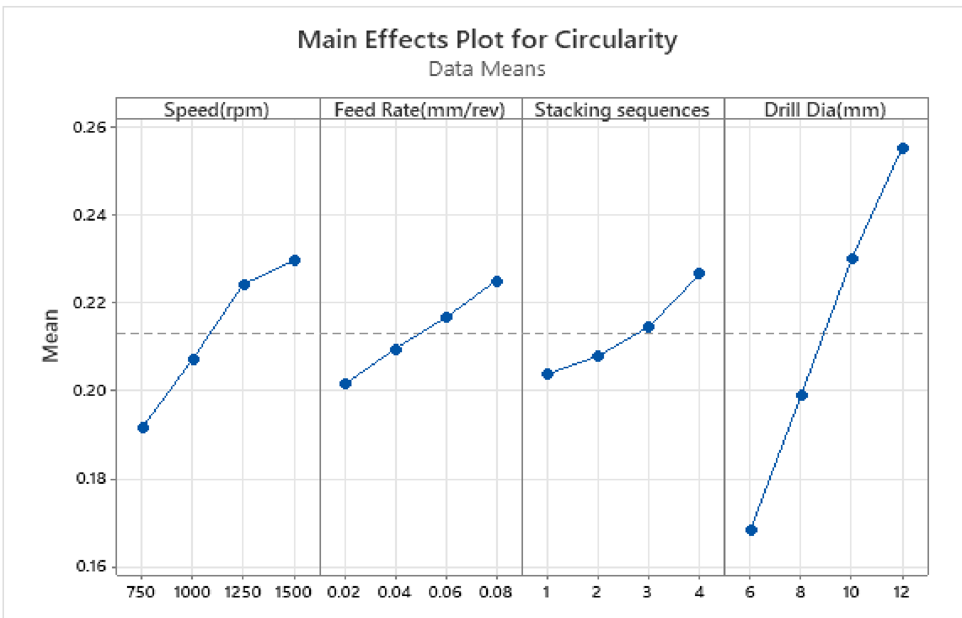

Figure 4.31: Main effect plot for roundness (circularity) error

The effect of drilling parameters namely spindle speed, feed rate, layer arrangement, and drill diameter on hole circularity (roundness error). In CNC drilling operation all parameter shows a linear effect on the roundness error of drilled holes. Figure 4.31 main effect plot, it was shown that the roundness error value was minimum for SGGS (1) that increased linearly up to the GGGG FRP composite. In dry drilling, layer arrangement was having a higher impact on drilled roundness error due to the contact surface of the drill with a different layer of the composite material which has a matrix and different reinforcement.

It was observed that drill diameter shows a linear effect on drilled glass-sisal FRP composite. For a drill diameter of 6 mm, the roundness error was a minimum. However, for a drill diameter of 12mm, the roundness error was high for all materials considered. It was seen that as the drill diameter increases it plays a crucial role in maintaining the quality of drilled holes in FRP composite. The effect of all parameters was shown in Figure 4.31. In dry drilling, tool diameter was having a higher impact on drilled roundness error due to the contact surface area of the drill with the workpiece material.

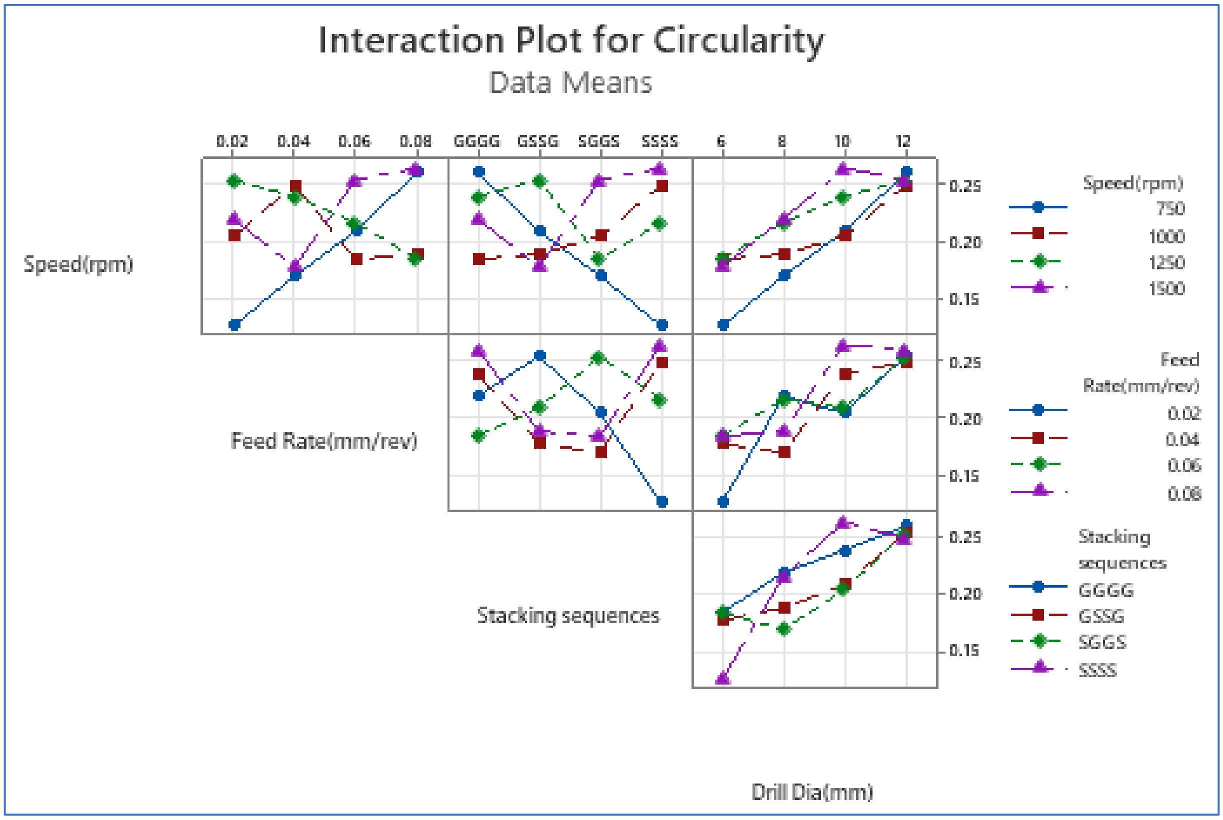

Figure 4.32: Interaction plot for circularity (Roundness) error

In Figure 4.32, it was observed that by increasing the feed rate, the roundness error of the drilled hole increases. It can be correlated with higher thrust force values at high feed rates resulting in more fiber pullouts. Because of these factors, the roundness error of the hole was getting larger. It was found from the response table that the hybrid fabric composite possesses less roundness error means good circularity than the non-hybrid sisal and glass fiber reinforced composites. It may be due to the variation in the physical and mechanical properties of the composites. Figure 4.31 the main effect plot of roundness error represents the effect of drilling parameters on the roundness error of pure sisal fiber-reinforced composites obtained with HSS drill bits. It was observed that the roundness error also shows a similar trend of delamination and surface roughness.

It was observed from the main effect plot that spindle speed also shows a linear effect on drilled glass-sisal FRP composite. At lower spindle speed i.e., at 750 rpm the roundness error was at a lower value. When the spindle speed increases up to 1000 rpm, the roundness error value increases. However, in the next step of the spindle speed of 1250 increments, the roundness error value suddenly dropped and constantly moved as in Figure 4.31.

3.3.3.2 Optimization of process parameters for roundness (circularity) error

To measure and characterize the exit delamination, the statical formula for the smaller the - better has been used. In the case of smaller is the better, the ratio of signal noise ratio can be given by Equation 3.16.

The signal-to-noise ratio analysis for circularity

Using Equation 3.16 the results for the S/N ratio for circularity are given in Table 4.7, and it indicates that drill diameter was the most significant factor influencing hole roundness error and ranked 1st.

Table 4.7: Response table for the signal-to-noise ratios of circularity (C_i)

Level	Speed(rpm)	Feed Rate(mm/rev)	Stacking sequences	Drill Dia. (mm)
1	14.66	14.28	13.76	15.57
2	13.73	13.70	13.81	14.07
3	13.13	13.18	13.55	12.66
4	12.56	12.92	12.97	11.78
Delta	2.09	1.36	0.85	3.79
Rank	**2**	**3**	**4**	**1**

The delta statistics of the S/N ratio for hole roundness (circularity) error depicted in Table 4.7 shows the ranks of factors affecting responses based on the S/N ratios obtained via the Taguchi orthogonal array. The delta statistics were computed based on the difference between the highest and lowest average value of each factor. The value of delta was assigned the first rank and represents the predominant factor affecting the hole roundness (circularity) error. The analysis showed that the drill bit diameter was assigned as rank 1 with a delta value of (3.79) signifying that it was the predominant factor that affects the roundness (circularity) hole of the glass-sisal composite. The speed, feed rate, and stacking sequences, were assigned by delta value in the second (2.09), third (1.36), and fourth (0.85) ranks respectively.

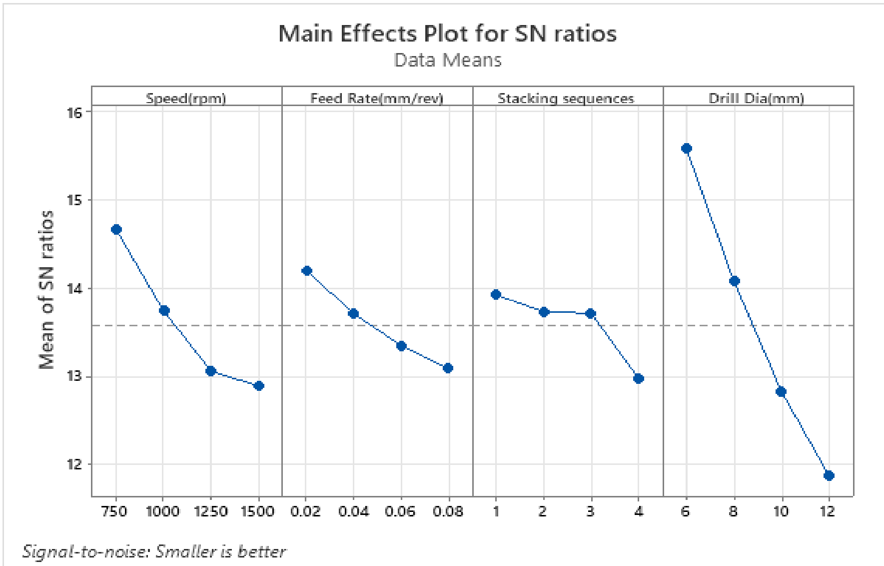

Where stacking sequences of SGGS=1, GSSG=2, SSSS=3, GGGG=4

Figure 4.33: The main effect plot for a signal-to-noise ratio of circularity

Figure 4.33 shows the optimum condition for the hole roundness error was the speed at level 1 (750rpm), feed at level 1 (0.02 mm/rev), and drill diameter at level 1 (6mm), with stacking sequences of SGGS hybrid composite material (**A1B1C1D1)**. It should be emphasized that these settings are capable of resulting in low hole roundness error (1.03mm) among the drilling conditions tested.

The hole roundness error values were found to be proportional to the feed rate for different spindle speeds at different drill diameters of the HSS drill bit in a sisal-glass FRP composite. The high hole roundness error in Hybrid Sisal Glass FRP indicates partially broken fibers, matrix pullout, or sometimes material crack also, a lower hole roundness error does not mean that it is perfectly circular. The hardness nature of Hybrid FRP laminate was highly influential on the HSS drill bit because the HSS material was a much softer drill bit. Therefore, the HSS tool exhibits more rapid tool wears which results in a poor hole roundness error (Shunmugesh & Kavan, 2017).

Analysis of Variance for roundness(circularity) error

Table 4.8: Analysis of variance results of roundness (circularity) error

Source	DF	Adj SS	Adj MS	F-Value	P-Value	%Contribution
Regression	4	0.026556	0.006639	96.12	0.000	
Speed(rpm)	1	0.005001	0.005001	72.40	0.000	18.31
Feed Rate(mm/rev)	1	0.002210	0.002210	32.00	0.000	8.09
Stacking sequences	1	0.000908	0.000908	13.14	0.004	3.32
Drill Dia. (mm)	1	0.018438	0.018438	266.94	0.000	67.49
Error	11	0.000760	0.000069			2.78
Total	15	0.027316				99.99
S = 0.0083108; R-sq = 97.22%; R-sq(adj) = 96.21%; R-sq(pred) = 94.31%.						

DF-degrees of freedom; SS-sum of squares; MS-mean squares; F - and P-values.

Table 4.8 shows the calculated ANOVA results of the hole roundness error. The results show that the roundness(circularity) error was mostly affected by the drill bit diameter. The analysis shows the significance of all parameters in affecting hole roundness error. F-values of drill diameter, spindle speed, feed rate, and stacking sequences were 266.94, 72.40, 32.00, and 13.14, respectively, and their corresponding P-values were 0.000, 0.000, 0.000, and 0.004. F-value and P-value show that the drill bit diameter contributed more to affecting the hole roundness (circularity) error. Thus, the 67.49% contribution of the drill bit diameter was the primary factor in deciding the roundness (circularity) error, followed by the speed of 18.31%, feed rate of 8.09%, and stacking sequences of 3.32%, i.e., at the level of confidence of 95%.

Regression Equation of circularity.

Based on the obtained roundness(circularity) error values for different experimental conditions, the linear polynomial model, as given in Eq, was developed to relate it to the drilling parameters.

$$\text{Circularity} = -0.0359 + 0.000063\, v + 0.5256\, f + 0.00674\, s + 0.015181\, d \quad (4.3)$$

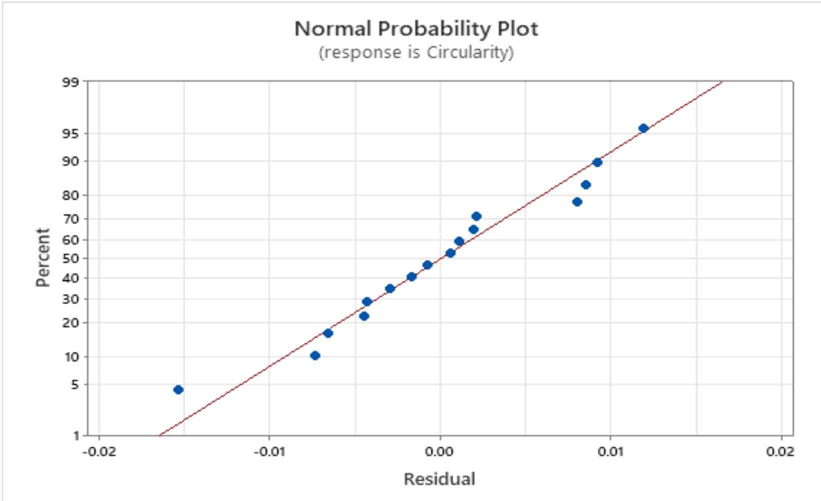

Figure 4.34: Normal probability graph for roundness (circularity) error

One of the assumptions in all the statistical models used in the design of experiments was that the experiment error (residuals) was normally distributed and a normal probability plot of effects was used to judge the significance of effects. If all the residuals fall along a straight line drawn, it was inferred that the residuals/errors follow a normal distribution. Figure 4.34 shows the data points are relatively close to the fitted normal distribution line. The results are scattered around the line which shows the minimum error value to be obtained from the experiment.

Determining optimum conditions for roundness(circularity) error

The optimum prediction condition for the S/N ratio in which, the lower roundness(circularity) error results are obtained with the terms set in Table 4.9. As shown in Table 4.7, the selected optimum parameters in this study were a lower spindle speed, lower feed rate, on sample two which was SGGS layer arrangement, and smaller drill diameter which was (**A1B1C1D1).**

Table 4.9: The optimum condition for roundness(circularity) error result prediction setting

Factors	Levels	Value of level	Rank of affecting	Prediction S/N Ratio	Values Mean
Spindle speed(v)	1	750rpm	2	17.6023	0.125906
Feed rate(f)	1	0.02mm/rev	3		
Stacking sequences (s)	1	SGGS	4		
Drill diameter(d)	1	6mm	1		

4.3.3 Surface Roughness Analysis (R_a)

Roughness plays an important role in determining how a real object will interact with its environment. Rough surfaces (Ra) usually wear more quickly and have a higher friction coefficient than smooth surfaces. In general, the surface finish of the drilled hole was essential, as the surface quality determines the precision of the drilled component. Roughness in fiber-reinforced composite laminates occurred due to the improper fracture of fibers, which tends to expose sharp fiber ends on the inner surface of the drilled hole. Variation in the surface roughness leads to the material failing under fatigue and fastener load, which cause misalignment, high friction, and heat generation at the drilled hole wall surfaces (Margabandu & Subramaniam, 2020). Roughness was often a good predictor of the performance of a mechanical component, since irregularities in the surface may form nucleation sites for cracks or corrosion.

In the present investigation, surface roughness found on the drilled surface was described by Ra (the average surface roughness). Surface roughness variation for the stacking sequences, drill diameter, spindle speed, and feed rate are shown in Figure 4.36. The figure shows that the roughness values were scattered; as such, the surface roughness values did not follow the trend of variation with drilling parameters at all. This was because of the non-homogeneous property of the composite and the availability of different layers. Under drilling, the surface may become more irregular due to the different cut mechanisms involved in Figure 4.37. The matrix material failed under high stress, while the fragmented matrix was found stuck to the cut surface. The matrix cracks were noted on the surface due to the high stress developed in the drill face during tool penetration. Due to high heat generation, the matrix became molten and smeared on the wall of the cut surface. The high drill force caused the fibers to pull out, protrude from, and become deboned from the matrix. In some regions, the fibers were broken and fragmented, while uncut fibers were. were also noticed at the exit point. These variations in the failure mechanism are the reason for the irregularity and scattering in the surface roughness value. Similar findings were reported by (Shanmugam et al., 2021).

4.4.1 Effect of process parameters on the surface roughness of the drilled hole

Effect of feed rate on surface roughness

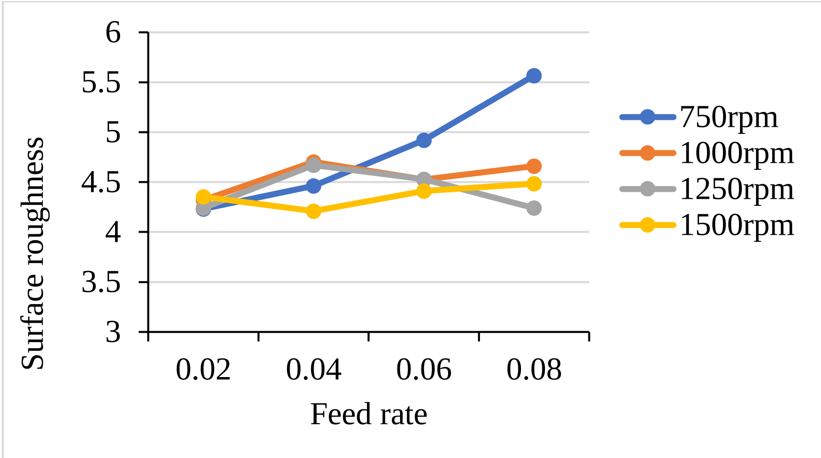

Figure 4.35: Effect of feed rate on surface roughness at a constant speed

Figure 4.35 shows the relationship between average surface roughness and feed rate. As the feed rate increase, the surface roughness increases for constant drilling speeds. Figure 4.35 shows the variation of surface roughness and feeds for a drilling speed of 750rpm, 1000rpm, 1250rpm, and 1500rpm which reveals that as the feed rate increases, there was almost a large increase in surface roughness value for all samples prepared. Moreover, surface roughness was high for the 750rpm drilling speed, 0.08mm/rev feed rate, and low for the 1250rpm speed, 0.08mm/rev feed rate which reveals the fact that the surface roughness increased along with an increase in feed rate and decrease in speed and vice versa.

Effect of drill diameter on surface roughness

Figure 4.36 shows the variation of surface roughness against the different feed rates for constant drill diameter. Generally, the surface roughness of the hybrid and no-hybrid sisal/glass FRP decreases as the drilling diameter decreases. In this experiment, the surface roughness gradually reduces when the drill diameter was 6mm. Then, the surface roughness value gradually increases when the drill bit diameter increases to 8mm, 10mm. Then finally it attains maximum surface roughness value as the drilling diameter increase to its maximum i.e., 12mm.

It observed that the surface roughness can be reduced to a larger extent by machining the composite sample at a drill diameter of 6mm and feed rate of 0.04mm/rev. The surface roughness was reduced with a decrease in drill diameter.

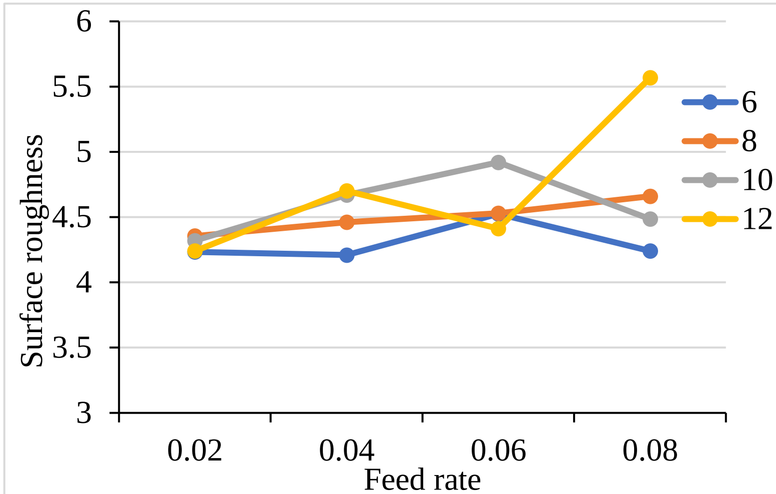

Figure 4.36: Effect of feed rate on surface roughness at constant drill diameter

Effect of speed on surface roughness at constant material layers

Figure 4.37 shows the relationship between average surface roughness and composite material layers at a constant speed. The surface roughness decreases with an increase in drilling speed. Figure 4.37 shows the variation of surface roughness and different materials layer arrangements for constant drilling speeds of 750rpm, 1000rpm, 1250rpm, and 1500rpm which reveals that as the material layer varies, there was almost a large increase in surface roughness for glass FRP samples prepared. Moreover, surface roughness was high for the 750rpm, 1000, 1250, and 1500 drilling speeds respectively. Stacking sequences reveals the fact that the exit delamination shows different along with speed. Poor exit delamination is seen at a point 750rpm with glass FRP composite and good quality at 1500rpm with SGGS FRP composite.

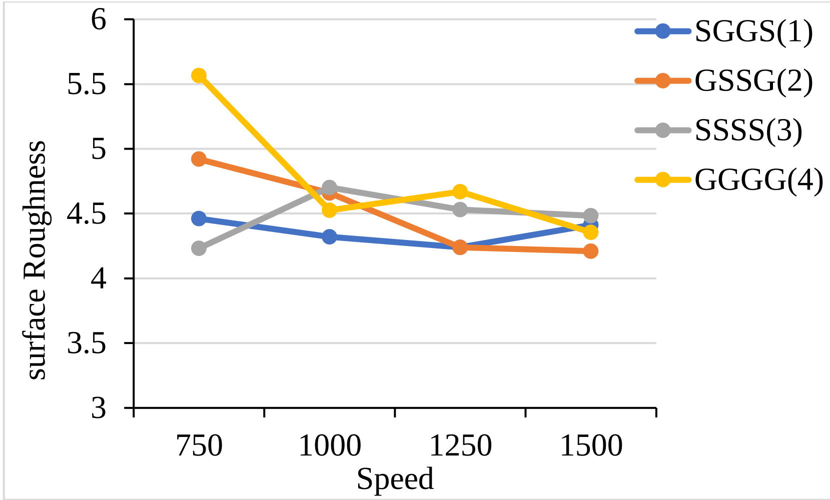

Figure 4.37: Effect of speed on surface roughness at constant material layers

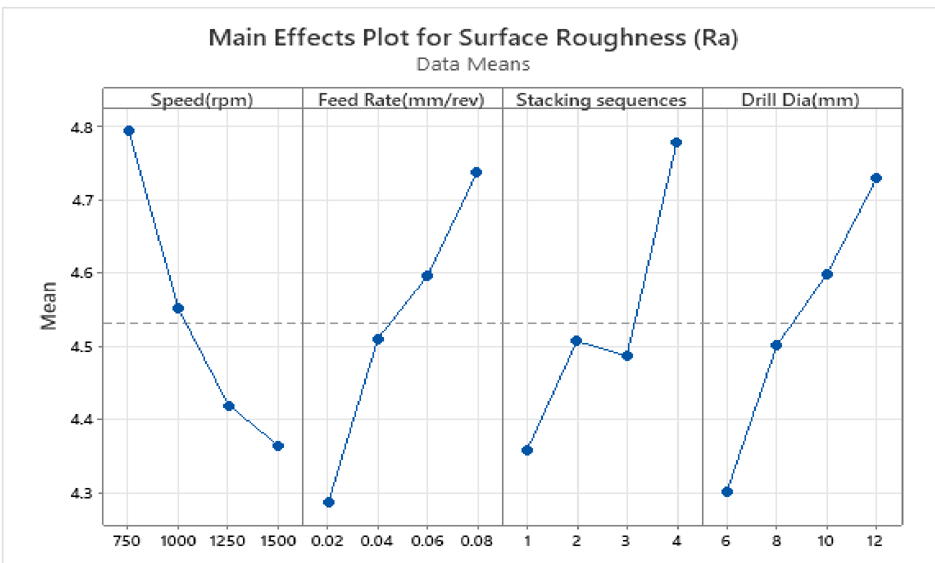

Figure 4.38: Main effect plot for surface roughness (Ra)

In CNC drilling operation layer arrangement shows a linear effect on the roughness of drilled holes. Figure 4.38 main effect plot, it was shown that the roughness value was minimum for SGGS that increased linearly up to the GGGG FRP composite. In dry drilling, layer arrangement was having a higher impact on drilled surface quality due to the contact surface of the drill with a different layer of the composite material which has a matrix and different reinforcement.

It was observed from the main effect plot that drill diameter shows a linear effect on drilled glass-sisal FRP composite. For a drill diameter of 6 mm, the roughness was a minimum. However, for a drill diameter of 12mm, the roughness was high for all materials considered. It was seen that as the drill diameter increases it plays a crucial role in maintaining the quality of drilled holes in FRP composite. The effect of all parameters was shown in Figure 4.39. In dry drilling, tool diameter was having a higher impact on drilled surface quality due to the contact surface area of the drill with the workpiece material.

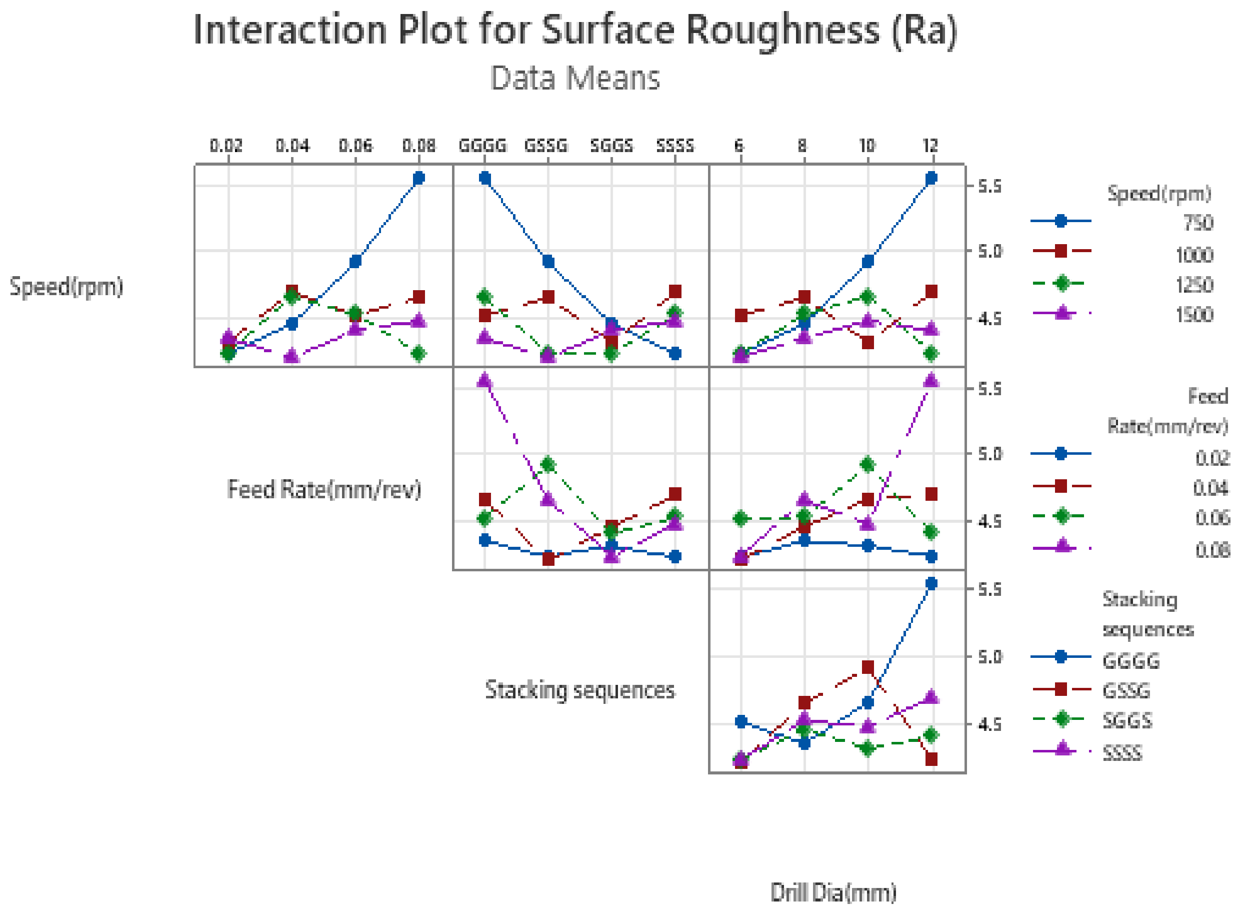

Figure 4.39: Interaction plot for surface roughness (Ra)

In Figure 4.38, it was observed that by increasing the feed rate, the surface roughness of the drilled hole increases. It can be correlated with higher thrust force values at high feed rates resulting in more fiber pullouts and delamination. Because of these factors, the surface quality of the hole was getting deteriorated. It was found from the response table that the hybrid fabric composite possesses less surface roughness means good surface quality than the non-hybrid sisal and glass fiber reinforced composites. It may be due to the variation in the physical and mechanical properties of the composites. Figure 4.37. The main effect plot of surface roughness represents the effect of drilling parameters on the surface roughness of pure sisal fiber-reinforced composites obtained with HSS drill bits. It was observed that the surface roughness also follows a similar trend of delamination.

It was observed from the main effect plot that spindle speed also shows a non-linear effect on drilled sisal glass fiber-reinforced composite. At lower spindle speed i.e., at 750 rpm the roughness was at a high value. When the spindle speed increases up to 1000 rpm, the roughness value decreases. However, in the next step of the spindle speed of 1250 increments, the roughness value suddenly dropped and constantly moved as in Figure 4.37.

4.4.2 Optimization of process parameters for surface roughness

Signal-to-noise ratios(S/N) for surface roughness

Similar to that of the delamination factor, the surface roughness response for each level and factor based on the S/N ratio were summarized in the response table and graph given below.

Table 4.10: Response table for a signal to noise ratios for surface roughness

Level	**Speed(rpm)**	**Feed Rate(mm/rev)**	**Stacking sequences**	**Drill Dia. (mm)**
1	-13.57	-12.64	-12.78	-12.67
2	-13.16	-13.08	-13.06	-13.06
3	-12.90	-13.24	-13.03	-13.24
4	-12.80	-13.47	-13.55	-13.45
Delta	0.77	0.82	0.76	0.78
Rank	**3**	**1**	**4**	**2**

Table 4.10. shows the influence of spindle speed, feed rate, stacking sequences, and drill diameter on the surface roughness of glass-sisal with different FRP composites drilled with different diameter HSS drill bits. It was found that the feed rate cutting and drill diameter made the largest contribution to the surface roughness assigned as the rank of first and second with a delta value which represents the predominant factor affecting surface roughness with the value of 0.82 and 0.78 while speed and stacking sequences affect in third and fourth order with the delta value of 0.77 and 0.76. It was observed that there was a decrease in values of the surface

roughness with a decrease in feed rate. The surface roughness was found to increase with the feed rate increase. Because, at an increased feed rate, more chips are produced and these chips were not easily removed due to their shapes and properties. Further, it was noticed that the surface roughness damage of the drilled hole obtained with the increased diameter HSS drill was higher than the smaller drill for all the process parameters in the considered composite.

In this regard, the minimum surface roughness (Ra) value was obtained at drill diameter 6mm stacking sequences SGGS, feed rate of 0.02mm/rev, and speed of 1500rpm.

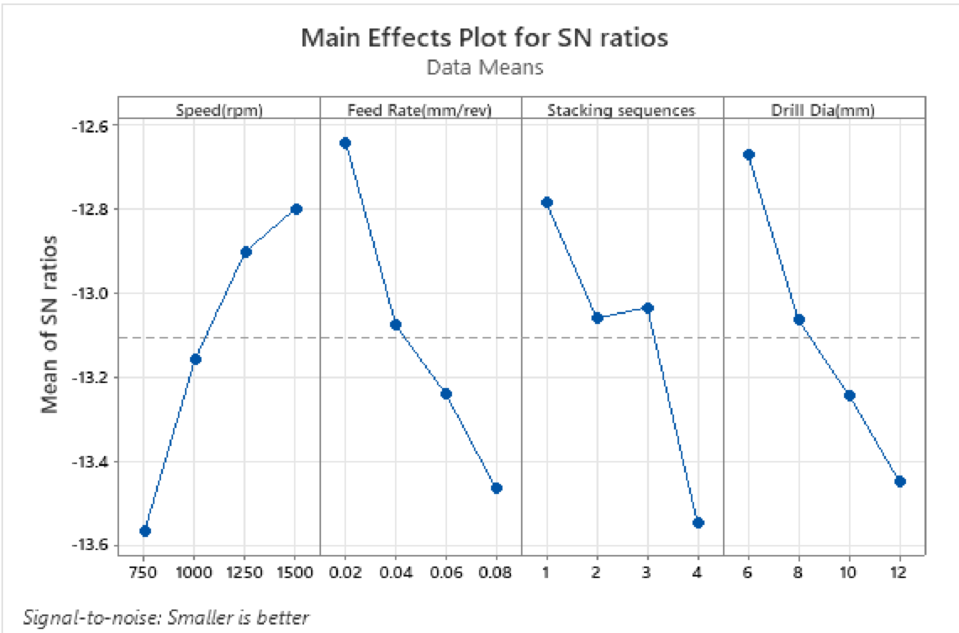

Figure 4.40: Main effect plot for S/N ratios for surface roughness

The desired parameter settings can often be determined based on the largest S/N ratio results of the response graph, Figure 4.40 As apparent, the optimum condition for the surface roughness was the speed at level 4 (1500rpm), feed at level 1 (0.02 mm/rev), and drill diameter at level 1 (6mm), with stacking sequences of SGGS hybrid composite material (**A4B1C1D1**). It should be emphasized that these settings are capable of resulting in low surface roughness (4.1µm) among the drilling conditions tested.

The surface roughness values were found to be proportional to the feed rate for different spindle speeds at different drill diameters of the HSS drill bit in a sisal-glass FRP composite. The high surface roughness in Hybrid Sisal Glass FRP indicates partially broken fibers, matrix pullout, or sometimes material crack; also, lower surface roughness does not mean that there was no crack in the surface but underlying may be there on the material.

The hardness nature of Hybrid FRP laminate was highly influential on the HSS drill bit because the HSS material was a much softer drill bit. Therefore, the HSS tool exhibits more rapid tool wears which results in a poor surface finish (Shunmugesh & Kavan, 2017).

Analysis of variance for surface roughness

Table 4.11: Analysis of variance for roughness value (Ra) of drilled sisal-glass composites

Source	DF	Adj SS	Adj MS	F-Value	P-Value	% Contribution
Regression	4	1.5094	0.37736	17.38	0.000	
Speed(rpm)	1	0.4040	0.40403	18.61	0.001	23.10
Feed Rate(mm/rev)	1	0.4142	0.41419	19.08	0.001	23.69
Stacking sequences	1	0.3094	0.30940	14.25	0.003	18.00
Drill Dia. (mm)	1	0.3818	0.38181	17.58	0.002	21.84
Error	11	0.2388	0.02171			13.66
Total	15	1.7483				
S=0.147353, R-sq=86.34%, R-sq(adj)= 81.37%, R-sq(pred)= 64.42%						

DF-degrees of freedom; SS-sum of squares; MS-mean squares; F - and P-values.

The desired setting from the response table was in agreement with the computed S/N ratio variability for individual parameters and respected the degree of freedom in this experiment or ANOVA. Table 4.11 shows the ANOVA output for surface roughness based on a 95% confidence level. The results indicate that feed rate, drill diameter, speed, and stacking sequences are significant in producing a smooth hole in which the F-value of the factors was higher than the table value; F (0.05, 1,15) = 4.54.

The ANOVA analysis shows the significance of the four parameters in affecting surface roughness. F-values of feed rate, drill diameter, and stacking sequences were 19.08, 18.61, 17.58, and 14.25 respectively, F-value and P-value show that the feed rate and speed contributed more to affect the surface roughness of the drilled hole. Thus, the 23.69% contribution of the feed rate was the primary factor in deciding the surface roughness, followed by the speed of

23.10% i.e., for a level of confidence of 95% and or with the P-value it was observed from the ANOVA that feed rate (0.001), speed (0.001), drill diameter (0.002), and stacking sequences (0.003) shows statistical significance on the roughness of drilled hole at a 95% confidence level as the P-value in the ANOVA for feed rate, speed, drill diameter, and stacking sequences was higher than 0.05 so, they are statically significant.

From Table 4.11, it was statistically proved that feed rate (23.69%) was the governing factor, which needs to be set at a low level (0.02 mm/rev) for improvement of the surface roughness during the drilling of the Glass-sisal FRP composite showing the higher impact of feed rate on the roughness of drilled hole.

Regression Analysis: Surface Roughness (Ra) versus Speed(rpm), Feed Rate(mm/rev), Stacking sequences, Drill Dia. (mm)

The correlations between the process parameters (spindle speed, feed rate, drill diameter, and stacking sequences) and the responses (delamination factor and surface roughness) in hybrid sisal/glass composite were obtained by multiple linear regression. The equations obtained were as follows:

$$\text{Surface Roughness (Ra)} = -0.56 - 0.000648\ s(\text{rpm}) + 17.91\ f(\text{mm/rev}) + 0.495\ s + 0.3907\ d\ (\text{mm}) \tag{4.4}$$

Normal probability graph of surface roughness

One of the assumptions in all the statistical models used in the design of experiments was that the experiment error (residuals) was normally distributed and a normal probability plot of effects was used to judge the significance of effects. If all the residuals fall along a straight line drawn, it was inferred that the residuals/errors follow a normal distribution. Figure 4.41 shows the data points are relatively close to the fitted normal distribution line. The results are scattered around the line which shows the minimum error value to be obtained from the experiment.

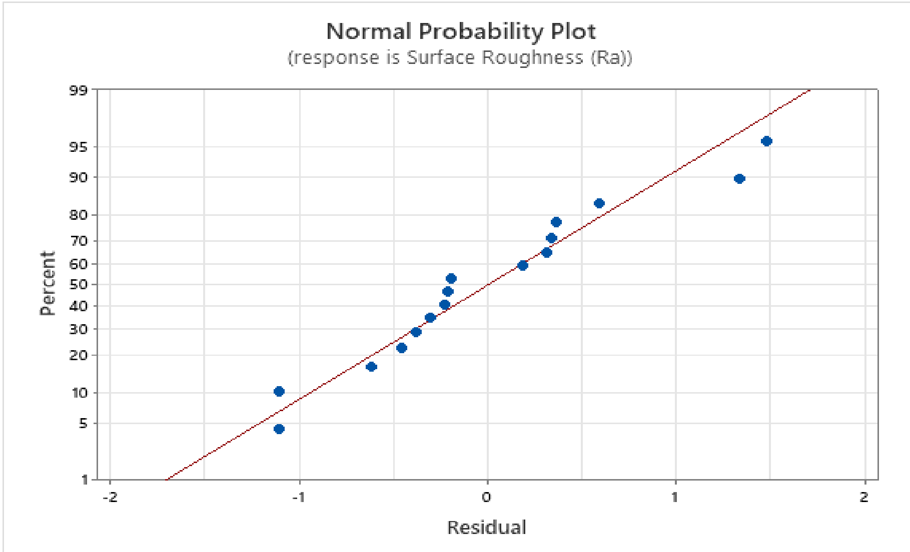

Figure 4.41: Normal probability graph of surface roughness

Determining optimum conditions for roundness(circularity) error

Table 4.12: The optimum condition for surface roughness result prediction setting

Factors	Levels	Value of level	Rank of affecting	Prediction S/N Ratio	Values Mean
Spindle speed(v)	4	1500rpm	2	17.6023	0.125906
Feed rate(f)	1	0.02mm/rev	1		
Stacking sequences (s)	1	SGGS	4		
Drill diameter(d)	1	6mm	3		

The optimum prediction condition for the S/N ratio in which, the lower surface roughness results are obtained with the terms set in Table 4.12. As shown in Table 4.10 the selected optimum parameters in this study were a higher spindle speed, lower feed rate, on sample two which was SGGS layer arrangement, and smaller drill diameter which was (**A4B1C1D1).**

4.4 Multi Response Grey Relational Analysis

The data obtained from the signal-to-noise ratio of entry and delamination, roundness error, and surface roughness tests were compiled into one to predict the optimal parameter combination for the best property of the drilled composites.

Step 1: Calculate the S/N ratio for the corresponding responses using Eq.3.16, Eq.3.17, and Eq.3.18.

Table 4.13: S/N ratio values and normalized S/N ratio values

S/N ratios				Normalized Value			
Entry Delamination	Exit Delamination	Circularity (Ci)	Surface Roughness (Ra)	Entry Delamination	Exit Delamination	Circularity	Surface Roughness (Ra)
-0.973	-1.533	17.993	-12.532	0.590	0.464	1.000	0.981
-1.054	-1.518	15.391	-12.989	0.380	0.476	0.597	0.793
-1.107	-1.726	13.576	-13.839	0.243	0.317	0.316	0.442
-1.201	-2.144	11.667	-14.912	0.000	0.000	0.020	0.000
-0.958	-1.434	13.765	-12.710	0.627	0.540	0.345	0.908
-1.052	-1.509	12.041	-13.446	0.386	0.483	0.078	0.604
-1.035	-1.553	14.657	-13.112	0.428	0.449	0.483	0.742
-1.051	-1.533	14.471	-13.368	0.388	0.464	0.455	0.637
-0.937	-1.108	11.869	-12.547	0.683	0.788	0.052	0.975
-0.971	-1.289	12.396	-13.387	0.594	0.650	0.133	0.629
-0.993	-1.161	13.271	-13.122	0.538	0.747	0.269	0.738
-0.899	-1.123	14.657	-12.547	0.781	0.776	0.483	0.975
-0.814	-0.906	13.152	-12.780	1.000	0.941	0.250	0.879
-0.820	-0.828	14.992	-12.486	0.985	1.000	0.535	1.000
-0.877	-1.027	11.869	-12.891	0.838	0.849	0.052	0.833
-0.945	-1.031	11.535	-13.035	0.662	0.846	0.000	0.774

Step 2: Normalization of the S/N values is the generation of grey relations within 0 and 1 using Eq.3.21.

Step 3: Calculation the grey relational coefficient using Eq.3.22.

Step 4: The grey relational grade using Eq.3.23.

Table 4.14: Grey relational co-efficient and grey relational grade values

Deviation Sequences				Grey Relation Coefficient				GRG.	Rank
Entrance Delamination	Exit Delamination	Circularity	Surface Roughness (Ra)	Entrance Delamination	Exit Delamination	Circularity	Surface Roughness (Ra)		
0.410	0.536	0.000	0.019	0.550	0.483	1.000	0.963	0.749	3
0.620	0.524	0.403	0.207	0.447	0.488	0.554	0.707	0.549	10
0.757	0.683	0.684	0.558	0.398	0.423	0.422	0.473	0.429	15
1.000	1.000	0.980	1.000	0.333	0.333	0.338	0.333	0.334	16
0.373	0.460	0.655	0.092	0.573	0.521	0.433	0.844	0.593	8
0.614	0.517	0.922	0.396	0.449	0.492	0.352	0.558	0.463	14
0.572	0.551	0.517	0.258	0.466	0.476	0.492	0.659	0.523	11
0.612	0.536	0.545	0.363	0.450	0.483	0.478	0.579	0.497	13
0.317	0.212	0.948	0.025	0.612	0.702	0.345	0.952	0.653	6
0.406	0.350	0.867	0.371	0.552	0.588	0.366	0.574	0.520	12
0.462	0.253	0.731	0.262	0.520	0.664	0.406	0.656	0.561	9
0.219	0.224	0.517	0.025	0.696	0.691	0.492	0.952	0.707	4
0.000	0.059	0.750	0.121	1.000	0.894	0.400	0.805	0.775	2
0.015	0.000	0.465	0.000	0.970	1.000	0.518	1.000	0.872	1
0.162	0.151	0.948	0.167	0.755	0.768	0.345	0.750	0.655	5
0.338	0.154	1.000	0.226	0.597	0.764	0.333	0.688	0.596	7

By analyzing the main effect of the grey relational grade value in Minitab 20 software, the optimal parameter was predicted for the best value of parameters for delamination, roundness error, and surface roughness minimization property.

Higher GRG means better machinability condition/product quality. Hence, based on the higher GRG or the rank, the optimum process level can be achieved (Shunmugesh & Kavan, 2017).

4.4.1 Optimization of Process Parameters for Grey Relational Grade

Taguchi Signal-to-Noise ratios (S/N), which are log functions of the desired output, serve as objective functions for optimization and help in data analysis and prediction of optimum results. In the Taguchi method, GRG response variation was studied with the help of the mean and signal-to-noise (S/N) ratio.

Analysis of Mean for GRG

The mean value of GRG for each factor i.e., entry delamination, exit delamination, roundness error, and surface roughness at each level was also obtained using Minitab 20 for GRG and the result was listed in Table 4.15:

Table 4.15: Response table for a mean of GRG

Level	**Speed(rpm)**	**Feed Rate(mm/rev)**	**Stacking sequences**	**Drill Dia. (mm)**
1	0.5153	**0.6922**	**0.6259**	**0.7130**
2	0.5190	0.6009	0.6128	0.5956
3	0.6103	0.5421	0.5922	0.5343
4	**0.7243**	0.5338	0.5381	0.5261
Delta	0.2090	0.1585	0.0877	0.1869
Rank	**1**	**3**	**4**	**2**

The factor with the greatest effect on the mean from above Table 4.15 was the drilling speed (Delta = 0.2090, Rank = 1). The factor with the least effect on the mean is stacking sequences (Delta = 0.0877, Rank = 4). To find out the predicted value of the responses (GRG the following linear regression equation is used (Ebrahim et al. (2020)):

Opt. = A4+B1+C1+D1-3m

Optimum = 0.7243 + 0.6922 + 0.6259 + 0.7130 -3 x 0.592

Opt. = 0.9794 (Predicted optimum value of GRG)

Where m is the average performance mean value for GRG (i.e.: m = 0.592)

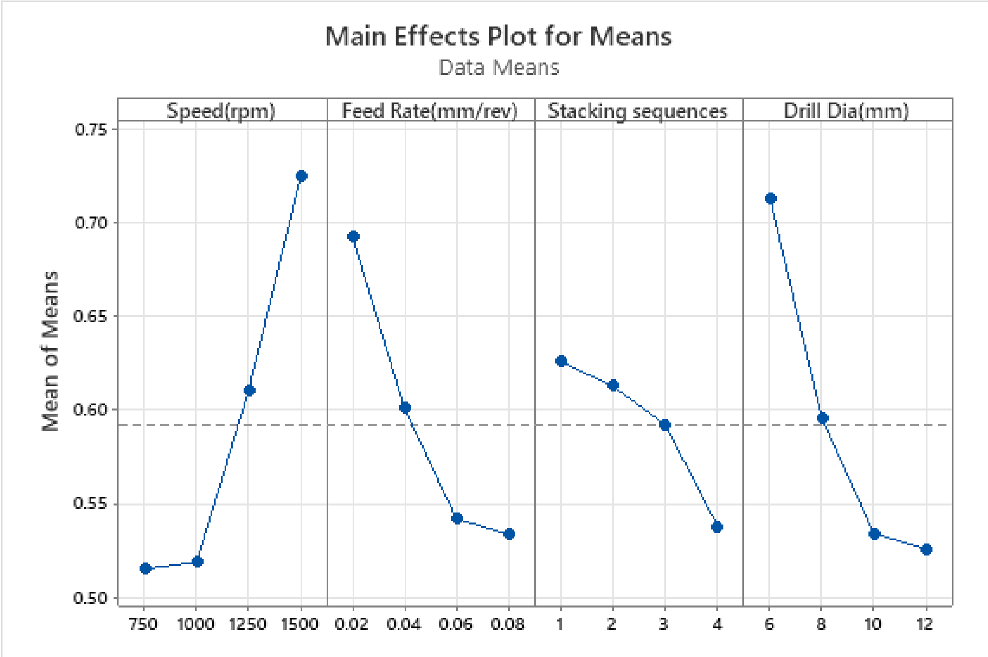

Figure 4.42: Main Effect Plot of Mean for GRG

Figure 4.42. it can be seen that within the scope of this study the maximum point in the graph for each factor is the optimum condition at which a larger GRG was obtained. The maximum point for drilling speed at level 4, lower feed rate at level 1, stacking sequences at level 1 SGGS, and lower drill diameter of level 1. This was why the identified optimum parameter was at high speed, lowest feed rate, hybrid stacking sequences with outer sisal fiber, and lowest drill diameter which was (**A4B1C1D1**).

4.4.2 Analysis of S/N ratio for Grey Relational Grade

Table 4.16: Signal-to-Noise ratios for GRG (larger is better)

Level	Speed(rpm)	Feed Rate(mm/rev)	Stacking sequences	Drill Dia. (mm)
1	-6.147	-3.245	-4.111	-3.083
2	-5.732	-4.694	-4.578	-4.627
3	-4.352	-5.418	-4.680	-5.520
4	-2.896	-5.771	-5.759	-5.899
Delta	3.251	2.526	1.648	2.817
Rank	**1**	**3**	**4**	**2**

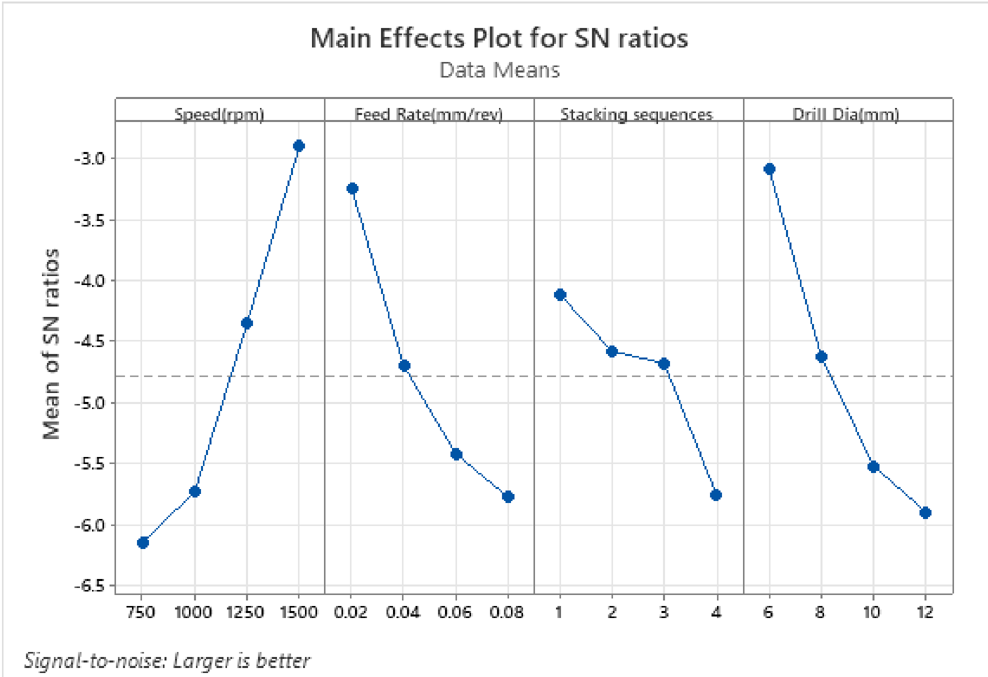

Figure 4.43: Main effect plots for S/N ratio of GRG response

Figure 4.43: shows the control factor's main effect plot for the S/N ratio and the optimal parameter combination on GRG response (larger the better GRG response). In the S/N ratio, the numerical value of the maximum point in each graph shows the best optimum combination of factors at that level and the above figure shows the maximum point for drilling speed at level 4 of 1500rpm, for feed rate level 1 of 0.02mm/rev, for stacking sequences level 1 of SGGS, and drill diameter of level 1of 6mm diameter that is (**A4B1C1D1**) was selected. The most effective parameter of GRG response is the drilling speed when compared with other factors and stacking sequences have the least effect on the GRG response.

4.4.3 Determining Optimum Condition for GRG

The optimum prediction condition for the S/N ratio in which, the GRG response result of the composite obtained with the terms set was shown in Table 4.17. The selected optimum parameters in this study were higher drilling speed, a lower feed rate, SGGS stacking sequences, and a lower drilling diameter which was (**A4B1C1D1)**.

Table 4.17: The optimum condition for GRG response result prediction-settings

Factors	Levels	Value of level	Rank of affecting	Prediction Values	
				S/N Ratio	Mean
Spindle speed(v)	4	1500rpm	1	1.01154	**0.9786**
Feed rate(f)	1	0.02mm/rev	3		
Stacking sequences (s)	1	SGGS	4		
Drill diameter(d)	1	6mm	2		

4.4.4 Analysis of Variance for GRG

ANOVA was used as an analytical tool to find out the significant factors in measurement by viewing the connection between the response variable and proposed factors. The Taguchi method could not choose the result of individual process parameters on the whole process; hence, the percentage of contribution was calculated using ANOVA on behalf.

Table 4.18: Analysis of variance of GRG

Source	**DF**	**Adj SS**	**Adj MS**	**F-Value**	**P-Value**	**% Contribution**
Regression	4	0.25379	0.063447	19.96	0.000	
Speed(rpm)	1	0.10322	0.103217	32.47	0.000	35.75
Feed Rate(mm/re)	1	0.05707	0.057070	17.95	0.001	19.76
Stacking sequences	1	0.01611	0.016106	5.07	0.046	5.58
Drill Dia. (mm)	1	0.07739	0.077394	24.35	0.000	28.80
Error	11	0.03496	0.003179			12.10
Total	15	0.28875				

DF-degrees of freedom; SS-sum of squares; MS-mean squares; F - and P-values.

From the ANOVA results shown in Table 4.18, the most influential factor on the grey relational grade was found to be the cutting speed (35.75 percent), followed by the drill diameter (28.80 percent), feed rate of (19.76 percent), and stacking sequences of (5.58 percent).

4.5 Confirmation Test

After obtaining the optimal process parameters and levels the next step was to verify that the predicted result was against the experimental results. If the combination of optimal process parameters level coincides with that of any experimental trial in the orthogonal array there will not be a need for a confirmation test. Unless performing experimentation at that new level should be performed. In these studies, the optimal process parameter combination for entry and exit delamination outputs, roundness (circularity error), and surface roughness were at A4B1C1D1.

The confirmation tests are conducted as per the optimum set point to confirm the standard qualities for drilling of glass-sisal FRP composite as suggested by the experimental work. The response values obtained from the confirmation test are Entry Delamination Factor = 1.054, Exit Delamination factor = 1.088, Circularity (roundness) error = 0.12mm, and Surface Roughness = 4.1µm. From the confidence interval of 95 percent, the optimum condition was predicted, and the grey relational grade estimate of the confirmation test shows an improvement of 5 percent from the average value. Hence, we can say that the hybrid Taguchi and GRA coupled gives a very good result to predict the entry and exit delamination factor, circularity, and surface roughness in the drilling of glass-sisal FRP materials.

4.6 Chip Analysis

During drilling operations, the chips are collected carefully to examine chip shapes and/or types in drilling operations. Continuous and discontinuous types of chips were separately formed. The chip types were affected by machining parameters including material type, cutting velocity, feed rate, stacking sequences, drill diameter, etc.

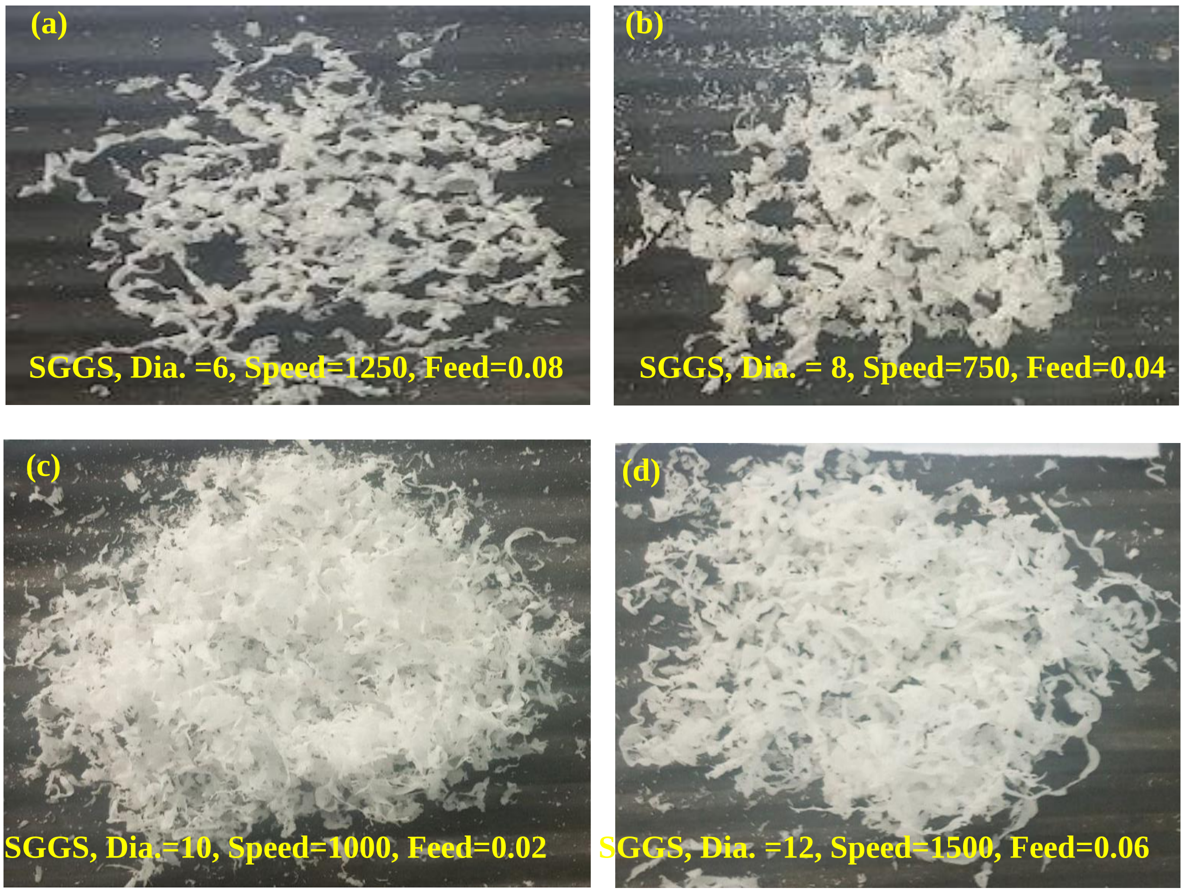

Figure 4.44: Chip formation during machining of SGGS (1) - hybrid composite

From Figure 4.44. We considered that chip sizes are highly influenced by layer sequences, drill diameter, speed, and feed rate. We observed that continuous, decrease in chip section, and curl-shaped chips are obtained at a diameter of 6mm, speed of 1250rpm, and feed rate of 0.08mm/rev. The chip at a drill diameter of 8mm and a lower speed of 750rpm was discontinuous but thicker in size. When drilling with a diameter of 12mm, speed of 1500rpm, and feed was 0.06mm/rev we obtain continuous but thin and not curled chip generation, whereas discontinued chips obtained at 10mm diameter, 0.02mm/rev feed, and 1000rpm speed and at a lower feed rate while the size of the chips was increasing with feed rate increases to 0.08mm/rev so that its surface roughness was affected in that manner for SGGS type of composite above. Generally, the chip length decreases as a result of the feed rate decreasing more for the SGGS stacking sequence material.

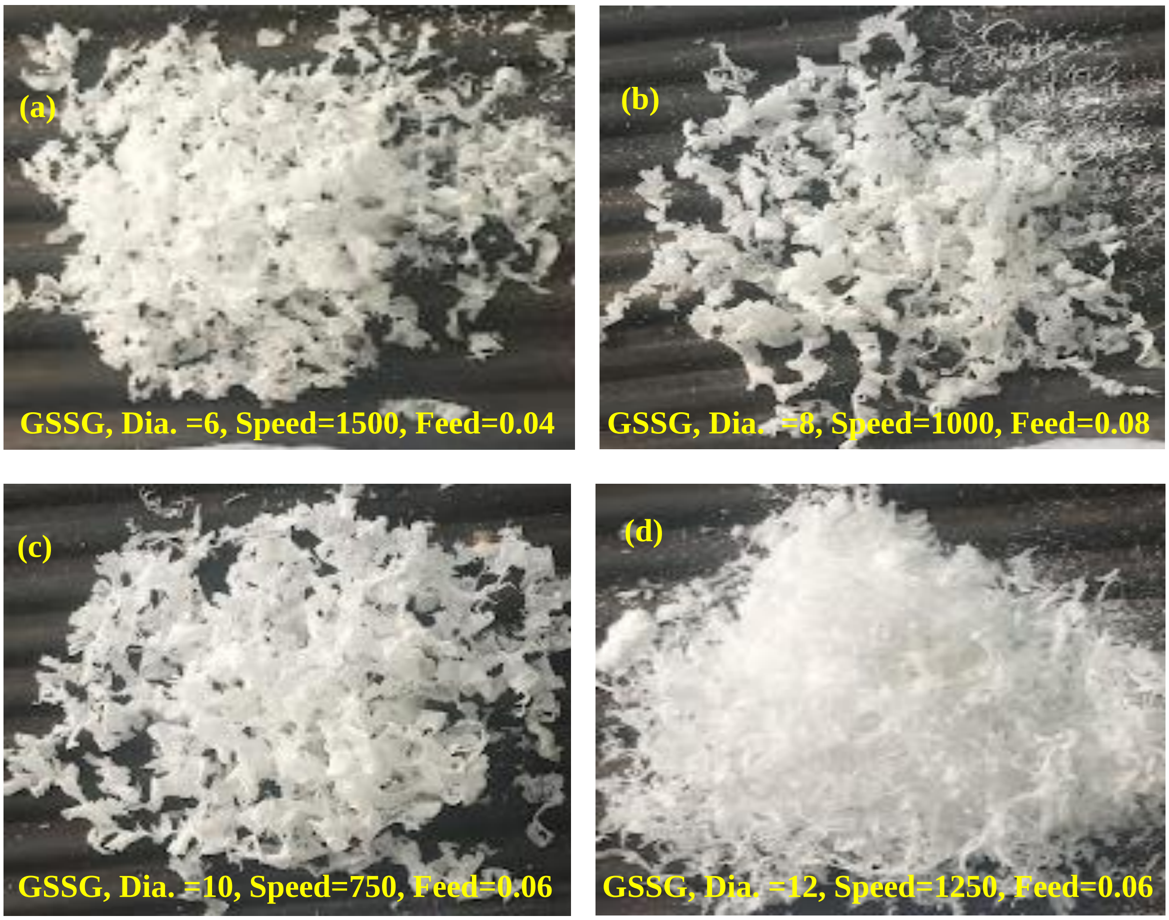

Figure 4.45: Chip formation during machining of GSSG (2) - hybrid composite

From Figure 4.45. We observed that GSSG layer arrangement material at a diameter of 6mm, speed 1500rpm, and feed of 0.04mm/rev shows thicker and discontinuous chips are obtained, at a diameter of 8mm, speed 1000rpm, and feed rate of 0.08mm/rev shows continuous and curled chips, whereas thicker, curled, and continuous at diameter 10mm, speed 750rpm and feed of 0.06mm/rev also, discontinuous, powdery, and brighter chips are obtained at diameter 12mm, speed 1250rpm, and feed of 0.06mm/rev due to the incorporation of synthetic fiber of glass.

Generally, during chip segment formation, the low hardness and higher ductility of HFRP chips caused an increase in the sticky period at the drill-chip interface and a reduction in the slip periods, as the polymer began to melt at a higher cutting temperature, usually around 60°C (Ismail et al., 2016).

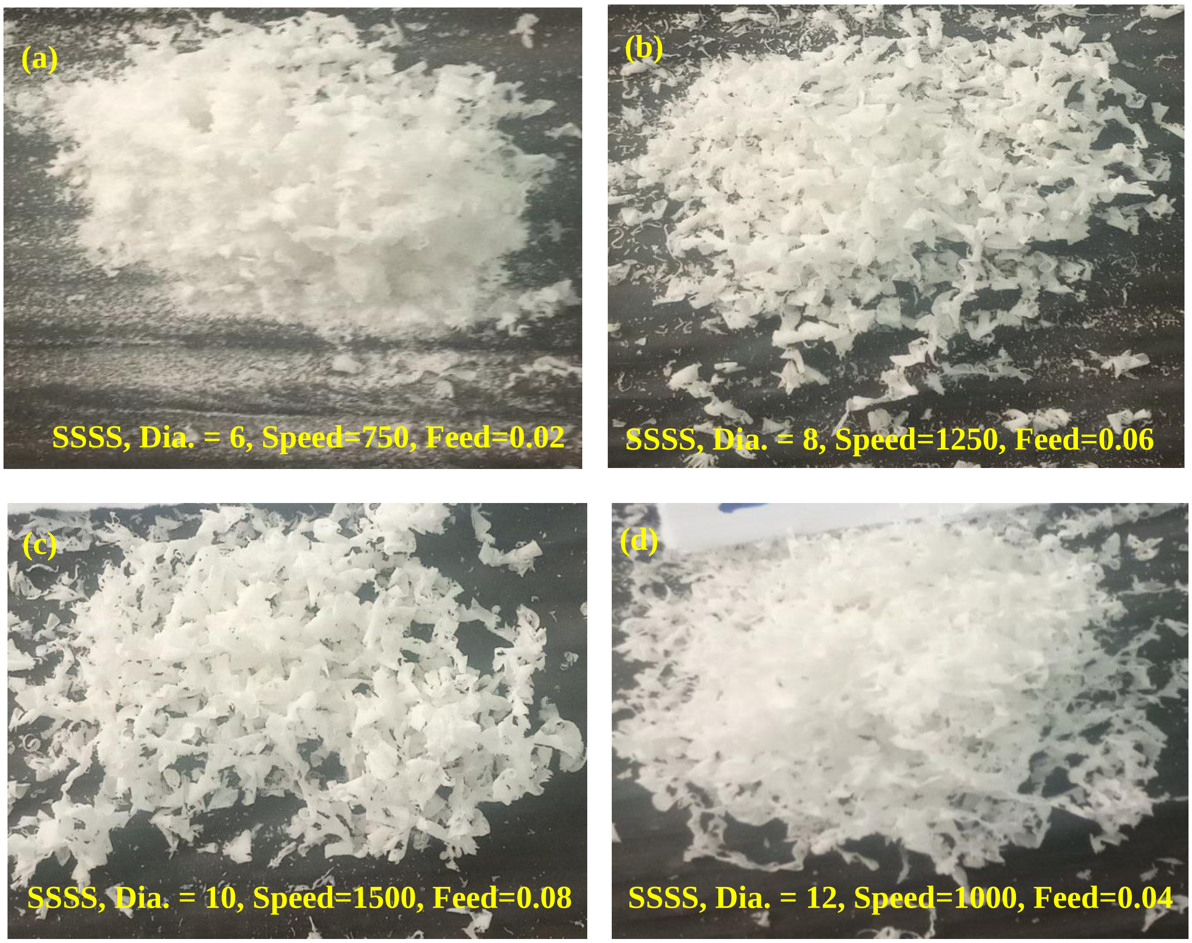

Figure 4.46: Chip formation during machining of SSSS (3) - hybrid composite

It is quite clear from Figure 4.46 that the length of the chips obtained from sisal (SSSS)-Polyester laminates are adequately short and powder forms at a diameter of 6mm, speed of 750rpm, and feed rate of 0.06mm/rev. Also, thicker and short chips are obtained at a diameter of 8mm, a speed of 1250rpm, 0.06mm/rev, a diameter of 10, a speed of 1500rpm, and a feed rate of 0.08mm/rev. Whereas continuous and curled chips are obtained at diameter 12, speed 1000, and feed of 0.04mm/rev. As compared to those of other materials due to their nature as a thermosetting polyester polymer and the higher brittleness of sisal fiber.

Short or smaller size, powder, and discontinuous chip phenomenon can be attributed to the greater thermal conductivity of the FRP sample as the chips of sisal FRP are subjected to more heat, and cooled instantly immediately after they are withdrawn from the cutting region or shearing zone and resultantly, became harder, brittle and produced dust-like chip sizes we observed the same phenomena on (Ismail et al., 2016).

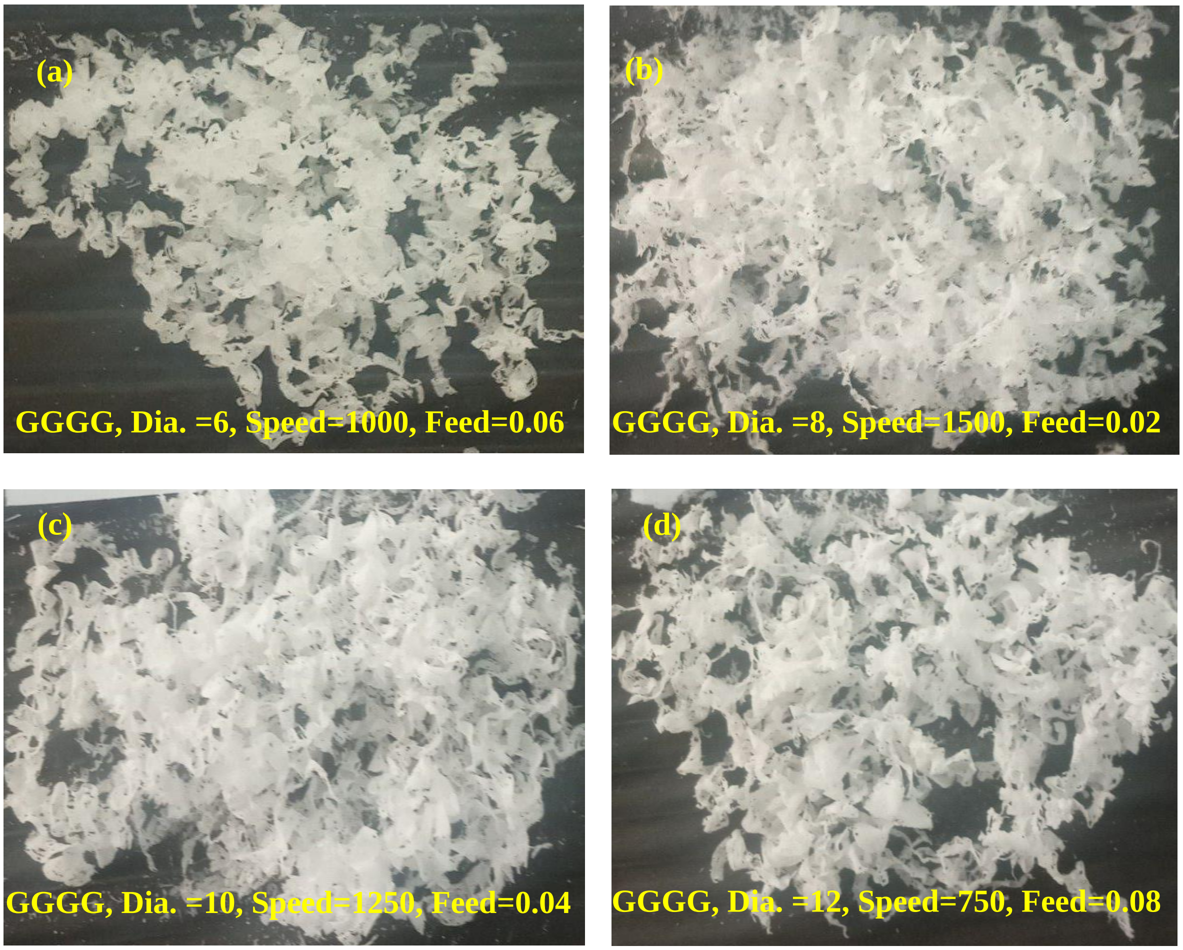

Figure 4.47: Chip formation during machining of GGGG (4) - hybrid composite

It was quite clear from Figure 4.47 that the length of the chips obtained from non-hybrid glass FRP composite laminates was adequately long and continuous but very thin as compared to that pure sisal and hybrids composite this characteristic of chips occurred mainly due to the differences in stacking sequences on the composite material and the lower brittleness nature of glass fiber.

Generally, the characteristic of the powder type of chip formed was also due to the brittle nature of the polymer material with a natural fiber combination. Low feed in conjunction with high spindle speed results in the formation of powdery chips as thermoset resin (polyester) fractures early because of the high strain rates induced. At the same time, the high feed and low spindle speed of SGGS of (c), GGGG (b) composite results in the formation of bulkier chips SSSS (d). Also, the diameter of the drill tool alters the chip characteristics. The chip obtained with different diameters such as a 6mm, 8mm, 10mm, and 12mm drilling tool for samples 1 (SGGS), 2 (GSSG), 3 (SSSS), and 4 (GGGG) was shown in Figure. 4.42, 4.43, 4.44, and 4.45 respectively.

It was observed that there was much difference in chip length and thickness for the different drill bit diameters in all composite specimens. But the thickness of the chips was lower when the chips are produced using a smaller diameter drill bit. With low feed in conjunction with low speed, a smaller diameter drill tool results in powdery chips for all composite specimens which are good for surface roughness in this research. However, with high feed-in conjunction with high speed, the chip length and thickness are somewhat higher for all composite specimens excluding sample 4 (GGGG). Because there was only glass fiber in sample 4 (GGGG) which was brittle so it fractures early.

4.7 Morphological Analysis of Drilled Hole

4.7.1.1 Morphological analysis of the drilled specimens

The surface morphology of the composites was examined through scanning electron microscopy (SEM) and 3D optical profilometer analysis. The SEM micrographs show the agglomeration of fiber, interfacial bonding between the fiber and the matrix, and dispersion of the fiber into the matrix (Manickam Ramesh et al., 2016). Figure 4.48. shows the micrographs of the drilled surfaces, observed in the drilling of hybrid sisal/glass composites shows the image of smooth surface texture for the drilled hole, drilled with a high-speed steel drill with 1500 rpm spindle speed, a feed rate of 0.02 mm/rev, SGGS layering arrangement, and 6mm drill diameter. It was attributed to the reduction in drill diameter, increase in speed, and lowering feed rate providing better quality drilled holes.

The drilling of composites with an HSS drill bit shows defects such as fiber fractures, fiber pull-out, delamination, groove, voids, deformation, porosity, cavities, and debonding of fibers from the matrix, etc. as illustrated in Figure 4.48 and Figure 4.49 rough surface texture that occurred with the high-speed steel tools. The surfaces of the hole drilled with an HSS drill have large fiber pullouts and high surface roughness because of the generation of a higher thrust force (Margabandu & Subramaniam, 2020). From the SEM images, it was visible that debonding, fiber pull-outs and matrix failure are the dominant factors, which affect the machinability of composite materials. Evaluation of surface morphology shows the typical defects such as fiber pullout, voids, and internal delamination in the experiments (Maleki et al., 2018).

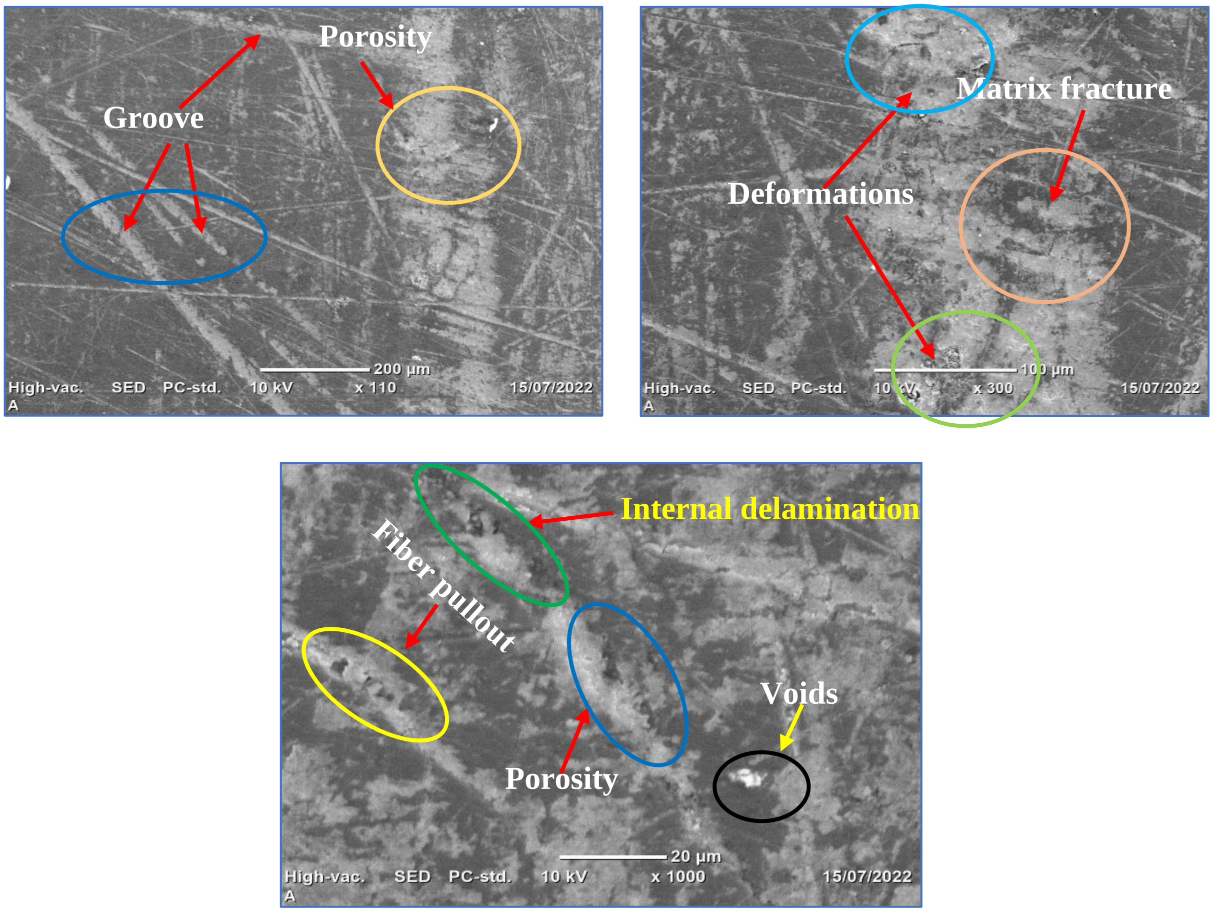

Figure 4.48: SEM micrographs of the optimum surface's roughness hole

For the same reason, fiber pullout and fiber debonding were observed during the drilling of sisal-glass polyester laminates. Therefore, the predominant form of damage observed during the drilling of sisal-glass polyester laminates was overhanging a bunch of uncut fibers at the exit of the hole. Debonding between the fibers and matrix was also detected in the microscopic image of the drilled hole side wall for sisal-polyester laminates. The bending of fibers protruding out of the hole side wall was specifically observed during the drilling of sisal and glass-polyester laminates. Furthermore, protrusion of clustered fibers was observed under 3D optical profilometer observation, during the drilling of sisal-glass polyester laminates. However, the buckling of fibers and debonding between the fibers and matrix are the two major damage phenomena observed during the 3D optical profilometer examination Figure 4.49. The appearance of internal delamination may be because of the material defect encountered during the process of the composite material. Fine scratches are observed on the drilled holes of the hybrid sisal glass FR polyester composite materials.

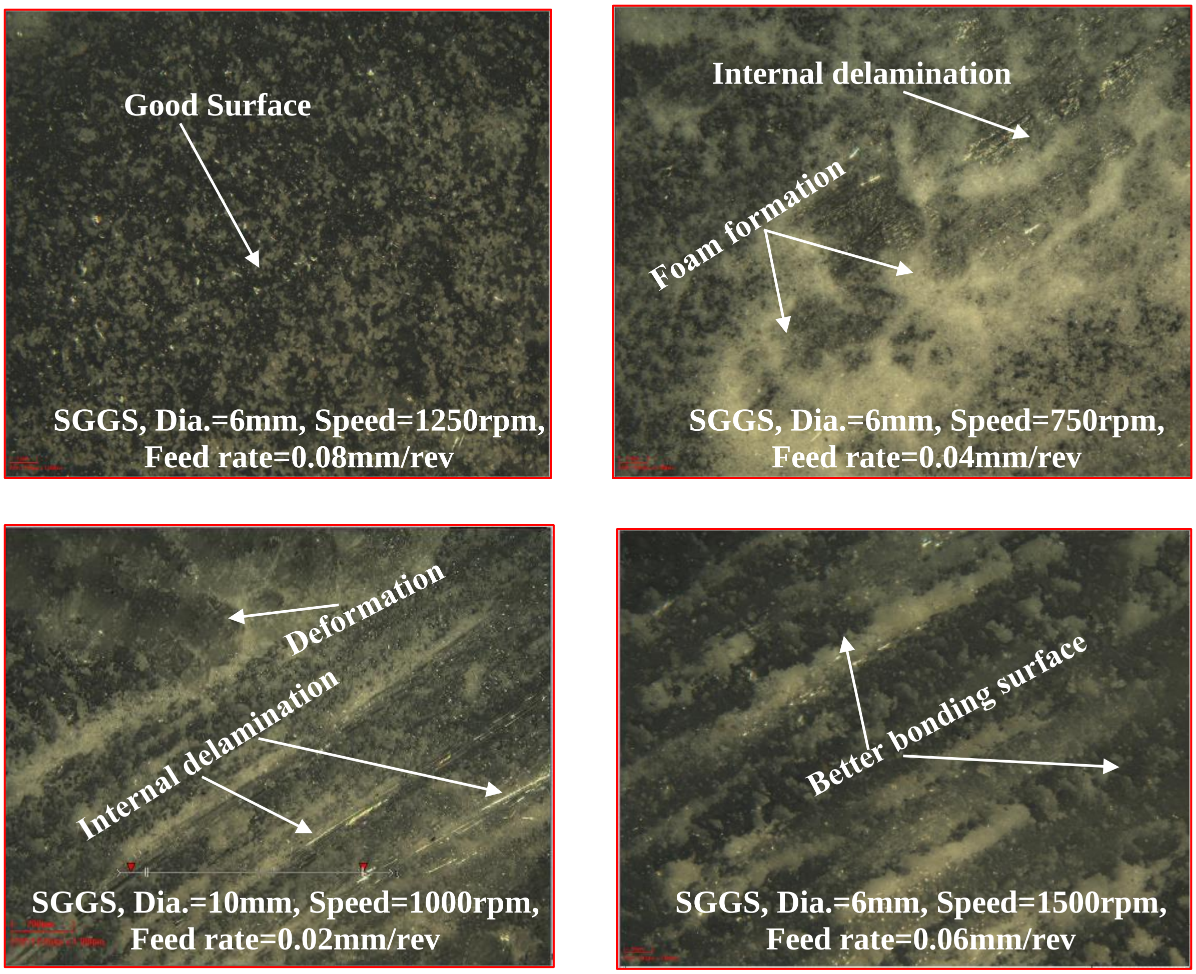

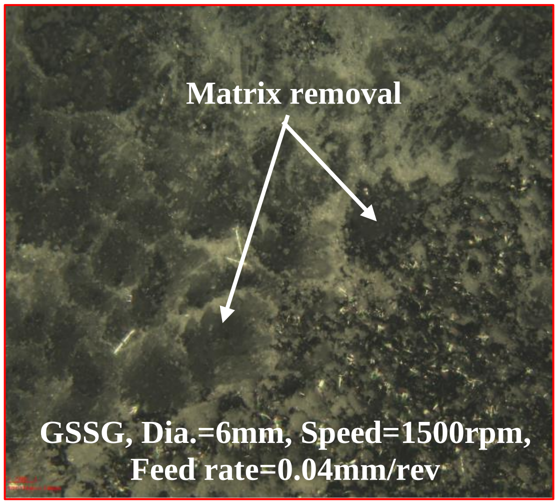

GSSG, Dia.=6mm, Speed=1500rpm, Feed rate=0.04mm/rev

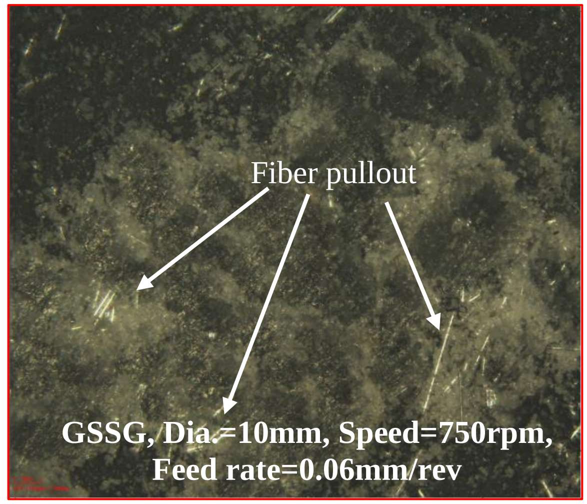

GSSG, Dia.=10mm, Speed=750rpm, Feed rate=0.06mm/rev

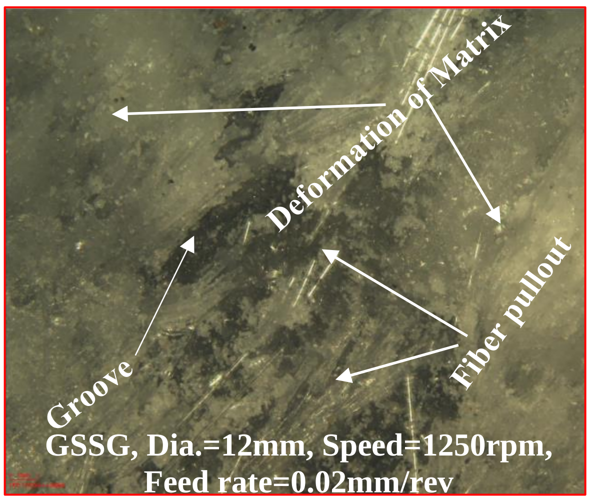

GSSG, Dia.=12mm, Speed=1250rpm, Feed rate=0.02mm/rev

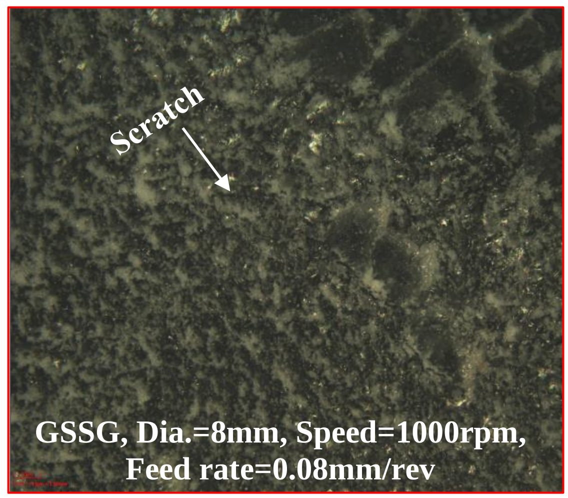

GSSG, Dia.=8mm, Speed=1000rpm, Feed rate=0.08mm/rev

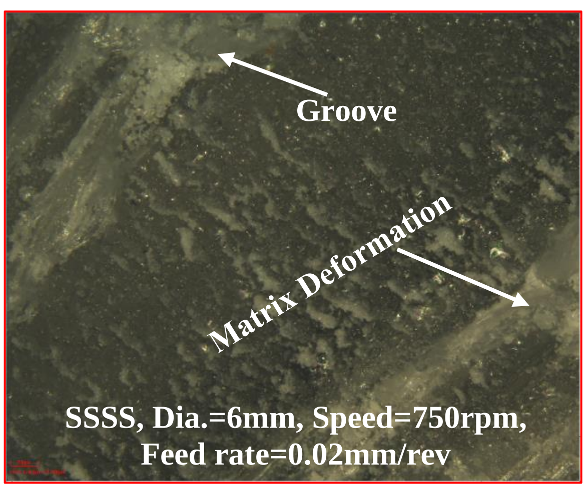

SSSS, Dia.=6mm, Speed=750rpm, Feed rate=0.02mm/rev

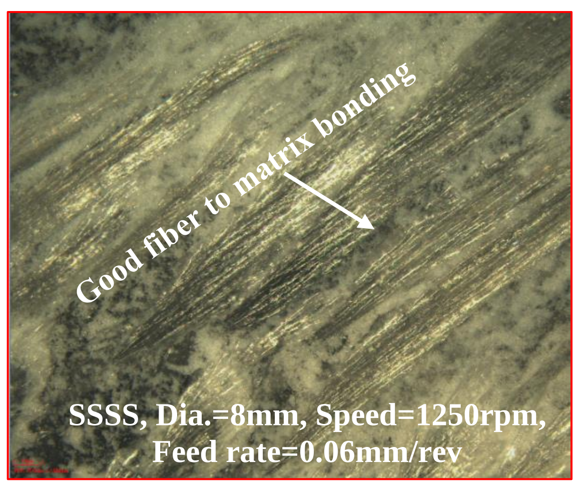

SSSS, Dia.=8mm, Speed=1250rpm, Feed rate=0.06mm/rev

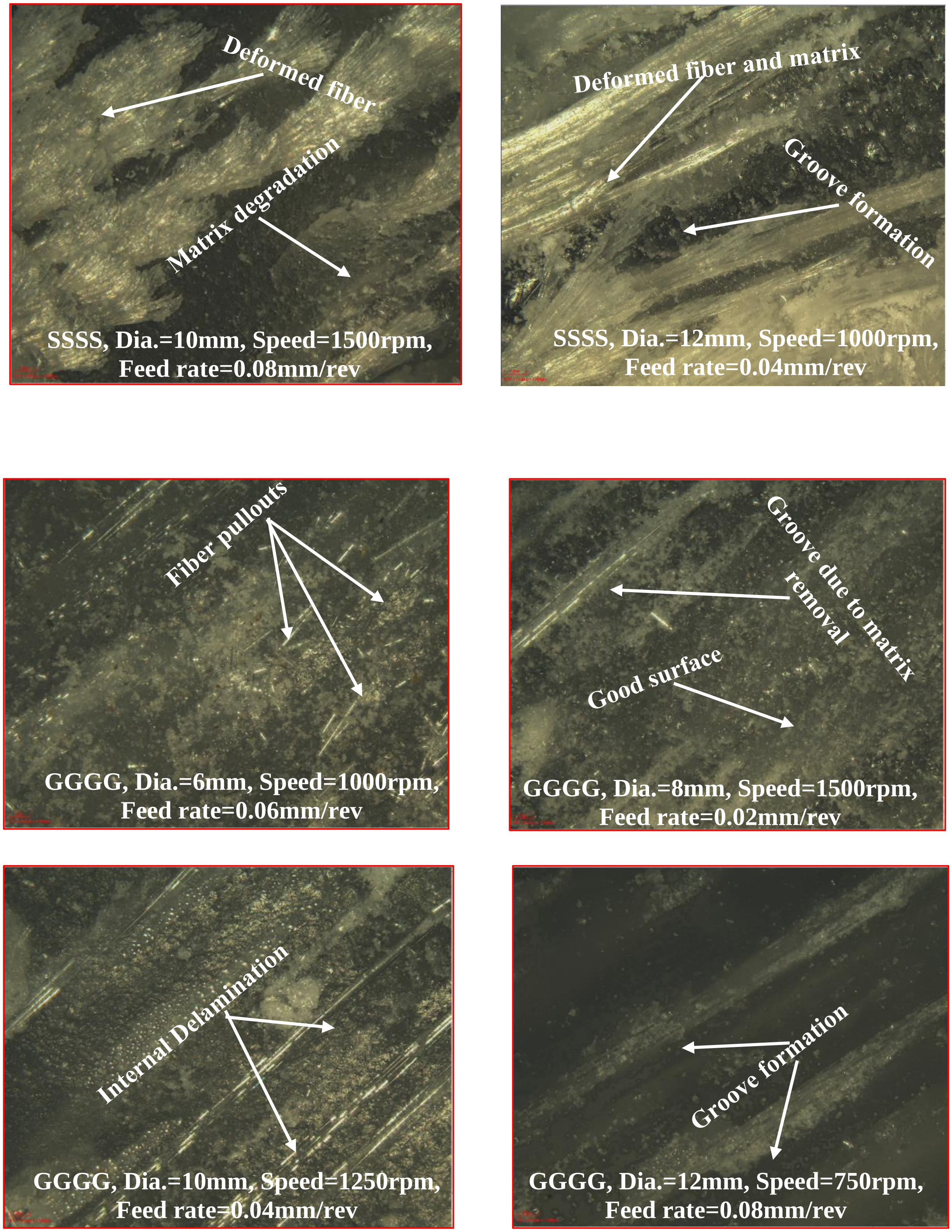

Figure 4.49: 3D optical profilometer view of hole for different drilling parameters

CHAPTER FIVE

CONCLUSIONS AND FUTURE WORKS

5.1 Summary of Findings and Conclusions

In this study, sisal fibers are extracted manually from sisal plants and glass fiber from the local market. Alkaline and acid treatment was carried out for sisal fiber at 5% NaOH and 2% HCl acid concentration to remove cellulose, lignin, and other fats and finally washed using distilled water. Next to that the sisal/glass fibers reinforced polyester hybridized composite material was fabricated and characterized the mechanical properties specifically Tensile, flexural, impact, and hardness strength by using laboratory tests.

Machining trials by drilling holes on glass-sisal hybrid polyester were developed, and the effect of cutting parameters (feed, speed, stacking sequence, and drill diameter) and the drilling-induced damages, mainly entry and exit delamination, circularity(roundness) error, and surface roughness. The quality of the drilled holes was compared based on the delamination factor and the surface roughness, as analyzed by the ImageJ software, and 3D optical surface profiles of drilled glass-sisal hybrid fiber-reinforced composite samples were carried out experimentally using Taguchi and grey relational analysis method. Also, the chip analysis and hole morphology is analyzed using SEM. In general, from the experimental results, the following conclusions were made:

- According to the literature, the behavior of natural fiber composites was inferior to that of synthetic fiber composites. However, the mechanical behavior of natural fiber was enhanced with hybridization, as confirmed by this work. The mechanical properties of the composite depend on the laminate stacking sequences and the best behavior was observed for the sisal/glass composite, being a potential replacement for glass fiber.
- The hybrid composites showed in-between properties between pure glass and pure sisal polyester composites. For greater impact and tensile strength, there must be glass fiber layers at the center of sisal fibers, whereas for hardness and flexural there must be glass fiber layers at extreme places.

- It was observed that during flexural testing the fracture was quite located with no damage in regions far from the fractures. This behavior indicates good adhesion between the layers of natural and synthetic fibers, despite the discrepancy in their properties.
- The hybrid composites with better drilling properties can withstand the maximum tensile strength of 78.4 MPa, flexural strength of 122.4MPa, impact strength of 9.333 $J/mm^{2,}$ and Hardness of 96.5 MPa.
- The hybrid composites showed in-between properties between pure sisal and pure glass polyester composites. For greater tensile and flexural strength for sisal-glass hybrid composites, there must be glass fiber layers at the center.
- The contribution made by cutting speed, feed rate, drill diameter, and stacking sequences, was high towards minimizing the entry and exit side of the delamination, circularity(roundness) error, and surface roughness outputs.
- The entry and exit delamination factors mainly depend on the material placed at the top and bottom of a composite plate thus, the entry and exit delamination factors for the produced holes can show large differences.
- An HSS twist drill with a smaller drill diameter was suggested for drilling the hybrid fiber-reinforced polymer composites as it produces lower delamination factors and roundness error with low surface roughness compared to non-hybrid composites but needs frequently changing to gate good surface finish.
- The minimum delamination factor and surface roughness of the composite sample for the optimum drilling are observed at spindle speeds of 1500 rpm, feed rate of 0.02 mm/rev, 6mm drill diameter, and sisal-glass hybrid composite with an outer layer with sisal fiber. Therefore, the optimum drilling condition, hole quality, and surface finish occur at higher speeds, and lower feed rates, with the HSS twist drill bit of diameter of 6mm, and SGGS type of composite.
- The minimum circularity(roundness) error of the composite sample for the optimum drilling was observed at spindle speeds of 750 rpm, feed rate of 0.02 mm/rev, 6mm drill diameter, and sisal-glass hybrid composite with an outer layer with sisal fiber. Which

was occur at the lowest speeds, and lower feed rates, with the HSS twist drill bit of diameter of 6mm, and SGGS type of composite.

- From hybrid Taguchi and grey relational analysis, we obtain that Cutting speed, feed rate, drill diameter, and stacking sequences all are influencing factors for minimizing the delamination factor, circularity, and surface roughness.
- The dimension and shape of the chip were highly influenced by the drilling parameters
- The image analysis using ImageJ, the 3D optical profilometer, and SEM micrographs image of the drilled hole revealed that Fiber pullouts, uncut fiber, fiber deformation, fiber and matrix uncut, matrix cracking and deterioration, internal delamination are the dominant factors of the hole during machinability was which affect the drilling of composite materials. Further, it was visible that the quality of the holes made with a small drill bit diameter in hybrid composites was much superior to the hole made with a big HSS drill bit diameter in woven sisal/random glass fabric-reinforced polyester composite laminates.
- From the experimental investigation result, it was generalized that the hybrid glass/sisal hybrid fiber reinforced polyester matrix composite material has significantly good mechanical strength and machinability.
- Although the replacement of a portion of E-glass will increase the overall cost of FRP composite, however, it was still worth supplanting the low cost of pure FRP composites. Hybrid composites with lighter weight and higher strength are one of the keys to moderating the shortage of petrol fuel as well as reducing the environmental burden of automotive vehicles or aerospace structures.

5.2 Recommendations

Based on the result and conclusions found from this study, the following recommendations were made

- It will be better to use the hybrid glass-sisal fiber reinforcement since we can get intermediate mechanical properties and have relatively good machinability properties also minimum cost relative to pure synthetic composites.
- This study was limited to four layers of glass-sisal fiber due to the cost of a lab from the preparation to mechanical testing and machining, so it's better to do the remaining layering arrangement.
- It will be good if the department prepared seminars for the postgraduate student during their thesis work so that they will accomplish their work competitively and timely.
- It will be good if there is a good relationship and collaboration between the departments as well as other outside institutes to facilitate fairly usage of different testing machines for student

5.3 Future Works

- Preparation of decorticating machines to get fiber from its leave easily. Also, it will be better to have a waving machine to wave the natural fiber in different fiber orientations.
- The study can be further extended to different fabrication techniques and study its parametric effect on mechanical, physical, and tool wear conditions.
- The study can be further extended to analyze the thrust force and torque of drilling.
- To understand the phenomenon of drilling-induced damage completely, the analysis of heat generation and its distribution in the drill and composite laminate interaction zone will be necessary to completely understand the drilling-induced damage both qualitatively and quantitatively so it will be essential to be done.
- The study can be further extended using a backplate to reduce the entry and exit delamination.
- The study can be conducted for the development of natural and synthetic fiber, optimization of drilling composite using simulation, and experimental analysis so that we can reduce the cost of machining.

Research Fund Acknowledgemnt

This research project is funded by Adama Science and Technology University under the grant number Reasearch Grant No: ASTU/SM-R/588/22, Adama , Ethiopia.

Reference

Abilash, N., & Sivapragash, M. (2016). Optimizing the delamination failure in bamboo fiber reinforced polyester composite. *Journal of King Saud University - Engineering Sciences*, *28*(1), 92–102. https://doi.org/10.1016/j.jksues.2013.09.004

Alagappan, K. M., Vijayaraghavan, S., Jenarthanan, M. P., & Giridharan, R. (2020). Optimization of process parameters on drilling of natural fibres reinforced in epoxy resin matrices using Taguchi–Grey relational analysis. *Multidiscipline Modeling in Materials and Structures*, *16*(5), 937–949. https://doi.org/10.1108/MMMS-06-2019-0108

Alavudeen, A., Rajini, N., Karthikeyan, S., Thiruchitrambalam, M., & Venkateshwaren, N. (2015). Mechanical properties of banana/kenaf fiber-reinforced hybrid polyester composites: Effect of woven fabric and random orientation. *Materials and Design*, *66*(PA), 246–257. https://doi.org/10.1016/j.matdes.2014.10.067

Ameur, M. F., Djilani, A. H., Zitoune, R., & Krishnaraj, V. (2022). *Experimental and numerical investigations of the damages induced while drilling fl ax / epoxy composite*. *56*(2), 295–312. https://doi.org/10.1177/00219983211055825

Baloyi, R. B., Ncube, S., Moyo, M., Nkiwane, L., & Dzingai, P. (2021). Analysis of the properties of a glass/sisal/polyester composite. *Scientific Reports*, *11*(1), 1–10. https://doi.org/10.1038/s41598-020-79566-7

Bekele, A. E., Lemu, H. G., & Jiru, M. G. (2022). Exploration of Mechanical Properties of Enset–Sisal Hybrid Polymer Composite. *Fibers*, *10*(2). https://doi.org/10.3390/fib10020014

Bhoopathi, R., & Ramesh, M. (2020). Optimization of drilling output responses of eggshell fillers reinforced hemp/glass fibres hybrid composites. *Materials Today: Proceedings*, *46*(xxxx), 3245–3250. https://doi.org/10.1016/j.matpr.2020.11.286

Caggiano, A. (2018). Machining of fibre reinforced plastic composite materials. In *Materials* (Vol. 11, Issue 3). MDPI AG. https://doi.org/10.3390/ma11030442

Chaudhary, V., & Ahmad, F. (2020). A review on plant fiber reinforced thermoset polymers for structural and frictional composites. *Polymer Testing*, *91*(May), 106792. https://doi.org/10.1016/j.polymertesting.2020.106792

Debnath, K., Singh, I., & Dvivedi, A. (2014). Drilling characteristics of sisal fiber-reinforced epoxy and polypropylene composites. *Materials and Manufacturing Processes*, *29*(11–12), 1401–1409. https://doi.org/10.1080/10426914.2014.941870

Durão, L. M. P., Gonçalves, D. J. S., Tavares, J. M. R. S., De Albuquerque, V. H. C., Panzera, T. H., Silva, L. J., Vieira, A. A., & Baptista, A. M. (2013). Drilling delamination outcomes on glass and sisal reinforced plastics. *Materials Science Forum*, *730–732*, 301–306. https://doi.org/10.4028/www.scientific.net/MSF.730-732.301

Durão, L. M. P., Tavares, J. M. R. S., de Albuquerque, V. H. C., Marques, J. F. S., & Andrade, O. N. G. (2014). Drilling damage in composite material. *Materials*, *7*(5), 3802–3819. https://doi.org/10.3390/ma7053802

Elsad, R. A., EL-Wazery, M. S., & EL-Kelity, A. M. (2020). Effect of Water Absorption on the Tensile Characteristics of Natural/ Synthetic Fabrics Reinforced Hybrid Composites. *International Journal of Engineering, Transactions B: Applications*, *33*(11), 2339–2346. https://doi.org/10.5829/ije.2020.33.11b.24

Flynn, J., Amiri, A., & Ulven, C. (2016). Hybridized carbon and flax fiber composites for tailored performance. *Materials and Design*, *102*, 21–29. https://doi.org/10.1016/j.matdes.2016.03.164

Hale, P., & Ng, E. G. (2021). 3D finite element model on drilling of cfrp with numerical optimization and experimental validation. *Materials*, *14*(5), 1–22. https://doi.org/10.3390/ma14051161

Ismail, S. O., Dhakal, H. N., Popov, I., & Beaugrand, J. (2016). Analysis and impacts of chips formation on hole quality during fibre-reinforced plastic composites machining. *Advances in Transdisciplinary Engineering*, *3*, 143–148. https://doi.org/10.3233/978-1-61499-668-2-143

Jani, S. P., Kumar, A. S., Khan, M. A., & Kumar, M. U. (2016a). Machinablity of Hybrid Natural Fiber Composite with and without Filler as Reinforcement. *Materials and Manufacturing Processes*, *31*(10), 1393–1399. https://doi.org/10.1080/10426914.2015.1117633

Jani, S. P., Kumar, A. S., Khan, M. A., & Kumar, M. U. (2016b). Machinablity of Hybrid Natural Fiber Composite with and without Filler as Reinforcement. *Materials and Manufacturing Processes*, *31*(10), 1393–1399. https://doi.org/10.1080/10426914.2015.1117633

Jayabal, S., & Natarajan, U. (2010). Optimization of thrust force, torque, and tool wear in drilling of coir fiber-reinforced composites using Nelder-Mead and genetic algorithm methods. *International Journal of Advanced Manufacturing Technology, 51*(1–4), 371–381. https://doi.org/10.1007/s00170-010-2605-7

Jayabal, S., Natarajan, U., & Sekar, U. (2011). Regression modeling and optimization of machinability behavior of glass-coir-polyester hybrid composite using factorial design methodology. *International Journal of Advanced Manufacturing Technology*, *55*(1–4), 263–273. https://doi.org/10.1007/s00170-010-3030-7

Jayabal, S., Velumani, S., Navaneethakrishnan, P., & Palanikumar, K. (2013). Mechanical and machinability behaviors of woven coir fiber-reinforced polyester composite. *Fibers and Polymers, 14*(9), 1505–1514. https://doi.org/10.1007/s12221-013-1505-5

Jenarthanan, M. P., Karthikeyan, M., & Neeli, N. (2017). Mathematical modeling of delamination factor on drilling of ARALL composites through RSM. *Multidiscipline Modeling in Materials and Structures, 13*(4), 578–589. https://doi.org/10.1108/MMMS-01-2017-0003

Jenarthanan, M. P., Prakash, A. L., & Jeyapaul, R. (2016). Experimental investigation and analysis of factors influencing delamination and surface roughness of hybrid GFRP laminates using Taguchi technique. *Pigment and Resin Technology*, *45*(6), 463–475. https://doi.org/10.1108/PRT-03-2015-0035

John, K. M., & Kumaran, S. T. (n.d.). *A feasible strategy to produce quality holes using temperature-assisted drilling on CFRP*. https://doi.org/10.1007/s00170-020-06089-w/Published

Köklü, U., Demir, O., Avcı, A., & Etyemez, A. (2017). Drilling performance of functionally graded composite: Comparison with glass and carbon/epoxy composites. *Journal of Mechanical Science and Technology, 31*(10), 4703–4709. https://doi.org/10.1007/s12206-017-0916-4

Kumar, D., Singh, K. K., & Zitoune, R. (2016a). Experimental investigation of delamination and surface roughness in the drilling of GFRP composite material with different drills. *Advanced Manufacturing: Polymer and Composites Science, 2*(2), 47–56. https://doi.org/10.1080/20550340.2016.1187434

Kumar, D., Singh, K. K., & Zitoune, R. (2016b). Experimental investigation of delamination and surface roughness in the drilling of GFRP composite material with different drills. *Advanced Manufacturing: Polymer and Composites Science*, *2*(2), 47–56. https://doi.org/10.1080/20550340.2016.1187434

Lee, J. H., Ge, J. C., & Song, J. H. (2021). Study on burr formation and toolwear in drilling cfrp and its hybrid composites. *Applied Sciences (Switzerland)*, *11*(1), 1–14. https://doi.org/10.3390/app11010384

Lopez-Arraiza, A., Amenabar, I., Agirregomezkorta, A., Sarrionandia, M., & Aurrekoetxea, J. (2012). Experimental analysis of drilling damage in carbon-fiber reinforced thermoplastic laminates manufactured by resin transfer molding. *Journal of Composite Materials*, *46*(6), 717–725. https://doi.org/10.1177/0021998311414218

Maleki, H. R., Hamedi, M., Kubouchi, M., & Arao, Y. (2018). *Experimental study on drilling of jute fiber reinforced polymer composites*. https://doi.org/10.1177/0021998318782376

Margabandu, S., & Subramaniam, S. (2020). An experimental investigation of thrust force, delamination and surface roughness in drilling of jute/carbon hybrid composites. *World Journal of Engineering*, *17*(5), 661–674. https://doi.org/10.1108/WJE-03-2020-0080

Mohammed, N. H., & Wolla, D. W. (2022). *Optimization of machining parameters in drilling hybrid sisal-cotton fiber reinforced polyester composites*. *9*(September 2021), 119–134. https://doi.org/10.3934/matersci.2022008

Mosisa, S., & Batu, T. (2021). Investigation of mechanical properties of bamboo/sisal fiber reinforced hybrid composite materials. *Material Science & Engineering International Journal*, *5*(2), 24–31. https://doi.org/10.15406/mseij.2021.05.00152

Nguyen, H., Zatar, W., & Mutsuyoshi, H. (2017). Mechanical properties of hybrid polymer composite. In *Hybrid Polymer Composite Materials: Properties and Characterisation*. Elsevier Ltd. https://doi.org/10.1016/B978-0-08-100787-7.00004-4

Njoku, R., Obayi, C., & Nnamchi, P. (2012). Hybrid Effect on the Mechanical Properties of Sisal Fiber and E-Glass Fiber Reinforced Polyester Composites. *Nigerian Journal of Technology*, *30*(3), 97–102. https://www.ajol.info/index.php/njt/article/view/123548

Patel, K., Gohil, P. P., & Chaudhary, V. (2018). Investigations on drilling of hemp/glass hybrid composites. *Materials and Manufacturing Processes*, *33*(15), 1714–1725. https://doi.org/10.1080/10426914.2018.1453150

Rafiquzzaman, M., Islam, M., Rahman, H., Talukdar, S., & Hasan, N. (2016). Mechanical property evaluation of glass–jute fiber reinforced polymer composites. *Polymers for Advanced Technologies*, *27*(10), 1308–1316. https://doi.org/10.1002/pat.3798

Rajkumar, D., Ranjithkumar, P., Jenarthanan, M. P., & Sathiya Narayanan, C. (2017). Experimental investigation and analysis of factors influencing delamination and thrust force during drilling of carbon-fibre reinforced polymer composites. *Pigment and Resin Technology*, *46*(6), 507–524. https://doi.org/10.1108/PRT-10-2016-0097

Rajmohan, T. (2019a). Experimental investigation and optimization of machining parameters in drilling of fly ash-filled carbon fiber reinforced composites. *Particulate Science and Technology*, *37*(1), 21–30. https://doi.org/10.1080/02726351.2016.1205686

Rajmohan, T. (2019b). Experimental investigation and optimization of machining parameters in drilling of fly ash-filled carbon fiber reinforced composites. *Particulate Science and Technology*, *37*(1), 21–30. https://doi.org/10.1080/02726351.2016.1205686

Ramesh, M., Deepa, C., Arpitha, G. R., & Gopinath, V. (2019). Effect of hybridization on properties of hemp-carbon fibre-reinforced hybrid polymer composites using experimental and finite element analysis. *World Journal of Engineering*, *16*(2), 248–259. https://doi.org/10.1108/WJE-04-2018-0125

Ramesh, M., Gopinath, A., & Deepa, C. (2016). Machining characteristics of fiber reinforced polymer composites: A review. *Indian Journal of Science and Technology*, *9*(42). https://doi.org/10.17485/ijst/2016/v9i42/101978

Ramesh, M., Palanikumar, K., & Reddy, K. H. (2014). Influence of Tool Materials on Thrust Force and Delamination in Drilling Sisal-glass Fiber Reinforced Polymer (S-GFRP) Composites. *Procedia Materials Science*, *5*, 1915–1921. https://doi.org/10.1016/j.mspro.2014.07.513

Ramesh, M, Palanikumar, K., & Reddy, K. H. (2014). Experimental Investigation and Analysis of Machining Characteristics in Drilling Hybrid Glass-Sisal-Jute Fiber Reinforced Polymer Composites Experimental Investigation and Analysis of Machining Characteristics in Drilling Hybrid Glass-Sisal-Jute Fiber Rei. *5th International & 26th All India Manufacturing Technology, Design and Research Conference (AIMTDR 2014), December*, 461(1-6).

Ramesh, Manickam, Palanikumar, K., & Reddy, K. H. (2016). *Influence of fiber orientation and fiber content on properties of sisal-jute-glass fiber-reinforced polyester composites*. *42968*, 1–9. https://doi.org/10.1002/app.42968

Rathinavel, S., Vigneshkumar, G., & Sathishkumar, U. (2015). *Optimization of thermal analysis of hybrid fibre composite on drilling process*. *2*(5), 28–37.

Refaai, M. R. A., Narayanasamy, S., Das, V. C., Prasad, D. V. S. S. S. V., Nalini, N., & Thanappan, S. (2022). Mechanical Properties of Ramie/Hemp Hybrid Composites Influenced by Stacking Arrangement and NaOH Treatment. *Advances in Polymer Technology*, *2022*. https://doi.org/10.1155/2022/8737669

Seyedbehzad G. (2015). Experimental Investigation and Modeling of Surface Machining of High-Performance Cfrp for the Aerospace Industry, MONTREAL.

Shamsuyeva, M., Hansen, O., Endres, H. J., & Abu-Jdayil, B. (2019). Review on Hybrid Carbon/Flax Composites and Their Properties. *International Journal of Polymer Science*, *2019*. https://doi.org/10.1155/2019/9624670

Shanmugam, V., Marimuthu, U., Rajendran, S., Veerasimman, A., Basha, A. M., Majid, M. S. B. A., Neisiany, R. E., Försth, M., Sas, G., Razavi, S. M. J., & Das, O. (2021). Experimental investigation of thrust force, delamination and surface roughness in drilling hybrid structural composites. *Materials*, *14*(16). https://doi.org/10.3390/ma14164468

Shireesha, Y., Nandipati, G., & Chandaka, K. (2019). Properties of hybrid composites and its applications: A brief review. *International Journal of Scientific and Technology Research*, *8*(8), 335–341.

Shunmugesh, K., & Kavan, P. (2017). Investigation and optimization of machining parameters in drilling of carbon fiber reinforced polymer (CFRP) composites. *Pigment and Resin Technology*, *46*(1), 21–30. https://doi.org/10.1108/PRT-03-2016-0029

Singh, H., Dewangan, B., & Jain, P. K. (2021). Experimental study on drilling characteristics of the hybrid sisal–jute fibre epoxy composites. *Journal of Micromanufacturing*, *4*(2), 157–168. https://doi.org/10.1177/25165984211015413

Sumesh, K. R., Kanthavel, K., & Kavimani, V. (2020). Machinability of hybrid natural fiber reinforced composites with cellulose micro filler incorporation. *Journal of Composite Materials*, *54*(24), 3655–3671. https://doi.org/10.1177/0021998320918020

Teja, P. V. S., Prakash, S., Prasad, B. N. D., Elijah, G., Ficici, F., Feito, N., Muñoz-Sánchez, A., Díaz-Álvarez, A., Loya, J. A., Milani, A. S., Muñoz-Sánchez, A., Díaz-Álvarez, J., Díaz-Álvarez, A., Cantero, J. L., Miguélez, M. H., Campos Rubio, J., Abrao, A. M., Faria,

P. E., Correia, A. E., … Giridharan, R. (2020). Analysis of the machinability of carbon fiber composite materials in function of tool wear and cutting parameters using the artificial neural network approach. *Materials*, *29*(6), 1–5. https://doi.org/10.1007/s00170-016-9010-9

Vigneshwaran, S., Uthayakumar, M., & Arumugaprabu, V. (2019). Development and sustainability of industrial waste-based red mud hybrid composites. *Journal of Cleaner Production*, *230*, 862–868. https://doi.org/10.1016/j.jclepro.2019.05.131

Vigneshwaran, Shanmugam, John, K. M., Deepak Joel Johnson, R., Uthayakumar, M., Arumugaprabu, V., & Kumaran, S. T. (2021). Conventional and unconventional machining performance of natural fibre-reinforced polymer composites: A review. *Journal of Reinforced Plastics and Composites*, *40*(15–16), 553–567. https://doi.org/10.1177/0731684420958103

Vinayagamoorthy, R., & Rajmohan, T. (2018). Machining and its challenges on bio-fibre reinforced plastics: A critical review. *Journal of Reinforced Plastics and Composites*, *37*(16), 1037–1050. https://doi.org/10.1177/0731684418778356

Xu, W., & Zhang, L. (2018). Tool wear and its effect on the surface integrity in the machining of fibre-reinforced polymer composites. *Composite Structures*, *188*(September 2017), 257–265. https://doi.org/10.1016/j.compstruct.2018.01.018

Yallew, T. B., Kumar, P., & Singh, I. (2016). A study about hole making in woven jute fabric-reinforced polymer composites. *Proceedings of the Institution of Mechanical Engineers, Part L: Journal of Materials: Design and Applications*, *230*(4), 888–898. https://doi.org/10.1177/1464420715587750

Zitoune, R., Krishnaraj, V., Sofiane Almabouacif, B., Collombet, F., Sima, M., & Jolin, A. (2012). Influence of machining parameters and new nano-coated tool on drilling performance of CFRP/Aluminium sandwich. *Composites Part B: Engineering*, *43*(3), 1480–1488. https://doi.org/10.1016/j.compositesb.2011.08.054

Appendix

Appendix-A: Mechanical Property Testing

Tensile Testing

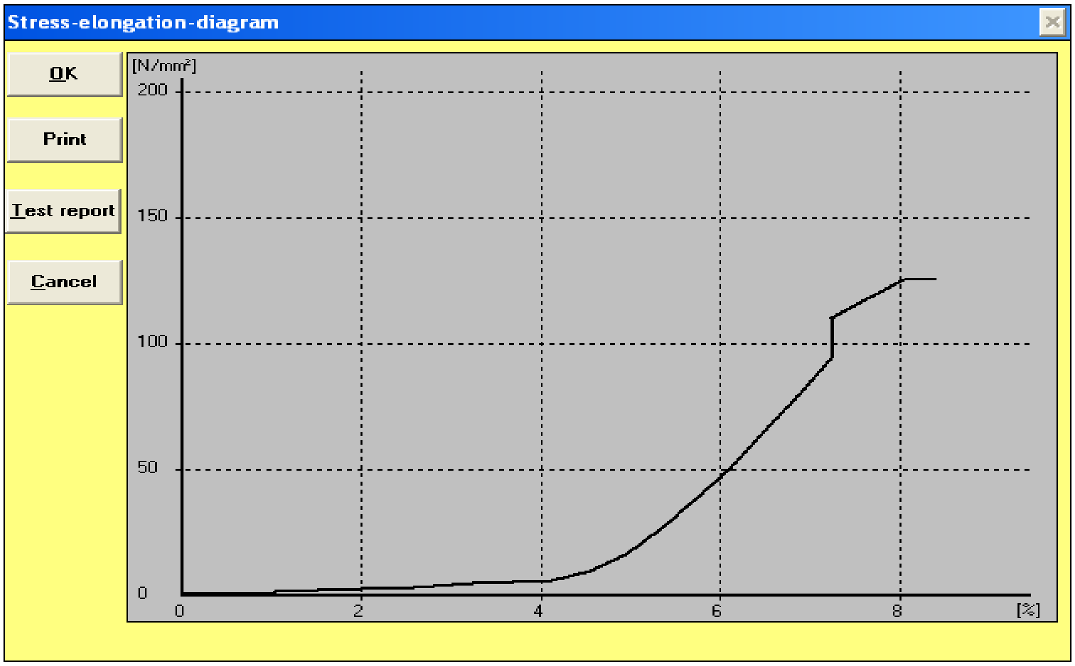

Flexural Testing

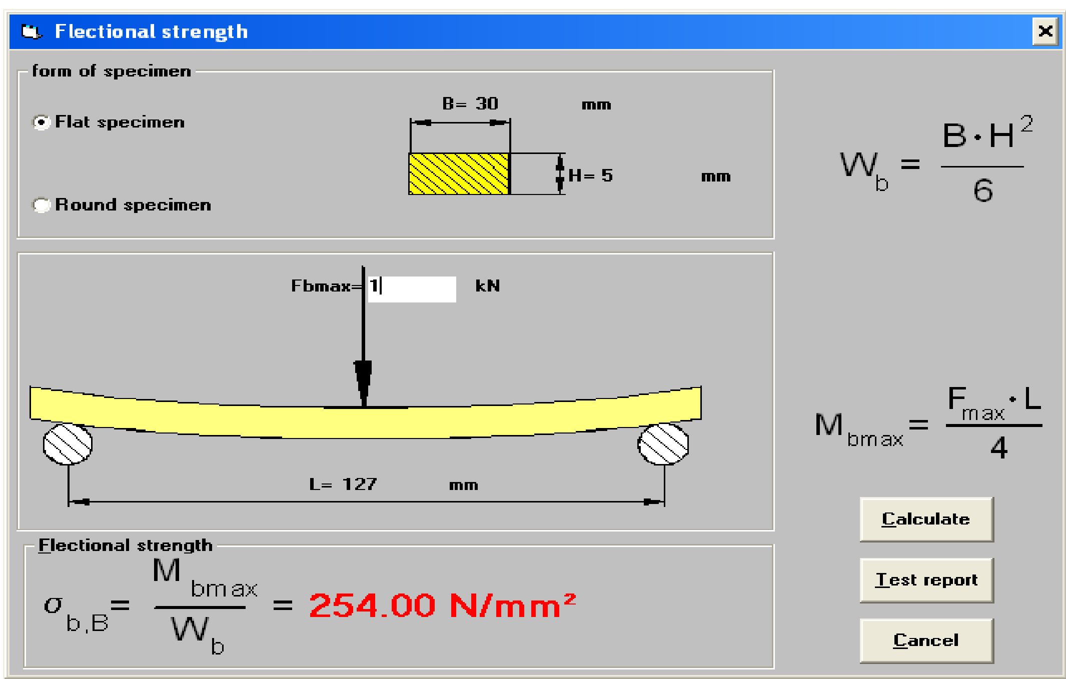

Appendix-B: Equipment, Software's and Machines used for the Study

Universal Testing Machine for Tensile, and Flexural Testing.

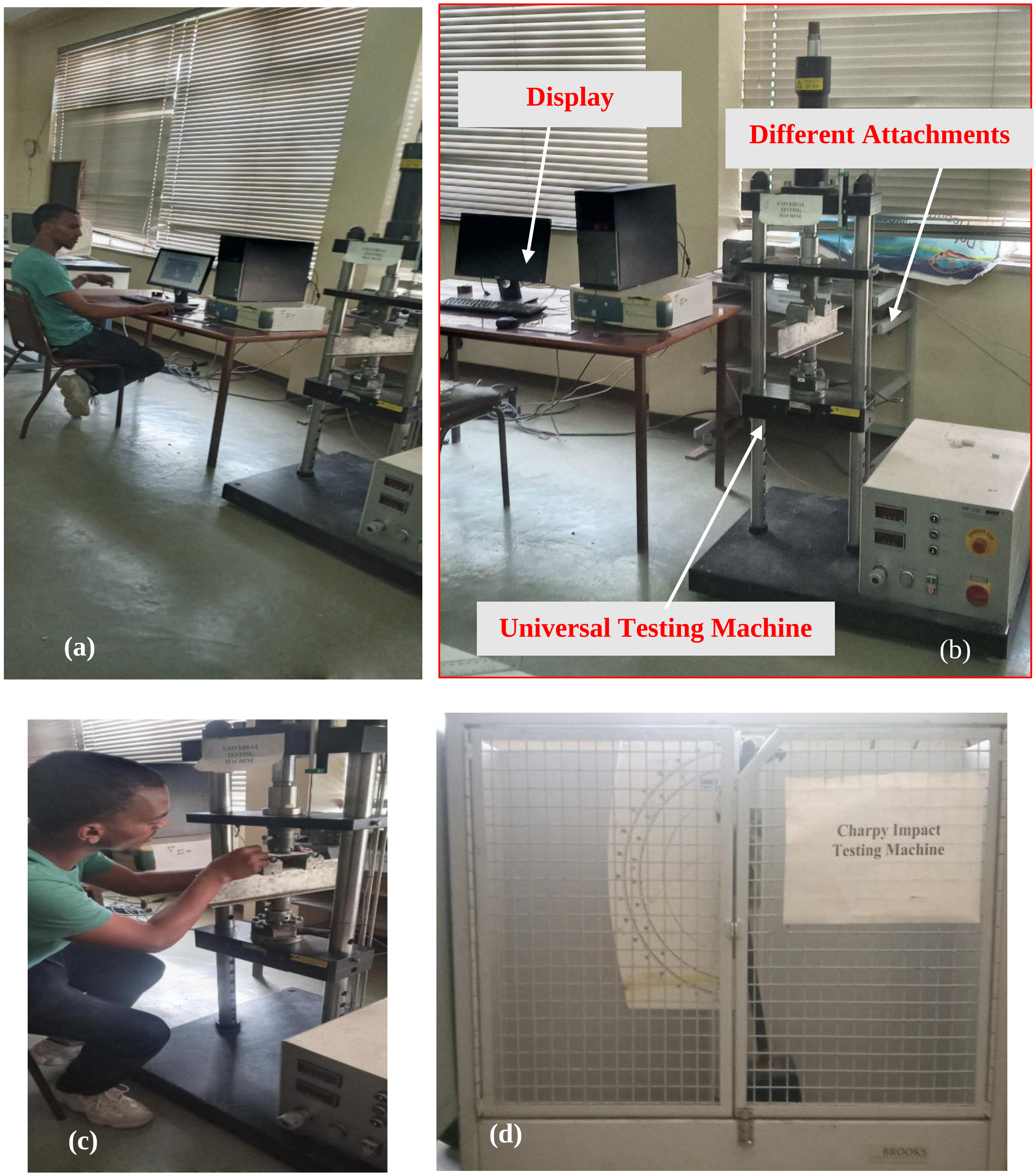

Figure 1: Mechanical Testing Machines (a) and (b) Tensile Testing, (c) Flexural Testing, (d) Impact Testing Machine

Hardness Testing

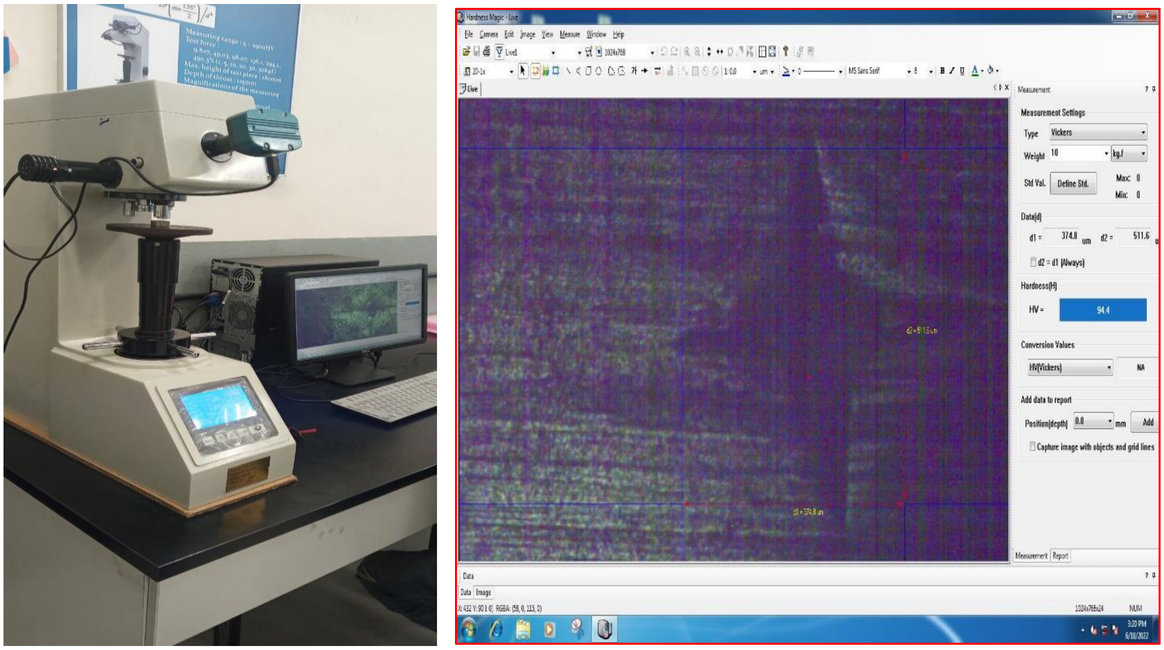

Figure 2: Vickery hardness Testing Machine and Sample Response

CNC Milling Machine

Figure 3: CNC vertical milling machine.

Mold, fiber mat preparation, and composite fabrication

Figure 4: Fabrication of composites

Surface Roughness Testing Machine

In this research 3D, the optical surface profiler was used to study the surface roughness.

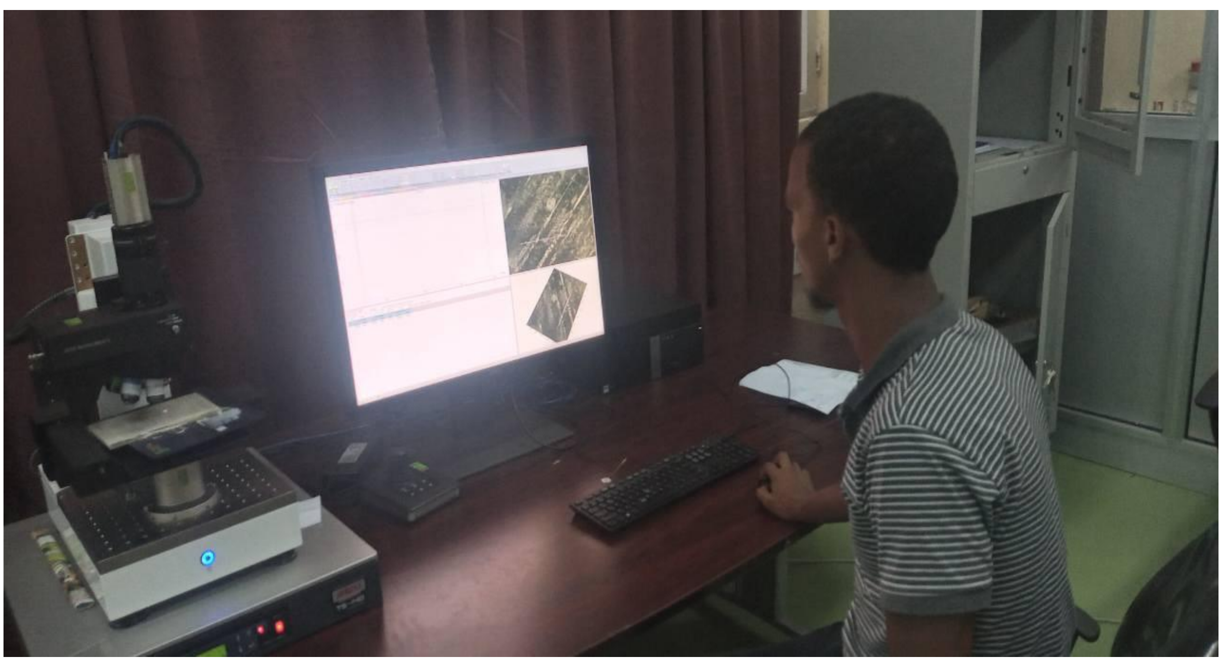

Figure 5: Zeta-20, 3D optical surface roughness measuring instrument.

Appendix-C: Drilling Code Used and Master CAM 3D Drawing

Table 1: The G-Code sample and its description for drilling composite materials.

PROGRAM	**O0250 N00000**
O0250 ………………………………	Program Name
O0250………………………………	Start with the program name
G90 G00 G95 G54 X0 YO S1250 M03; …………	Absolute positioning system, rapid move, feed per revolution, Work offset, X0, Y0, Spindle speed 1250, Spindle speed in a clockwise direction.
Z100; ………………………………	Start Z-axis at 100.
G83 X-49 Y40.5 R5. Z-10. Q1. F0.02; …………	Machine to run a peck drilling cycle, X-49, Y40.5, Quickly approach, at Z 10, depth of each peck is 1, feed equals to 0.02.
G80; ………………………………	Cancels canned cycles for drilling to perform normal operation.
G00 Z5.; ………………………………	Rapid Move, to Z value of 5.
G83 X-49.5 Y-40.5 R5. X-10. Q1. F0.02…………	The second hole Machine to run a peck drilling cycle, X-49.5, Y-40.5, Quickly approach, X-10, depth of each peck is 1, Feed 0.02.
G80; ………………………………	Cancels canned cycles for drilling to perform normal operation.
G00 Z100.; ………………………………	Rapid Move to Z100.
X0 Y0 M05; ………………………………	Return to X00, Y0 and Spindle stop.
M30; ………………………………	It also stops the spindle, turns off the coolant, and returns the program cursor to the start of the program.

Appendix D: Layout of Taguchi L_{16} orthogonal array design with results.

Design Summary

Taguchi $L_{16}(4^4)$

Table 2: Experimental Drilling Outputs Response

S. No	Speed (rpm)	Feed Rate (mm/rev)	Stacking sequences	Drill Dia. (mm)	Entry Delamination	Exit Delamination	Circularity (Roundness) error	Surface Roughness (µm)
1	750	0.02	3	6	1.11849	1.1930	0.1260	4.2325
2	750	0.04	1	8	1.12900	1.1910	0.1700	4.4610
3	750	0.06	2	10	1.13592	1.2199	0.2095	4.9200
4	750	0.08	4	12	1.14829	1.2800	0.2610	5.5670
5	1000	0.02	1	10	1.11666	1.1795	0.2050	4.3200
6	1000	0.04	3	12	1.12870	1.1897	0.2500	4.7020
7	1000	0.06	4	6	1.12660	1.1958	0.1850	4.5250
8	1000	0.08	2	8	1.12861	1.1930	0.1890	4.6600
9	1250	0.02	2	12	1.11389	1.1360	0.2550	4.2400
10	1250	0.04	4	10	1.11830	1.1600	0.2400	4.6702
11	1250	0.06	3	8	1.12110	1.1430	0.2170	4.5300
12	1250	0.08	1	6	1.10900	1.1380	0.1850	4.2400
13	1500	0.02	4	8	1.09825	1.1099	0.2200	4.3550
14	1500	0.04	2	6	1.09900	1.1000	0.1780	4.2100
15	1500	0.06	1	12	1.10620	1.1255	0.2550	4.4110
16	1500	0.08	3	10	1.11490	1.1260	0.2650	4.4850

Appendix-E: Surface Roughness Response Using Zeta-20, 3D Optical Surface Roughness Measuring Instrument

Table 3: Response of surface roughness value from 3D-optical profilometer

Zeta Analysis Report									
Ra	Rq	Rpv	Rp	Rv	Rsk	Rz	Rku		
3.49	4.398	19.84	11.8	8.036	0.6253	10.36	2.97	SGGS	6
2.985	3.965	20.36	8.012	12.34	-0.5798	10.38	3.593		8
3.352	4.355	27.58	17.58	9.993	0.4913	12.44	4.462		10
4.341	5.922	46.17	10.11	36.05	-1.371	18.15	6.526		12
3.85	4.781	29.95	14.26	15.68	-0.7837	14.35	3.361	GSSG	6
3.224	4.214	19.6	11.81	7.79	0.7438	12.75	3.302		8
4.468	5.772	31.88	12.21	19.66	-0.7133	17.02	3.609		10
5	6.446	30.76	8.47	22.29	-1.091	10.64	4.298		12
3.449	4.232	19.35	10.06	9.298	-0.0582	11.99	2.451	SSSS	6
4.494	6.218	35.24	24.19	11.05	1.114	18.93	5.432		8
5.073	6.932	37.21	20.2	17.01	0.1043	11.14	3.871		10
6.037	8.171	49.52	23.85	25.68	-0.696	22.15	4.109		12
3.573	4.893	26.77	13.96	12.8	0.043	11.73	4.012	GGGG	6
3.702	4.503	22.26	10.42	11.84	0.1559	9.737	2.665		8
4.125	5.025	21.4	9.669	11.73	-0.1691	16.93	2.441		10
8.531	10.72	49.26	11.42	37.84	-1.445	29.04	4.57		12